

MONOLITHIC SILICA – BONDED STATIONARY  
PHASES FOR CAPILLARY  
ELECTROCHROMATOGRAPHY

By

DARIN JAMES ALLEN

Bachelor of Science

Southeastern Oklahoma State University

Durant, Oklahoma

1998

Submitted to the Faculty of the Graduate College at  
Oklahoma State University in partial fulfillment  
of the requirements for the degree of  
DOCTOR OF PHILOSOPHY  
December 2003

MONOLITHIC SILICA – BONDED STATIONARY  
PHASES FOR CAPILLARY  
ELECTROCHROMATOGRAPHY

Thesis Approved:



Thesis Advisor









Dean of the Graduate College

## ACKNOWLEDGEMENTS

First and foremost I would like to thank my Lord and Savior, Jesus Christ for all of the blessings and opportunities that He has given me. He has kept my family and myself out of harms way and has always provided us with everything that we need. Whenever there were times that I thought I could not handle the difficulties of research or whenever my family was under financial stress I went to Him in prayer and He has always remained faithful and delivered. I find strength in Him and someday I hope to be the Christian He wants me to be.

I would like to express my sincere gratitude to my research advisor, Dr. Ziad El Rassi for sharing his expertise and giving me guidance throughout graduate school. Working in his research group the last 5 years has really allowed me to develop as an analytical investigator. The knowledge and wisdom he has shared with me will prove to be invaluable as I pursue my future career, and I am truly grateful.

I would also like to thank the members of my committee: Dr. Darrell Berlin, Dr. Allen Apblett, and Dr. Andrew Mort. Their dedication to teaching and research has helped open my mind and has helped my learning experience during my stay here at Oklahoma State.

I am deeply indebted to all of the members of Dr. El Rassi's research group for their assistance in all things pertaining to my research. I would like to thank Mohamed

Bedair for his helpful suggestions concerning my experiments and support in all of my “computer-related” difficulties. My eternal gratitude goes out to Eric Wall for being my “in-lab” mentor during most of my time in this research group. He has never made me feel like a burden whenever I needed assistance with the instrumentation or my research (even after he graduated) and he has become a true friend. Additional thanks to my fellow graduate students, Chad Brown and Lara Johnson, for their friendship and encouragement in my times of need. Many thanks to “the ladies who run this joint”: Carolyn Schwabe, Glenda Edwards and Cheryl Malone. They have always been there to assist me in anything that I have needed and have ensured that I always receive a paycheck.

Special thanks to my early scientific influences: Orda Selph, an extraordinary high school science teacher who taught me that Chemistry was not the nightmare that I thought it was, and Dr. Tim Smith, my undergraduate advisor at Southeastern Oklahoma State for introducing me to analytical research. I have frequently called upon his exceptional scientific knowledge to guide me through the stumbling blocks of research, and I consider him a good friend.

To my parents, Jim Allen and Janis Huff, I cannot begin to express my gratitude for the countless number of things you have done for me growing up. You raised me to appreciate the value of a good work ethic and have taught me the importance of loyalty, honor and integrity. Despite some of the rough times you worked so hard to make sure that I had everything that I needed and have always expressed your love. I think you are the coolest parents in the world, you are my best friends, and I love you so much.

I also want to express my gratefulness to all of my friends and family that have been so patient with me while I have been in graduate school; my best friend J.P. and my brother Dustin in particular. I know there were many times that I may have missed out on things or disappointed you guys because of the time that I spent in the lab, and I just want you to know that I am thankful for your understanding and I cherish your friendships.

Finally, I would like to dedicate this thesis to my wife Aimee and my son Marshall (a.k.a. "J.M."). You two are my life and without you I am nothing. Aimee, it is incomprehensible how supportive and understanding you have been in our marriage and I will never take that for granted. Already, you have been the most remarkable, loving mother to our child. You have made me a better man, and I am proud to call myself your husband. Marshall, being a father has been the most rewarding experience of my life. I never thought that I could love something so much until you came into this world. I want you to know that every decision I make involves you and your mother's happiness and wellbeing as my ultimate goal, and I will do everything in my power to make sure that it happens.

## TABLE OF CONTENTS

Chapter	Page
I. SOME BASIC PRINCIPLES OF CAPILLARY ELECTROCHROMATOGRAPHY- SCOPE OF THE STUDY.....	1
Introduction.....	1
The Development of Capillary Electrochromatography:	
A Historical Background .....	3
Basic Principles of CEC.....	4
Theory of Electroosmosis .....	4
Theoretical Considerations for Flow in a Packed Capillary .....	8
Retention in CEC .....	10
Neutral solutes .....	10
Charged species .....	11
Other Performance Parameters Used in CEC .....	14
Selectivity factor .....	14
Separation efficiency .....	14
Resolution .....	15
Band Broadening in CEC .....	16
Instrumentation .....	21
General Aspects of Instrumentation .....	21
Sample Introduction.....	22
Detection.....	23
Column Technologies .....	25
Packed Columns .....	25
Open Tubular Columns.....	27
Fritless Columns (Monoliths) .....	28
Organic polymer monoliths .....	29
Conclusions.....	30
References.....	31
II. SILICA-BASED MONOLITHS FOR CAPILLARY ELECTROCHROMATOGRAPHY. BACKGROUND AND RATIONALE FOR THE INVESTIGATION.....	38
Introduction.....	38
Silica-Based Monoliths.....	40
Particle-Fixed Monoliths .....	40
Agglomeration of silica microparticles by thermal treatment .....	41

Chapter	Page
Entrapment/bonding of particles using sol-gels.....	44
Design and characterization .....	45
Chiral separations and non-aqueous CEC.....	49
Sol-Gel Monoliths.....	51
Nonpolar sol-gel monoliths for reversed-phase CEC .....	53
Design and characterization .....	53
Chip format .....	60
Use of nonpolar sol-gel monoliths in on-line preconcentration.....	60
Ionic sol-gel monoliths for ion-exchange CEC – Chip CEC.....	62
Chiral sol-gel monoliths for enantiomeric separations by CEC .....	64
Rationale of the Investigation .....	69
Conclusions.....	71
References.....	72
III. CAPILLARY ELECTROCHROMATOGRAPHY WITH MONOLITHIC SILICA COLUMNS. PREPARATION OF SILICA MONOLITHS HAVING SURFACE- BOUND OCTADECYL MOIETIES AND THEIR CHROMATOGRAPHIC CHARACTERIZATION AND APPLICATIONS TO THE SEPARATION OF NEUTRAL AND CHARGED SPECIES .....	77
Introduction.....	77
Experimental .....	78
Instrumentation .....	78
Chemicals and Materials.....	78
Column Preparation .....	79
Results and Discussion .....	81
Optimization of Column Fabrication .....	81
Coating of the stationary phase.....	81
Pore-tailoring .....	84
Evaluation of the Chromatographic Retention .....	89
Neutral solutes .....	89
Ionizable species .....	94
Conclusions.....	101
References.....	103
IV. CAPILLARY ELECTROCHROMATOGRAPHY WITH MONOLITHIC SILICA COLUMNS. PREPARATION OF AMPHIPHILIC SILICA MONOLITHS HAVING SURFACE-BOUND CATIONIC OCTADECYL MOIETIES AND THEIR CHROMATOGRAPHIC CHARACTERIZATION AND APPLICATION TO THE SEPARATION OF PROTEINS AND OTHER NEUTRAL AND CHARGED SPECIES .....	104
Introduction.....	104

Chapter	Page
Experimental .....	105
Instrumentation .....	105
Chemicals and Materials.....	106
Preparation of the Silica Backbone.....	107
Surface Modification to the Silica Monoliths – Formation of Bonded Phases.....	108
Results and Discussion .....	110
Characterization of the Stationary Phases .....	110
Evaluation of the Chromatographic Retention .....	115
Neutral and slightly polar solutes .....	115
Ionizable species .....	119
Conclusions.....	125
References.....	126
V. CAPILLARY ELECTROCHROMATOGRAPHY WITH MONOLITHIC SILICA COLUMNS. PREPARATION OF HYDROPHILIC SILICA MONOLITHS HAVING SURFACE-BOUND CYANO GROUPS: CHROMATOGRAPHIC CHARACTERIZATION AND APPLICATION TO THE SEPARATION OF CARBOHYDRATES, NUCLEOSIDES, NUCLEIC ACID BASES AND OTHER NEUTRAL POLAR SPECIES .....	127
Introduction.....	127
Experimental .....	129
Instrumentation .....	129
Chemicals and Materials.....	129
Preparation of the Silica Backbone.....	131
Surface Modification of the Silica Monoliths – Formation of the Bonded Phases.....	132
Results and Discussion .....	134
Comparison of the Cyano Phases .....	134
Characterization of the CN-OH-Monolith with Polar Solutes.....	136
Mobile phase composition .....	136
Correlation of solute retention and structure .....	140
Phenols .....	140
Nucleic acid bases and their nucleosides .....	141
Nitrophenyl derivatives of mono- and oligosaccharides.....	142
Conclusions.....	147
References.....	149



## LIST OF TABLES

Table		Page
Chapter III		
1.	Values of retention parameters for anilines obtained with a mobile phase consisting of 5 mM sodium phosphate monobasic (pH 3.5) at 40% (v/v) acetonitrile.....	95
2.	Values of $k_e^*$ and the mobility moduli ( $\eta$ ) for DNP-AA obtained with a mobile phase consisting of 10 mM ammonium acetate (pH 4.5) at 30 % (v/v) acetonitrile .....	100
Chapter IV		
1.	Retention factor and selectivity factor for AB's obtained with the different C <sub>18</sub> -monoliths at 60% (v/v) acetonitrile (65% (v/v) for ODS column) .....	111
2.	Retention factor and selectivity factor for anilines obtained on the different C <sub>18</sub> -monoliths using 5 mM sodium phosphate monobasic (pH 7.0) at 40% (v/v) acetonitrile.....	115
3.	Retention factor and selectivity factor for PTH-AA obtained on the different C <sub>18</sub> -monoliths using 5 mM sodium phosphate monobasic at pH 6.0 (ODS) or pH 2.5 (C <sub>18</sub> -NQ1 and C <sub>18</sub> -NSec) at 25% (v/v) acetonitrile .....	118
4.	Values of retention parameters for anilines obtained on the different stationary phases using 5 mM sodium phosphate monobasic (pH 3.5) at 40% (v/v) acetonitrile.....	120
5.	Values of retention parameters of some standard proteins obtained on C <sub>18</sub> -NSec column using 20 mM sodium phosphate monobasic (pH 2.5) at 60% (v/v) acetonitrile.....	123

## Chapter V

1. Comparison of CN-monolith and CN-OH monolith using 5 mM TEAPO <sub>4</sub> (pH 6.5) at 95% (v/v) acetonitrile.....	135
2. Effect of the mobile phase composition on the behavior of the CN-OH-monolith column.....	139
3. Retention factor for phenols obtained on CN-OH-monolith using 5.0 mM TEAPO <sub>4</sub> (pH 6.5) at 95% (v/v) acetonitrile .....	140

## LIST OF FIGURES

Figure	Page
Chapter I	
1. Illustration of the electrical double layer formed at a charged surface and the Stern-Gouy-Chapman model depicting potential gradient with respect to distance from the charged surface.....	5
2. Comparison of mobile phase flow profiles through channels of varying diameter under pressure and electro-driven conditions and its effect on eluted peak shape .....	7
3. Illustration of the plate height contribution for each van Deemter term and the resulting observed curve under pressure-driven and electro-driven conditions for packing material having pores $\geq 300 \text{ \AA}$ .....	19
4. Schematic illustration of a manual instrument used in CEC/CZE.....	21
Chapter II	
1. Hydrolysis and condensation reactions involved in the sol-gel process.....	52
Chapter III	
1. Typical electrochromatograms of APK's obtained on monolithic silica column bonded with octadecyl moieties in the absence and presence of 2,6-lutidine in the silanization reaction with dimethyloctadecylchlorosilane .....	82
2. Effects of the reaction time between the silica monolith and dimethyloctadecylchlorosilane on the retention factor of AB's and the mobile phase flow velocity .....	83
3. Schematic illustration for converting micropores into mesopores within the monolithic silica skeleton during $\text{NH}_4\text{OH}$ treatment.....	84

Figure	Page
4. Effect of pore tailoring on retention of AB's and the mobile phase velocity .....	85
5. Comparison of electrochromatograms of AB's obtained on monolithic C <sub>18</sub> -silica columns previously treated with NH <sub>4</sub> OH for 0, 180 and 360 minutes .....	87
6. Van Deemter plots obtained on monolithic C <sub>18</sub> -silica columns previously treated by NH <sub>4</sub> OH for different time periods using APK's and a typical electrochromatogram of the APK's obtained on the column treated with NH <sub>4</sub> OH for 270 min at u <sub>opt</sub> .....	88
7. Plots of log k' for AB's and APK's versus percent acetonitrile (v/v) in the mobile phase .....	89
8. Electrochromatograms of anilines .....	91
9. Structures of the phenylthiohydantoin amino acids (PTH-AA) .....	92
10. Electrochromatogram of PTH-amino acids .....	93
11. Comparison of aniline separations by CZE and CEC.....	94
12. Comparison of DNP-AA separations by CZE and CEC .....	97
13. Comparison of DNP-AA separations by CZE and CEC .....	98

#### Chapter IV

1. Schematic of the 3 reaction pathways investigated .....	109
2. Comparison of the separations of AB's achieved by columns C <sub>18</sub> -NQ1, C <sub>18</sub> -NQ2 and C <sub>18</sub> -NSec .....	112
3. van Deemter plots for columns C <sub>18</sub> -NQ1 and C <sub>18</sub> -NSec .....	113
4. Plot of mobile phase velocity as a function of pH for columns C <sub>18</sub> -NQ1 and C <sub>18</sub> -NSec .....	114
5. Separation of anilines on column C <sub>18</sub> -NQ1 .....	117
6. Separation of PTH-amino acids on column C <sub>18</sub> -NQ1.....	119
7. Comparison of aniline separations on column C <sub>18</sub> -NSec and C <sub>18</sub> -NQ1 .....	122

Figure	Page
8. Separation of proteins .....	124

## Chapter V

1. Schematic of the two reaction pathways investigated .....	133
2. Electrochromatograms of some model compounds on cyano columns made by two different pathways.....	136
3. Comparison of mobile phase conditions for the separation of model compounds on the CN-OH-monolith column .....	138
4. Electrochromatograms of nucleic acid bases and nucleosides on the CN-OH-monolith column .....	142
5. Electrochromatogram of the pNP-oligosaccharide homologous series and plot of log k' vs. number of glucose residues.....	143
6. Electrochromatograms of pNP monosaccharides and pNP N-acetyl monosaccharides obtained on the CN-OH-monolith column.....	144
7. Structures of the pNP and oNP oligosaccharides .....	145
8. Electrochromatograms of oNP derivatives of monosaccharides obtained on the CN-OH-monolith column .....	146

## LIST OF SYMBOLS

$\alpha$	selectivity factor
$\alpha_{Glc}$	glucosyl group selectivity factor
$\alpha_{GlcNAc}$	glucosyl amino group selectivity factor
$\alpha_{mOH}$	hydroxyl group selectivity factor at the meta position
$\alpha_{oOH}$	hydroxyl group selectivity factor at the ortho position
$\alpha_{pOH}$	hydroxyl group selectivity factor at the para position
$B_o$	specific permeability
$\Delta p$	pressure drop
$\Delta t_m$	difference in migration times
$\delta$	thickness of the double layer
$d.p.$	degree of polymerization
$D_m$	diffusion of solute in the mobile phase
$d_p$	particle diameter
$d_x$	diameter of the channel
$E$	electric field strength
$\varepsilon$	dielectric constant
$\varepsilon'$	porosity of packed column
$\varepsilon_o$	permittivity of the vacuum
$\gamma_m$	obstruction factor

$\eta$	viscosity <i>or</i> mobility moduli
$H$	height equivalent to a theoretical plate
$H_{col}$	plate height contribution from the column
$H_{conn}$	plate height contribution from connections
$H_{det}$	plate height contribution from the detector
$H_f$	plate height contribution from maldistribution of flow
$H_{inj}$	plate height contribution from injection of the sample
$H_{joule}$	plate height contribution from joule heating
$H_{md}$	plate height contribution from longitudinal molecular diffusion
$H_{min}$	minimum plate height
$H_{obs}$	observed plate height
$H_p$	plate height contribution from mass transfer resistance in the pore
$i_{open}$	current observed in open tube
$i_{packed}$	current observed in packed column
$k'$	retention factor
$k^*$	CEC retention factor
$k_{cc}^*$	peak locator in CEC
$k_e^*$	velocity factor
$k_o$	ratio of pore volume to interstitial volume
$\lambda$	measure of flow inequality
$L$	total length of the column
$l$	effective length of column to detection point
$\mu_{app}$	apparent electrophoretic mobility

$\mu_{eo}$	electroosmotic mobility in CZE
$\mu_{eo}^*$	apparent electroosmotic mobility in CEC
$\mu_{ep}$	electrophoretic mobility
$N$	number of theoretical plates
$\theta$	tortuosity factor
$R_s$	resolution
$\sigma_{open}$	conductivity of open segment filled with electrolyte
$\sigma_{packed}$	conductivity of packed segment filled with electrolyte
$\sigma$	peak standard deviation
$\sigma_t$	peak standard deviation in units of time
$\overline{\sigma_t}$	mean peak standard deviation in units of time
$\sigma_L^2$	peak variance in units of length
$t$	elution time
$t_m$	migration time of charged species
$t_o$	elution time of inert and neutral tracer
$t_R$	retention time of neutral species
$u$	mobile phase velocity
$u_{eo}$	electroosmotic velocity in CZE
$u_{eo}^*$	electroosmotic velocity in CEC
$u_{eo,opt}^*$	optimum electroosmotic flow velocity in CEC
$u_{opt}$	optimum velocity
$V$	applied voltage
$v'$	average velocity in pressure driven flow



$w_b$	width at the base of a Gaussian peak
$w_h$	width at half height of a Gaussian peak
$w_i$	width at the inflection point of a Gaussian peak
$\psi_d$	potential at the interface between compact and diffuse regions
$\psi_o$	potential at the interface between the surface and the solution
$\zeta$	zeta potential
$\zeta_p$	zeta potential at the surface of the packing material

## LIST OF ABBREVIATIONS

ACN	Acetonitrile
ABs	Alkyl benzenes
APKs	Alkyl phenyl ketones
BGE	Background electrolyte
BSA	Bovine serum albumin
C <sub>8</sub>	n-Octadimethyl
C <sub>18</sub>	Octadecyl
CE	Capillary electrophoresis
CF <sub>13</sub>	Perfluorohexyl
C <sub>3</sub> F <sub>3</sub>	3,3,3-Trifluoropropyl
CEC	Capillary electrochromatography
CP	Chlorophenol
3-CPDCS	3-Cyanopropyldimethylchlorosilane
CPTS	Chloropropyltrimethoxysilane
CZE	Capillary zone electrophoresis
DCP	Dichlorophenol
DMF	<i>N,N'</i> -Dimethylformamide
DMODA	<i>N,N'</i> -Dimethyloctadecylamine
DNP-AA	2,4-Dinitrophenyl amino acids

DS	Dextran sulfate
EOF	Electroosmotic flow
$\gamma$ -GPTS	( $\gamma$ -Glycidoxypropyl)trimethoxysilane
HPLC	High performance liquid chromatography
3-HPN	3-Hydroxypropionitrile
I.D.	Inner diameter
LIF	Laser-induced fluorescence
NH <sub>2</sub>	Aminopropyl
$\mu$ -HPLC	Micro high performance liquid chromatography
MIP	Molecularly imprinted polymer
MPTS	Methacryloxypropyltrimethoxysilane
MS	Mass spectrometry
NMR	Nuclear magnetic resonance
NPC	Normal phase chromatography
ODS	Octadecylated silica
oNP	o-Nitrophenyl
oNP- $\alpha$ GlcNAc	oNP <i>N</i> -Acetyl- $\alpha$ -D-glucosaminide
oNP- $\beta$ GalNAc	oNP <i>N</i> -Acetyl- $\beta$ -D-galactosaminide
OT	Open tube
OVM	Ovomucoid
PDDAC	Poly (diallyldimethylammonium chloride)
PEG	Poly (ethylene glycol)
PEM	Polyelectrolyte multilayer

PEO	Poly (ethylene oxide)
PFP	Pentafluorophenyl
PFPDM	Pentafluorophenylpropyldimethyl
pNP	p-Nitrophenyl
pNP- $\alpha$ Glc	pNP $\alpha$ -D-glucopyranoside
pNP- $\beta$ chitobiose	pNP <i>N,N'</i> -Diacetyl- $\beta$ -D-chitobioside
pNP- $\beta$ Gal	pNP $\beta$ -D-Galactopyranoside
pNP- $\beta$ GalNAc	pNP <i>N</i> -Acetyl- $\beta$ -D-galactopyranoside
pNP- $\beta$ Glc	pNP $\beta$ -D-Glucopyranoside
pNP- $\beta$ GlcNAc	pNP <i>N</i> -Acetyl- $\beta$ -D-glucosaminide
pNP-Mal	pNP $\alpha$ -D-Maltoside
PSG	Photopolymerized sol-gel
PSS	Poly (sodium styrene-p-sulfonate)
PTH-AA	Phenylthiohydantion amino acids
RPC	Reversed phase chromatography
TEA	Triethylamine
TMOS	Tetramethylorthosilicate
TODAC	[3-(Trimethoxysilyl)propyl]octadecyldimethylammonium chloride

## CHAPTER I

### SOME BASIC PRINCIPLES OF CAPILLARY

### ELECTROCHROMATOGRAPHY –

### SCOPE OF THE STUDY

#### Introduction

Capillary electrochromatography (CEC) is a hybrid analytical separation technique that combines the advantages of both high performance liquid chromatography (HPLC) and capillary zone electrophoresis (CZE) [1-5]. It involves the application of an electric field across a narrow bore, fused-silica capillary (typically 25-100  $\mu\text{m}$  inner diameter or I.D.) possessing some type of stationary phase. Analytes are separated based on chromatographic partitioning between stationary and mobile phases (as in HPLC) or, in the case of charged solutes, undergo an additional separative component resulting from their differential migration (as in CZE). A wide variety of robust stationary phases provide selectivity that can be altered by adjusting parameters such as pH, electrolyte concentration or organic content. As in CZE, mobile phases are transported through the separation channel by means of an electroosmotic flow (EOF). The plug flow profile of the EOF decreases band broadening as compared to laminar flow observed with methods that involve a pressure gradient (e.g., HPLC). This leads to very high separation

efficiencies that give CEC its superior resolution power and peak capacity, thereby promoting rapid analysis times. Since flow is generated at the surface of the support, efficiency can be improved even further by incorporating small diameter packing materials that would require very high pressures if used in HPLC but has no effect on flow velocity in CEC. In addition, CEC affords the advantages of CZE in that it consumes very little reagents, requires small sample volumes, is relatively inexpensive and exhibits high mass sensitivity.

The purpose of this chapter is to introduce fundamental aspects associated with CEC along with basic principles of operation. After a brief historical introduction, the behavior of EOF and the electrophoretic migration of charged solutes in packed columns will be discussed in detail. In addition, performance parameters such as retention factor ( $k'$ ), selectivity factor ( $\alpha$ ) and resolution ( $R_s$ ) will be defined, as well as investigation into the causes of band broadening. Different CEC modes will be introduced, and various instrumentation and column technologies will be discussed.

In addition to this introductory chapter, this dissertation contains 4 other chapters. Chapter II encompasses a thorough review of recent published reports involving the use of monolithic silica column technology for CEC. Several aspects will be highlighted including investigations of column behavior, methods of design, the wide array of bonded phases used and application to the separation of various species. Any shortcomings or areas that could be further investigated will be mentioned. This chapter will also provide an in depth look into the chemistries involved in monoliths developed using the sol-gel process, being that it was the method of choice used to develop columns used in this dissertation.

Chapter III is an investigation into the various parameters that affect the development of sol-gel derived monolithic supports. The effects of pore tailoring and bonded phase reaction time are evaluated in terms of retention factor and separation efficiency. The preparation of an amphiphilic silica monolith possessing cationic octadecyl ligands is described in Chapter IV. Several reaction schemes are investigated to produce either quaternary or secondary amine functionalities on the surface resulting in strong anodal EOF velocities at acidic conditions. Chapter V introduces the application of some cyano-bonded phases for use in normal phase chromatography (NPC). Two separate reaction pathways were investigated and subsequently evaluated using several different sets of polar model compounds. In the following sections, a description of the basic principles and concepts of CEC are summarized in order to familiarize the reader with common terms and fundamental equations used throughout this dissertation.

#### The Development of Capillary Electrochromatography: A Historical Background.

The earliest report on the use of both electrophoretic and chromatographic forces in a separation was in 1939 when Strain separated several dyes by adsorption chromatography on an alumina column in the presence of an electric field [6, 7]. In the early 1950's, Mould and Synge separated polysaccharides on a collodion membrane with the assistance of electroosmotic flow (EOF) [8, 9]. In 1974, Pretorius *et al.* suggested this EOF as an alternative to pressure for driving mobile phases through a 1 mm glass tube packed with a particulate stationary phase of 75-125  $\mu\text{m}$  particle diameter ( $d_p$ ), demonstrating substantially smaller band broadening as compared to HPLC [10]. Four

decades after the concept of using electrophoresis in conjunction with chromatography was first introduced, Jorgenson and Lukacs demonstrated its feasibility by performing electrochromatography in a capillary packed with chromatographic particles [11, 12]. Tsuda *et al.* demonstrated the use of pressure-assisted CEC in both open-tubular [13] and packed capillary columns [14] to perform separations. Knox and co-workers thoroughly investigated the use of CEC as a viable separation technique in the late 1980's and early 1990's [15-18] by using capillaries packed with C<sub>18</sub>-coated silica particles of 3 and 5 μm mean particle diameter to separate a mixture of aromatic hydrocarbons at a reduced plate height < 1. These works have been credited to generating an increased interest in the method, making it responsible for the popularity it experiences today [19-22].

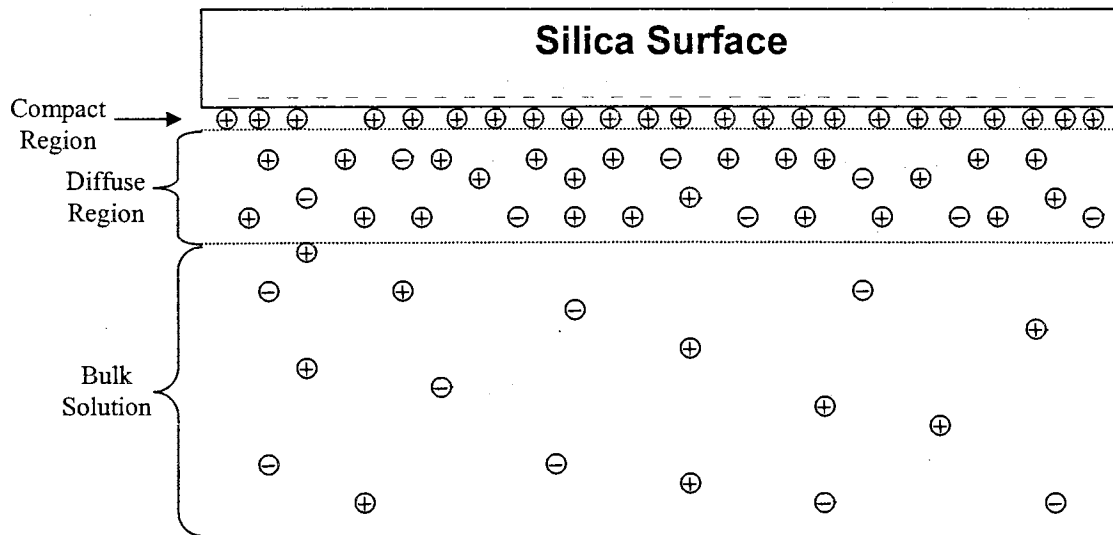
## Basic Principles of CEC

### Theory of Electroosmosis

In CEC, mobile phases are transported through the column by electroosmosis. When a charged surface comes in contact with an electrolyte solution, an electrical double layer forms thus producing a potential gradient. Figure 1a illustrates the electrical double layer in the case of a negatively charged surface (e.g., silica). At pH > 3.5, the silanol groups on the surface of silica will begin to ionize thereby producing a negatively charged surface. In an attempt to balance this charge, counter-ions in solution (i.e., cations) will begin to accumulate near the charged surface while co-ions (i.e., anions) are repelled. At the solid-liquid interface, the cations are tightly bound by electrostatic forces



**a.**



**b.**

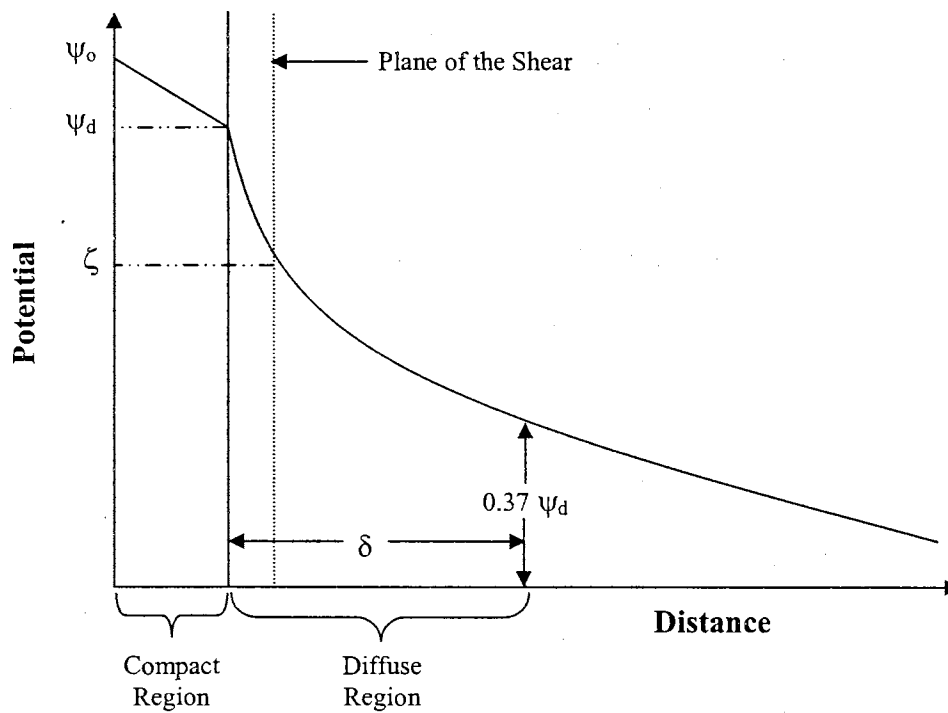
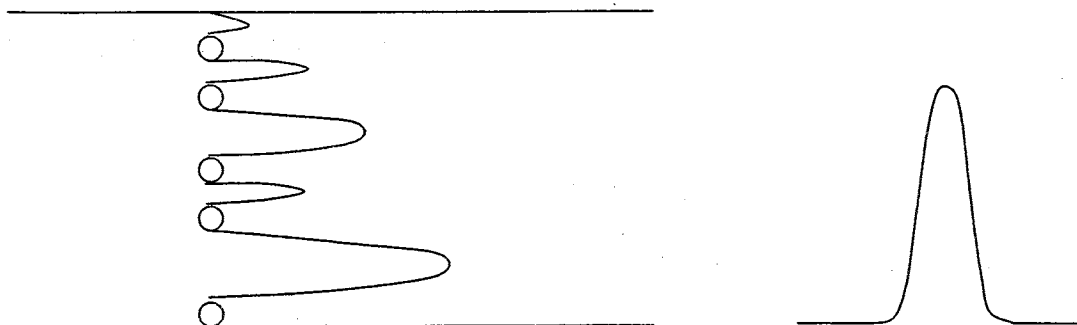


**Figure 1.** (a) Illustration of the electrical double layer formed at a charged surface, (b) Stern-Gouy-Chapman model depicting potential gradient with respect to distance from the charged surface.

resulting in a compact region, or a stern layer. Thermal motion causes some of these ions in the compact region to diffuse further into the solution producing the diffuse region. The compact and diffuse regions are collectively known as the electrical double layer. Since the double layer contains an excess positive charge, a potential gradient is established that decreases linearly in the compact region and exponentially in the diffuse region. Figure 1b illustrates this potential gradient where  $\psi_0$  and  $\psi_d$  represent the electrical potentials at the silica-solution interface and compact-diffuse region interface, respectively. The potential value at the plane of the shear (where the bulk solution flows tangentially to the surface) is known as the zeta potential ( $\zeta$ ). The thickness of the double layer is represented by  $\delta$  and is defined as the distance between the compact-diffuse region interface and the point where the potential is equal to  $0.37 \psi_d$ .

Upon the application of an electric field that is tangential to the surface, hydrated cations in the diffuse region migrate toward the cathode, dragging the bulk solution concurrently and creating an electroosmotic flow (EOF). The sign for the zeta potential dictates the direction of EOF once the electric field is applied. Negatively charged surfaces have a negative zeta potential exhibiting a cathodal EOF. In the event a positive surface is implemented (e.g., covalent bonding of amine, or dynamic coating of cationic surfactant), a double layer is formed containing an excess of anions whereby the application of an electric field would generate an anodal EOF (flow in the direction of the anode). The plug flow profile thus generated in either instance does not introduce band broadening and generates superior separation efficiency as compared to pressure gradient techniques (e.g., HPLC) that exhibit a parabolic flow profile (Figure 2). This issue

**a.**



**b.**

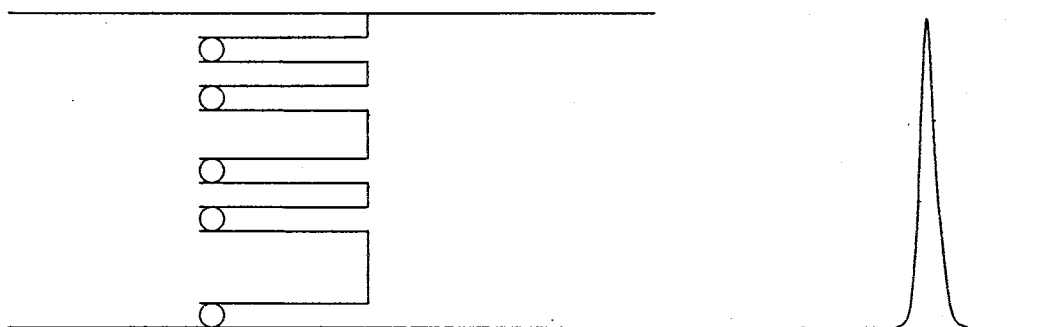


**Figure 2.** Comparison of mobile phase flow profiles through channels of varying diameter and their effect on column efficiency. (a) Laminar flow profile observed in hydraulically driven methods and its band broadening effect on eluted peak shape. (b) Plug flow profile observed in electrically driven flow and the resulting peak shape observed.

concerning the effect of flow profile on separation efficiency will be discussed in more detail later in this chapter.

### Theoretical Considerations for Flow in a Packed Capillary

For porous/nonporous non-conducting packing materials of arbitrary shape and uniform zeta potential, Overbeek [23] suggested the following equation to describe the average electroosmotic velocity,  $u_p$ , generated in the interstices

$$u_p = -\frac{\varepsilon\varepsilon_o\zeta_p E}{\eta} \left( \frac{\sigma_{packed}}{\sigma_{open}} \right) \quad (1)$$

where  $\varepsilon$  is the dielectric constant of the medium,  $\varepsilon_o$  is the permittivity of the vacuum,  $\zeta_p$  is the zeta potential at the surface of the packing material,  $E$  is the electric field strength,  $\eta$  is the viscosity of the bulk solution and  $\sigma_{packed}$  and  $\sigma_{open}$  are the conductivities of a completely packed column and an open tube, both filled with the electrolyte solution, respectively. The EOF generated by the stationary phase is viewed as a bundle of open tubes that obey the Smoluchowski's equation for EOF in open tubes [24, 25] and was modified by adding the conductivity ratio expression ( $\sigma_{packed}/\sigma_{open}$ ), making it applicable to packed columns. Under equivalent conditions, packed capillaries exhibit a lower conductance than a corresponding open capillary and generate lower mobile phase velocities due to the presence of the packing material. Therefore, any difference in the conductivity between open and packed conditions is indicative of the effect the particles have on the average flow velocity and can be monitored by recording differences in current.

Recently, there have been more thorough formulations that consider factors such as difference in flow rate, conductivity and potential drop between open and packed segments, difference in zeta potential between the capillary and the stationary phase, conservation of flow rate between open and packed segments and intersegmental pressure [24, 26-29]. However, since the columns fabricated for this dissertation are silica-based monoliths without open segments, and since the reaction of bonded phases was performed on both the monolith and the surface of the capillary simultaneously, these factors do not need to be considered. Therefore, there is no reason to think that Eq. 1 is not applicable in this particular case.

Note that Eq. 1 does not include particle size in the expression, suggesting that particles of very small size ( $\leq 1 \mu\text{m}$ ) could be used in CEC without sacrificing EOF velocity, an advantage that pressurized techniques do not possess. The use of small stationary phase particles is desirable for analytical separation techniques to reduce mass transfer resistance between analytes and the stationary phase, promoting high separation efficiencies. For pressure driven flow, the average velocity,  $v'$ , can be expressed using the Kozeny-Carman equation [30]

$$v' = \frac{\varepsilon'^2 d_p^2 \Delta p}{180(1 - \varepsilon')^2 \eta L} \quad (2)$$

where  $\varepsilon'$  is the porosity,  $d_p$  is the particle diameter of the stationary phase and  $\Delta p$  is the pressure drop over the length of the column,  $L$ . In this instance, decreasing particle size would have a two-fold effect on the velocity since a decrease in porosity would accompany the decrease in particle size. A drastic increase in the applied pressure would be necessary to compensate these effects on the average flow velocity.

Despite the omission of particle diameter in Eq. 1, it should be mentioned that a limit of 0.5  $\mu\text{m}$  has been predicted for CEC [18, 31]. To obtain good flow in CEC, it is necessary to use particles with diameters that are at least 10 times greater than the thickness of the double layer (which can reach a thickness of 100 nm) [15]. The use of particles that fall below this threshold can result in a double layer overlap that disturbs the potential gradient, thereby eliminating EOF.

### Retention in CEC

Neutral solutes As in HPLC, the mechanism of retention for a neutral solute in CEC is based on chromatography. Components of a sample mixture are separated as they partition differentially between stationary and mobile phases. Solutes that spend more time in the stationary phase are more retarded than those that spend more time in the mobile phase; therefore more time is required for their elution. Separation can be achieved by a variety of processes (e.g. adsorption or ion-exchange), and many parameters can be altered to adjust their retention (e.g. pH, ionic strength or organic content).

In chromatography, retention of a neutral solute can be determined experimentally using the following equation

$$k' = \frac{t_R - t_o}{t_o} \quad (3)$$

where  $k'$  is the dimensionless retention factor,  $t_R$  is the retention time of a retained species and  $t_o$  is the retention time of an inert, neutral tracer (i.e., EOF marker). The tracer selected must not interact with the stationary phase (i.e., not be retained) so that the “dead time” of the column can be accurately determined. The values for  $k'$  can range from 0 to  $\infty$ , with higher values indicating a higher degree of partitioning with the stationary phase.

Charged species In CEC, analytes that carry a charge are retained by both chromatographic and electrophoretic mechanisms simultaneously. Upon application of an electric field, charged species will migrate towards the oppositely charged electrode (as in EOF generation). This migration can be in the same direction as EOF (co-directional) or in the opposite direction (counter-directional). To gain insight into this concept, a few basic principles involved in electrophoresis-based techniques that do not impart chromatographic retention (e.g., CZE) will be discussed.

In CZE, migration of a charged analyte is dependent on the mobilities of EOF ( $\mu_{eo}$ ) and the resulting electrophoretic mobility ( $\mu_{ep}$ ) of the charged species under application of an electric field. The magnitude of  $\mu_{ep}$  is dependent on the mass-to-charge ratio of the species and is determined by taking the difference between  $\mu_{eo}$  and the *observed* mobility of the charged species, known as the apparent mobility ( $\mu_{app}$ ).

$$\mu_{ep} = \mu_{app} - \mu_{eo} \quad (4)$$

$\mu_{ep}$  represents the true mobility since it subtracts the contribution of EOF from  $\mu_{app}$ . Negative values for  $\mu_{ep}$  indicate mobility against the flow of EOF, while positive values are indicative of mobilities that move in the same direction as EOF. For the majority of

applications, separations are based on counter-directional conditions where the magnitude of  $\mu_{eo}$  is greater than  $\mu_{ep}$ .

Mobility is calculated experimentally by dividing the observed velocity,  $v$ , of the species by the electric field strength ( $E$ ). Since  $v = l/t$  and  $E = V/L$ , mobility can also be represented as

$$\mu = \frac{v}{E} = \frac{lL}{tV} \quad (5)$$

where  $l$  is the effective length from column inlet to detection point,  $L$  is the total length of the column,  $t$  is the species elution time and  $V$  is the applied voltage. Therefore,  $\mu_{eo}$  and  $\mu_{app}$  are calculated by substituting  $t_o$  and  $t_m$  for  $t$ , respectively. Here,  $t_m$  is the migration time of the analyte of interest while  $t_o$  is the elution time of an inert, unretained species (i.e., EOF tracer). Substitution of these expressions into Eq. 4 yields

$$\mu_{ep} = \mu_{app} - \mu_{eo} = \frac{lL}{V} \left( \frac{1}{t_m} - \frac{1}{t_o} \right) \quad (6)$$

As mentioned earlier, charged components in a separation mixture undergo both electrophoretic and chromatographic mechanism when analyzed in CEC. Due to the increased complexity of the separation mechanism, calculation of  $k'$  does not indicate the extent of chromatographic partitioning (as in HPLC), but rather it serves only as a useful peak locator. There have been several reports that have attempted to describe retention of a charged species in CEC [32-34] although none have been widely accepted. However, one of the more insightful characterizations for migration of a charged solute has been introduced recently by Rathore and Horváth [24, 35]. They have defined a CEC retention factor ( $k^*$ ) as:



$$k^* = \frac{t_m(1+k_e^*) - t_0}{t_0} \quad (7)$$

where velocity factor,  $k_e^*$ , is introduced as a modification. The velocity factor describes the contribution of electrophoretic mobility to the separation of a charged species in CEC and is given by

$$k_e^* = \frac{\mu_{ep}}{\mu_{eo}} \quad (8)$$

where,  $\mu_{eo}$  is the actual “interstitial” electroosmotic mobility of the mobile phase in the monolithic CEC column. For neutral solutes  $k_e^*$  is zero and, therefore, Eq. 7 becomes Eq. 3 which is the  $k'$  found in chromatography. Since  $\mu_{ep}$  is the same for a charged species in CZE and CEC, its value is usually obtained by running in the CZE mode at the same conditions as the CEC analysis [24, 35]. The value of  $\mu_{eo}$  is obtained by multiplying the “apparent” electroosmotic mobility  $\mu_{eo}^*$  within the CEC column by the tortuosity factor of the column. The column tortuosity factor is usually estimated by the quotient of the currents observed in the CZE ( $i_{open}$ ) and CEC ( $i_{packed}$ ) modes for the same running conditions [36]. Thus, Eq. 2 is explicitly expressed as follows:

$$k_e^* = \frac{\mu_{ep}}{\mu_{eo}^* \cdot \frac{i_{open}}{i_{packed}}} \quad (9)$$

Because of the presence of  $k_e^*$  in Eq. 1,  $k^*$  does not serve as a useful peak locator as its counterpart  $k'$  does in chromatography. To facilitate the description of the elution order of charged solutes in CEC, a peak locator,  $k_{CC}^*$ , based on chromatographic formalism, has been suggested [24, 35]:

$$k_{cc}^* = \frac{t_m - t_0}{t_0} \quad (10)$$

Unlike  $k^*$  and  $k_e^*$ ,  $k_{cc}^*$  is devoid of any mechanistic insight, and so has limited utility [24, 35]. For neutral species, both  $k^*$  and  $k_{cc}^*$  become the true chromatographic retention factor,  $k'$ .

### Other Performance Parameters Used in CEC

Selectivity factor Selectivity factor ( $\alpha$ ) is a measure of the stationary phase's chromatographic discriminating power for a given set of conditions, and is calculated by taking the quotient of retention factors for the analytes in question.

$$\alpha = \frac{k_2'}{k_1'} \quad (11)$$

Here,  $k_2'$  is always greater than  $k_1'$ ; thus,  $1 \leq \alpha < \infty$ . Note that the above equation is expressed in terms of the conventional retention factor used in HPLC. The CEC equivalent would involve substitution of  $k_{cc}^*$  for  $k'$  to obtain the *overall* selectivity of both separative components (i.e., chromatography and electrophoresis) [35].

Separation efficiency Separation efficiency is used to measure the degree of band broadening for eluted peaks in chromatography. Plate height (H), or height equivalent to a theoretical plate, provides this information as the peak variance ( $\sigma_L^2$ ) per effective unit length of the column.

$$H = \frac{\sigma_L^2}{l} \quad (12)$$

Plate number ( $N$ ), or number of theoretical plates, is a dimensionless value and is a more common means of expressing separation efficiency. Since  $N = l/H$ , dividing both sides of Eq. 12 by  $l$  and inverting gives

$$N = \frac{l^2}{\sigma_L^2} = \left( \frac{t_m}{\sigma_t} \right)^2 \quad (13)$$

As illustrated in the last expression above (Eq. 13), retention time can be substituted for effective length, and the variance is changed accordingly to maintain the unitless value. Since migration time ( $t_m$ ) is easily obtained from the electrochromatogram, this expression is preferred for simplicity. Peak width for a Gaussian peak can be measured at the base ( $w_b$ ), half height ( $w_h$ ) or at the inflection point ( $w_i$ ) and are equal to  $4\sigma$ ,  $2.354\sigma$  and  $2\sigma$ , respectively. The inflection point of the peak is defined as 0.607 of the peak height. Substitution of the peak standard deviation ( $\sigma$ ) for each case gives

$$N = 4 \left( \frac{t_m}{w_i} \right)^2 = 5.54 \left( \frac{t_m}{w_h} \right)^2 = 16 \left( \frac{t_m}{w_b} \right)^2 \quad (14)$$

Often the plate number is divided by the effective length of the column to give a better indication to the degree of band broadening that is occurring as it transverses the separation channel, and is given in units of plates per meter.

Resolution Resolution ( $R_s$ ) measures the extent of separation between two neighboring peaks in terms of overlap and is calculated by dividing the difference in peak maximums by the mean band width of the two peaks. This can be expressed as

$$R_s = \frac{\Delta t_m}{4\sigma_t} \quad (15)$$

where  $\Delta t_m$  is the difference in migration times of the adjacent peaks and  $\overline{\sigma_t}$  is the mean standard deviation of the two peaks. As in chromatography, resolution can also be expressed in terms of selectivity, retention factor and efficiency

$$R_s = \left( \frac{\alpha - 1}{\alpha} \right) \left( \frac{k_2'}{1 + k_2'} \right) \left( \frac{\sqrt{N}}{4} \right) \quad (16)$$

where  $k_2'$  is the retention factor of the more retarded peak of the two neighboring peaks in question. Recall, that selectivity for CEC is calculated using peak locator  $k_{cc}^*$  and likewise is the appropriate substitute for  $\overline{k'}$  here [35]. From Eq. 16 we can see the importance of using columns that provide high separation efficiency and mobile phases of optimal composition to enhance selectivity and retention, thereby promoting maximum resolution. Since CEC exhibits superior separation efficiency over HPLC (as high as 10-fold or more), equivalent resolutions can be obtained at lower retention and selectivity; factors that could be sacrificed if rapid analysis times were desired.

### Band Broadening in CEC

It is well known that the high efficiencies obtained in CEC are a result of the plug flow profile characteristic of the technique [1, 2, 37]. However, to fully understand the superior separation efficiency observed for CEC over HPLC, it is necessary to delve into the factors that contribute to band broadening. For any LC technique, the observed plate height is established by the plate height contributions of sample injection ( $H_{inj}$ ),

connections ( $H_{conn}$ ), detection ( $H_{det}$ ) and passage of sample through the column ( $H_{col}$ ). Connections are not a factor in CEC, but plate height contribution stemming from heat generated by the passage of current, or Joule heat ( $H_{joule}$ ), is an additional consideration, and therefore

$$H_{obs} = H_{joule} + H_{inj} + H_{det} + H_{col} \quad (17)$$

Joule heating causes non-uniform temperature gradients and local changes in viscosity that lead to band broadening. However, since this effect can be minimized by using nonconductive packing material, narrow bore capillaries, field strengths no greater than 1000 V/cm, and temperature controlled systems,  $H_{joule}$  can be considered negligible for most applications. In fact, a systematic examination of band broadening between pressure and electro-driven conditions performed by Horvath and coworkers established that plate height contributions  $H_{joule}$ ,  $H_{inj}$ , and  $H_{det}$  were all negligible compared to  $H_{col}$  [37]. Therefore, it can be assumed that the observed plate height is determined by passage of the sample through the column. For LC techniques, factors involved with  $H_{col}$  include maldistribution of flow ( $H_f$ ), longitudinal molecular diffusion ( $H_{md}$ ) and mass transfer resistance in the pore ( $H_p$ ). After dropping the negligible terms and substituting these terms for  $H_{col}$  Eq. 17 becomes

$$H_{obs} = H_f + H_{md} + H_p \quad (18)$$

If we substitute the corresponding parameters that define these plate height contributions into Eq. 18 we obtain the van Deemter equation

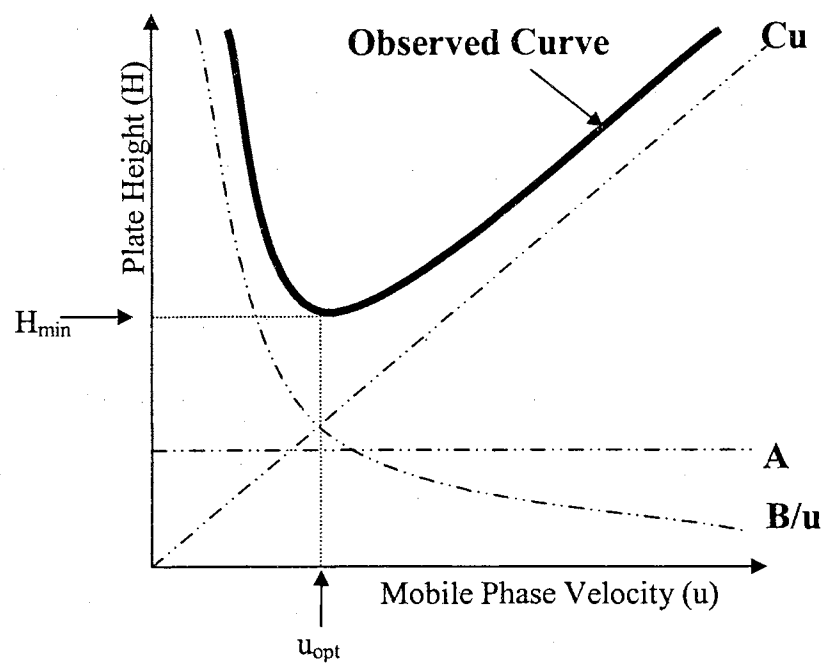
$$H_{obs} = 2\lambda d_p + \frac{2\gamma_m D_m}{u} + \frac{\theta(k_o + k' + k_o k')^2 d_p^2 u}{30D_m k_o (1 + k_o)^2 (1 + k')^2} \quad (19)$$

where  $\lambda$  is the measure of flow inequality through channels of differing diameter,  $\gamma_m$  is an obstruction factor coming from the presence of the packing,  $D_m$  is diffusion of the solute in the mobile phase,  $u$  is mobile phase velocity (in CEC  $u$  is  $u_{eo}^*$ ),  $\theta$  is the tortuosity factor of the porous structure and  $k_o$  is the ratio of the pore volume to the interstitial volume. A simplified version of the van Deemter equation that consolidates the constants for a given set of conditions and relates each plate height contributor in terms of mobile phase velocity is usually preferred

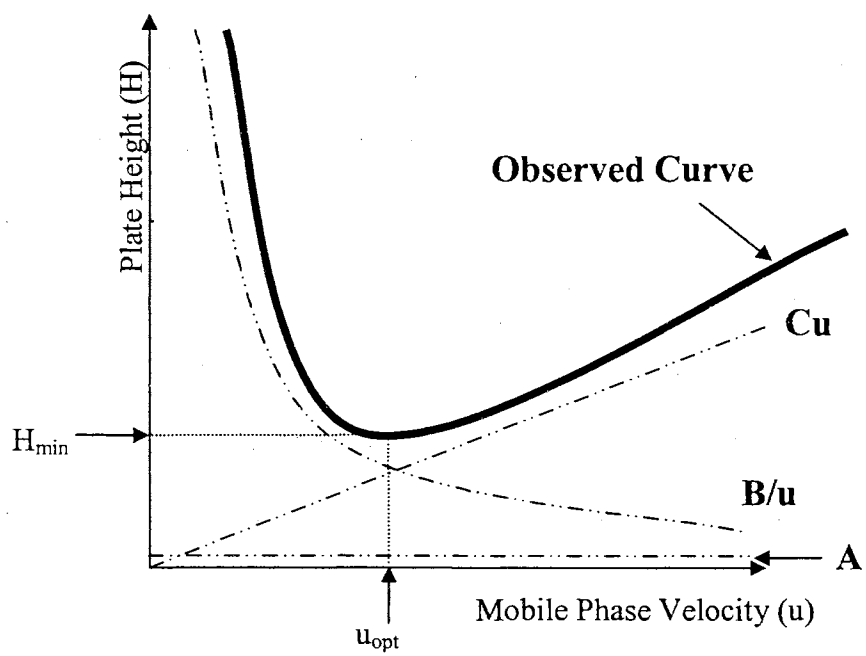
$$H = A + \frac{B}{u} + Cu \quad (20)$$

Figure 3 illustrates a typical van Deemter plot and the relative plate height contributions of each term in the van Deemter equation as a factor of mobile phase velocity for pressure-driven and electro-driven conditions. Optimum velocity that produces the minimum plate height is represented as  $u_{opt}$  (in CEC,  $u_{eo,opt}^*$ ) and  $H_{min}$ , respectively. Since longitudinal molecular diffusion is dependent on the nature of the solute, the effect of the “B” term is the same for both modes and can be minimized by increasing mobile phase velocity (as can be seen in Eq. 20). The plate height contribution resulting from mass transfer resistance in the pores increases with an increase in mobile phase velocity for both modes. However, for packing materials that possess pores  $\geq 300 \text{ \AA}$ , the effect of increasing mobile phase velocity on observed plate height is reduced in CEC mode due to the EOF generated within the pore [37]. The EOF facilitates mass transfer within the pore, thereby increasing the kinetics associated with the process. This trend is illustrated by the decrease in slope of the “C” term contribution plot in Fig. 3b. At pore sizes  $< 300 \text{ \AA}$ , double layer overlap begins to occur and the

a.



b.



**Figure 3.** Illustration of the plate height contribution for each van Deemter term and the resulting observed curve under (a) pressure-driven and (b) electro-driven conditions for packing material having pores  $\geq 300 \text{ \AA}$ .

mobile phase within the pores becomes stagnant, thus deteriorating this effect.

While the observed improvements in the “C” term contribute to a lowered overall plate height, the highest gains in separation efficiency result from differences in flow profiles between the two modes. As mentioned earlier, pressure gradient techniques generate laminar flow profiles between the interstices of particles at low mobile phase velocities (Fig. 2). Mobile phase velocity is at a maximum in the center of the channel, with velocity decreasing as distance from the wall decreases due to the increasing effect of the drag force at the liquid-solid interface. The flow velocity through each channel in a packed bed varies with the square of the channel diameter ( $d_c$ ) at equivalent path length and  $\Delta p$  as given by the following expression [24]

$$\frac{u_2}{u_1} = \left( \frac{d_2}{d_1} \right)^2 \quad (21)$$

It is apparent, that differences in channel diameter lead to magnified differences in flow velocities that cause excessive band broadening. This maldistribution of flow observed for packed columns in pressure driven mode is known as “Eddy diffusion” [30]. Conversely, the EOF velocity in CEC is independent of channel diameter (or,  $u_1 \sim u_2$ ) as long as there is no double layer overlap (see Eq. 1). Therefore, the plug flow profile in CEC causes the “A” term to become negligible in determining overall separation efficiency (Fig. 3b). The end result to reducing these band broadening effects (in both A and C terms) is separation efficiencies that are 5-10 times better than those observed in pressure-driven mode under otherwise equivalent running conditions [2].



## Instrumentation

### General Aspects of Instrumentation

Instrumental design in CEC can be either manual or automated in nature and is identical for that used in CZE. Figure 4 is a schematic representation of a typical manual instrument used in CEC. The separation column is composed of a narrow bore fused-silica capillary containing some type of packing material as a stationary phase. The capillary contains an external polyimide coating, thereby increasing its durability. This

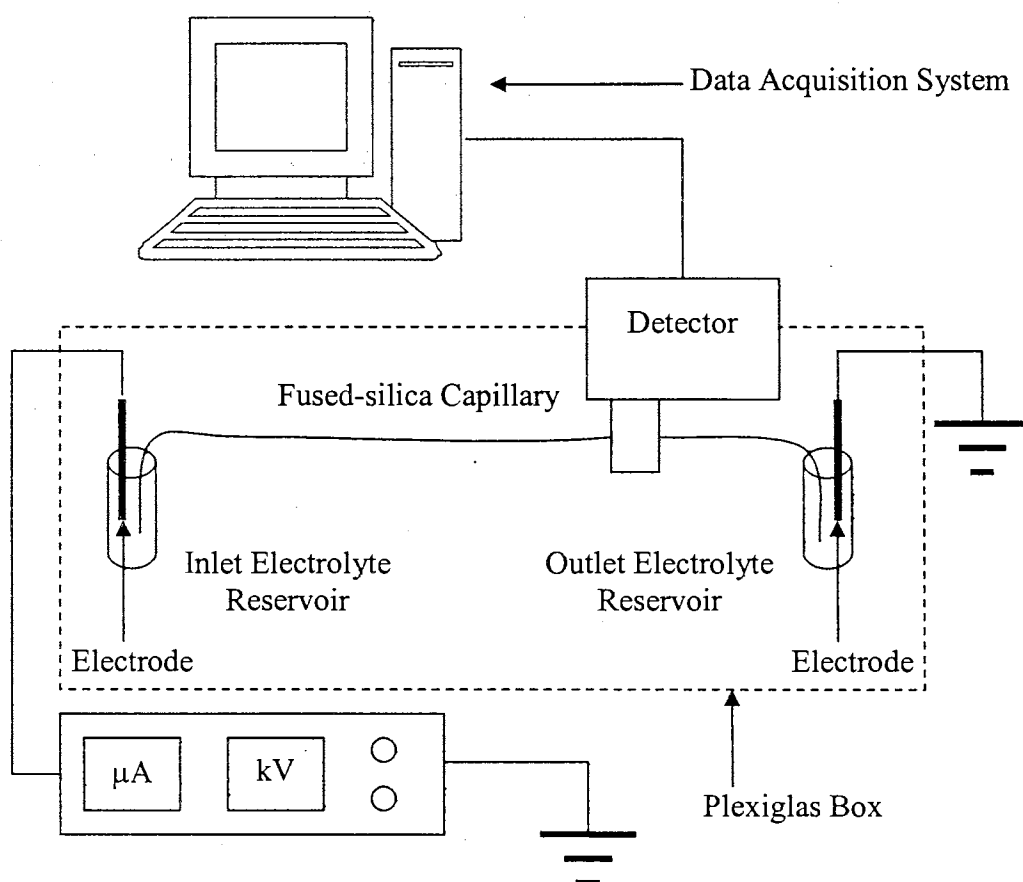


**Figure 4.** Schematic illustration of a manual instrument used in CEC/CZE.

coating is removed at the detection point (~2 mm in length) to facilitate transmittance of light. Each end of the capillary is immersed in electrolyte reservoirs containing the mobile phase. A platinum electrode connected to a high voltage power supply is allowed to make contact with the inlet reservoir (i.e., vial with inlet end of capillary). The power supply is typically capable of introducing electrical potentials up to 30kV. The platinum electrode located in the outlet reservoir is connected to ground to complete the circuit. On-column detection for CEC is most commonly accomplished using a UV-Vis detector, which is connected to a data acquisition device (e.g., integrator or computer). The capillary, the high voltage connections and the reservoirs are all enclosed in a Plexiglas box equipped with a safety cutoff switch for obvious safety reasons. In the event the lid is opened while the high voltage is being supplied, the power supply is automatically switched off. Automated instruments can also include temperature control components, auto-samplers and pressurized systems.

### Sample Introduction

There are predominantly two methods of introducing sample components onto the separation column in CEC, namely hydrodynamic injection and electrokinetic injection. Hydrodynamic injection in CEC involves application of an external pressure within the sample vial in which the capillary inlet is immersed (also known as headspace pressurization). Other types of hydrodynamic injection techniques used in CE (e.g., vacuum injection or gravimetric siphoning) are usually not well suited for CEC due to the packing material that interferes with these processes. For instrumental setups that

employ pressurized systems, hydrodynamic injection is the most frequently used. However, when CEC columns exhibit extremely high backpressures resulting from separation beds of low porosity, commercial instrumentation that makes use of low-pressure sample injections may not be sufficient. In this instance, electrokinetic injection is preferred. Electrokinetic injection involves the siphoning of the sample matrix onto the column by means of EOF. As the buffer moves along the capillary by electroosmosis, the sample is pulled into the inlet of the column at the sample-buffer interface. This method of sample introduction is most popular when dealing with manual instruments, but it does have its drawbacks. Since the quantity of sample injected is dependent on the relative conductivities of sample matrix and running electrolyte, altering their respective compositions can cause problems in terms of injection reproducibility. This effect can be magnified when dealing with samples that contain charged species. Nonetheless, this issue can be remedied by careful selection of running conditions for applications that necessitate high detection sensitivity.

### Detection

UV detection has been the workhorse of LC methods (e.g., HPLC) due to its durability, simplicity and low cost requirements. In addition, many analytes absorb in the UV range, and those that do not can be derivatized with chromophores that allow their detection. While the popularity of UV detection has carried over into CEC, several factors must be considered when dealing with on-column capillary detection. These include [19, 20, 38] low peak volumes, short optical path length (usually 50-100  $\mu\text{m}$ ),

light scattering due to the curved surface of the capillary and “in-column” detection. In column detection refers to measurement of the signal across the packed portion of the column which leads to increased separation efficiency but decreases in detection sensitivity [39, 40]. The following are some advances reported in CEC that have tried to address these issues.

In an attempt to address the problem of optical path length, Ross *et al.* tried to increase detection sensitivity by incorporating a high sensitivity detection cell design [41]. A path-length of 1.2 mm was obtained for a 100  $\mu\text{m}$  I.D. capillary by using a detection cell channel that was perpendicular to the capillary and aligned with the beam path. This concept was implemented a few years later by Hewlett-Packard when they introduced capillaries possessing a bubble cell that expanded the capillary at the point of detection 3-fold [42].

An alternative to using specially designed detection cells or capillaries is making use of more sensitive detection methods. Fluorescence, especially laser induced fluorescence (LIF), can provide a more sensitive alternative to UV detection although it is limited to a certain number of analytes without the use of derivatization [21, 43-45]. Mass spectrometry (MS) and nuclear magnetic resonance (NMR) have also been used as detectors for CEC because of their ability to provide additional structural information of the analytes. One group in particular has focused on designing a coupling device for NMR detection in CEC [46-49] with applications to the separations of metabolites [47, 49] and analgesics [46]. The volumetric flow rates ( $\sim 50\text{-}100$  nL/min) and solvent compatibility associated with CEC are well suited for the interfacial requirements of MS (e.g., electrospray ionization). The interface is critical in establishing the viability of

CEC-MS and has received a lot of attention [50-58]. The success of these interfacial designs has led to a plethora of recent applications towards analysis of enantiomers [59-61], oligosaccharides [62-64], carbohydrates [62, 64, 65], metabolites [66, 67], proteins [65, 68, 69], peptides [65, 70, 71] and fatty acids [53, 58], among others.

### Column Technologies

For capillary electrochromatography (CEC) to realize its full potential as a hybrid separation technique of micro-high-performance liquid chromatography ( $\mu$ -HPLC) and capillary electrophoresis (CE), advanced column technologies have been introduced to produce a variety of stationary phases for achieving the CEC separations of a wide range of analytes. From these investigations, three major categories of column design have surfaced, namely packed, open tubular (OT) and monolithic.

#### Packed Columns

The most commonly used columns in CEC are packed columns. Packed columns for CEC involve the incorporation of highly characterized, microparticulate stationary phases into narrow bore fused-silica capillaries [72]. Most generally, these columns consist of packed and open segments used for separation and detection, respectively. The packed segment requires retaining frits at each end to keep the stationary phase particles in place. The most common frit involves the sintering of the packing material or bare silica at elevated temperature in an attempt to fuse the particles to each other and the

capillary wall. Other alternatives for frit fabrication include silicate polymerization [73, 74] and photopolymerization of organic polymer solutions [75], while others have eliminated frits altogether by incorporating external or internal tapers and restrictors [56, 76]. In any case, careful production of the frits is necessary to avoid increased problems with bubble formation [77, 78].

The success of packed capillaries for CEC can be attributed to the increased loading capacity of highly characterized and commercially available packing materials. In selecting these materials, it is desirable for the particles to be charged to assist in the generation of EOF (e.g., uncapped silanols), but still possess the retentive properties of the bonded phase [20, 79]. For this reason, the majority of applications involve the use of uncapped, silica-based materials. However, in some instances, the unreacted silanols on the surface may not be sufficient to provide good EOF velocity. To remedy this problem these columns may incorporate segments packed with bare silica particles (known as segmented capillaries) [29]. To avoid EOF dependence on pH altogether, many groups have made use of mixed-mode stationary phases that incorporate ionic exchange sites [80-83]. These materials exhibit strong EOF as a result of the fixed charges on the surface while still providing good retention.

There are a variety of methods used to pack capillaries for CEC with pressure packing being the most common [84]. These columns are primarily packed at elevated pressure (> 5000 psi) by connecting the capillary to a slurry reservoir (containing the packing material suspended in organic solvent) connected to a high-pressure pump. In an attempt to produce more stable separation beds, this procedure has been modified by using supercritical CO<sub>2</sub> as the transporting media [85, 86]. One group has made use of

centripetal force to pack capillaries by placing the slurry reservoir in the center of a rotating packing apparatus [87, 88]. Using this method, capillaries can be packed in 5 min at 2000 rpm. Others have taken advantage of the inherent charges fixed on the packing material and packed capillaries by pseudoelectropacking [89, 90]. In this situation, a high electric field is applied in conjunction with hydrodynamic flow to produce well-packed columns.

### Open Tubular Columns

Open tubular CEC (OT-CEC) utilizes narrow bore fused-silica capillary columns (ca. 10  $\mu\text{m}$  I.D.) having stationary phases coated onto their inner walls [91]. Due to the slow rate of solute diffusion in the liquid phase, these narrow channels are necessary to promote interaction with the immobilized ligands [92]. Fabrication of these columns is relatively simple, and they provide very high separation efficiencies [93]. Many times an etching process is performed to increase the surface area prior to ligand attachment to the inner surface [94].

There are primarily four major groups of stationary phases used for OT-CEC [95], namely chemically bonded, physically or dynamically adsorbed, organic polymer-based and sol-gel coated. Chemically bonded phases involve bonding of an organic moiety to the etched surface via silanization or hydrosilation processes [91]. As its name implies, adsorbed stationary phases make use of the electrostatic interactions between the silica surface and the desired ligand [96] (e.g., surfactants and proteins). Physically adsorbed phases involve stronger interactions compared to dynamically adsorbed ligands, and so

addition of the adsorbing agent to the mobile phase is necessary for the latter [97]. The final two categories involve column fabrication by the polymerization of organic polymers [98, 99] (organic polymer-based) and inorganic alkoxides [100, 101] (sol-gel coatings). These processes are congruent with the methods used for the generation of monolithic columns (see following section), except the process is limited to the coating of the walls with a porous layer as opposed to generating a continuous bed that occupies the entire volume of the capillary. These columns proved to promote the most retention due to an increase in surface area, while the adsorbed columns are the easiest to produce.

### Fritless Columns (Monoliths)

Monolithic columns are composed of a continuous piece of macroporous material cross linked to the inner walls of a fused-silica capillary. This porous network provides high surface area and functionality that can be tailored to a desired separation problem. The majority of monoliths are created by the *in situ* polymerization of monomers (also called rods). The high permeability of these monoliths generates back pressures that are three times lower than that of a packed bed and, since the “backbone” of the skeleton is attached to the inner walls of the capillary, monolithic columns do not require retaining frits that can lead to bubble formation. These monoliths have been applied to a variety of applications and are classified as either inorganic or organic polymer-based. Since the work of this dissertation was accomplished using inorganic polymer-based monoliths using the sol-gel process, an in depth discussion is provided in Chapter II. Therefore, only polymer-based monoliths will be presented at this time in the following section.



Organic polymer monoliths Organic polymer-based monoliths are created by a one step polymerization of an organic monomer in the presence of a cross-linker, initiator and porogenic mixture of solvents [102-104]. The concentration of the cross-linker can be adjusted to alter column porosity, and polymerization is usually initiated either by UV light or thermal treatment of a free radical. Polymerization proceeds until the polymer reaches a threshold of insolubility in the porogenic solvent, at which point the polymer precipitates and cross-links with other precipitated macroporous globules producing a three-dimensional organic network.

These organic monoliths can be classified as either soft or rigid. Soft gels involve polymerization within an aqueous environment and have mostly involved the use of acrylamide monomers [105, 106]. While successful, the use of these columns for reversed phase chromatography (RPC) separations is limited due to the number of desirable monomers that are soluble in water, and therefore rigid polymers prepared in the presence of organic solvents receive the most attention [104]. This area is dominated by the use of polystyrene [107, 108] and polymethacrylate polymers [102, 109]. Of particular interest is the use of these monomers for the generation of molecularly imprinted polymers (MIPs) [110]. In this process, monomeric units are combined with the desired template to produce site-specific imprints of the target molecule upon polymerization of the mixture. Due to the specific nature of this stationary phase, most applications have involved the selective separation of enantiomers [111, 112].

## Conclusions

This chapter has outlined the scope of this dissertation and presented some of the basic principles and fundamental equations that pertain to the works described in the remaining chapters. In addition to the presentation of the parameters used to evaluate electrochromatographic systems, instrument and column technologies were discussed to provide the reader with the background necessary to understand the development of CEC as a valid analytical separation technique.

## References

1. Colon, L.A., Guo, Y., Fermier, A., *Anal. Chem.* **1997**, 69, 461A-467A.
2. Dittmann, M.M., Wienand, K., Bek, F., Rozing, G.P., *LC-GC* **1995**, 13, 800-814.
3. Ross, G., Dittmann, M., Bek, F., Rozing, G., *Amer. Lab.* **1996**, 28, 34-38.
4. Grant, I.H., *Capillary Electrochromatography*, in *Capillary Electrophoresis*, K. Altria, Editor. 1996, Humana Press Inc.: Totowa, NJ. pp. 197-209.
5. Krull, I.S., Stevenson, R.L., Mistry, K., Swartz, M.E., *Capillary Electrochromatography and Pressurized Flow Capillary Electrochromatography: An Introduction*. 2000, HNB Publishing: New York, NY.
6. Strain, H.H., *J. Am. Chem. Soc.* **1939**, 61, 1292-1293.
7. Strain, H., Sullivan, J., *Anal. Chem.* **1951**, 23, 816-823.
8. Mould, D.L., Synge, R.L., *Analyst* **1952**, 77, 964-969.
9. Mould, D.L., Synge, R.L., *Biochem. J.* **1954**, 58, 571-585.
10. Pretorius, V., Hopkins, B.J., Schieke, J.D., *J. Chromatogr.* **1974**, 99, 23-30.
11. Jorgenson, J.W., Lukacs, K.D., *J. Chromatogr.* **1981**, 218, 209-216.
12. Jorgenson, J.W., Lukacs, K.D., *Anal. Chem.* **1981**, 53, 1298-1302.
13. Tsuda, T., Nomura, K., Nakagawa, G., *J. Chromatogr.* **1982**, 248, 241-247.
14. Tsuda, T., *Anal. Chem.* **1988**, 60, 1677-1680.
15. Knox, J.H., Grant, I.H., *Chromatographia* **1987**, 24, 135-143.
16. Knox, J.H., *Chromatographia* **1988**, 26, 329-337.
17. Knox, J.H., McCormack, K.A., *J. Liq. Chromatogr.* **1989**, 12, 2435-2470.
18. Knox, J.H., Grant, I.H., *Chromatographia* **1991**, 32, 317-328.

19. Colon, L.A., Reynolds, K.J., Alicea-Maldonado, R., Fermier, A.M., *Electrophoresis* **1997**, 18, 2162-2174.
20. Colón, L.A., Burgos, G., Maloney, T.D., Cintron, J.M., Rodriguez, R.L., *Electrophoresis* **2000**, 21, 3965-3993.
21. Dadoo, R., Yan, C., Zare, R.N., Anex, D.S., Rakestraw, D.J., Huz, G.A., *LC-GC* **1997**, 15, 630-635.
22. Dittmann, M.M., Rozing, G.P., Ross, G., Adam, T., Unger, K.K., *J. Cap. Elec.* **1997**, 4, 201-212.
23. Overbeek, J.T.G., *Colloid Science*. 1952, Elsevier: New York, pp. 194-203.
24. Rathore, A.S., *Electrophoresis* **2002**, 23, 3827-3846.
25. Rathore, A.S., Horvath, C., *J. Chromatogr. A* **1997**, 781, 185-195.
26. Rathore, A.S., Horvath, C., *Capillary Electrochromatography*, in *Journal of Chromatography Library*, Z. Deyl and F. Svec, Editors. 2001, Elsevier: Amsterdam, pp. 1-38.
27. Choudhary, G., Horvath, C., *J. Chromatogr. A* **1997**, 781, 161-183.
28. Wen, E., Rathore, A.S., Horvath, C., *Electrophoresis* **2001**, 22, 3720-3727.
29. Yang, C., El Rassi, Z., *Electrophoresis* **1999**, 20, 18-23.
30. Giddings, J.C., *Unified Separation Science*. 1991, New York: Wiley.
31. Smith, N.W., Evans, M.B., *Chromatographia* **1995**, 4, 197-203.
32. Xiang, R., Horvath, C., *Anal. Chem.* **2002**, 74, 762-770.
33. Grimes, B.A., Liapis, A.I., *J. Col. Inter. Sci.* **2001**, 234, 223-243.
34. Grimes, B.A., Liapis, A.I., *J. Chromatogr. A* **2001**, 919, 157-179.
35. Rathore, A.S., Horvath, C., *Electrophoresis* **2002**, 23, 1211-1216.

36. Rathore, A.S., Wen, E., Horvath, C., *Anal. Chem.* **1999**, 71, 2633-2641.
37. Wen, E., Asiaie, R., Horvath, C., *J. Chromatogr. A* **1999**, 855, 203-216.
38. Steiner, F., Scherer, B., *J. Chromatogr. A* **2000**, 887, 55-83.
39. Banholczer, A., Pyell, U., *J. Microcol. Sep.* **1998**, 10, 321-328.
40. Chen, H., Horvath, C., *Anal. Methods Instrum.* **1995**, 2, 122-128.
41. Ross, G., Kaltenbach, P., Heiger, D., *Today's Chemist at Work* 1997, 6, 31-36.
42. Heiger, D.N., Kaltenbach, P., Sievert, H.-J., *Electrophoresis* **1994**, 15, 1234-1247.
43. Bruin, G.J.M., Tock, P.P.H., Kraak, J.C., Poppe, H., *J. Chromatogr. A* **1990**, 517, 557-572.
44. Rebscher, H., Pyell, U., *J. Chromatogr. A* **1996**, 737, 171-180.
45. Yan, C., Schaufelberger, D., Erni, F., *J. Chromatogr. A* **1994**, 670, 15-23.
46. Gfroerer, P., Schewitz, J., Pusecker, K., Bayer, E., *Anal. Chem.* **1999**, 71, 315A-321A.
47. Pusecker, K., Schewitz, J., Gfroerer, P., Tseng, L.-H., Albert, K., Bayer, E., Wilson, I.D., Bailey, N.J., Scarfe, G.B., Nicholson, J.K., Lindon, J.C., *Anal. Comm.* **1998**, 35, 213-215.
48. Pusecker, K., Schewitz, J., Gfroerer, P., Tseng, L.-H., Albert, K., Bayer, E., *Anal. Chem.* **1998**, 70, 3280-3285.
49. Schewitz, J., Gfroerer, P., Pusecker, K., Tseng, L.-H., Albert, K., Bayer, E., Wilson, I.D., Bailey, N.J., Scarfe, G.B., Nicholson, J.K., Lindon, J.C., *Analyst* **1998**, 123, 2835-2837.
50. We, J.-T., Qian, M.G., Li, J.X., Zheng, K., Huang, P., Lubman, D.M., *J. Chromatogr. A* **1998**, 794, 377-389.

51. Warriner, R.N., Craze, A.S., Games, D.E., Lane, S.J., *J. Rapid Commun. Mass Spectrom.* **1998**, 12, 1143-1149.
52. Špikmans, V., Lane, S.J., Tjaden, U.R., Van Der Greef, J., *J. Rapid Commun. Mass Spectrom.* **1999**, 13, 141-149.
53. Rentel, C., Gfrorer, P., Bayer, E., *Electrophoresis* **1999**, 20, 2329-2336.
54. Palmer, M.E., Clench, M.R., Tetler, L.W., Little, D.R., *Rapid Commun. Mass Spectrom.* **1999**, 13, 256-263.
55. Ludtke, S., Unger, K.K., *Chimia* **1999**, 53, 498-500.
56. Lord, G.A., Gordon, D.B., Myers, P., King, B.W., *J. Chromatogr. A* **1997**, 768, 9-16.
57. Lane, S.J., Tucker, M.G., *Rapid Commun. Mass Spectrom.* **1998**, 12, 947-954.
58. Bayer, E., Gfrorer, P., Rentel, C., *Angew. Chem.* **1999**, 38, 992-995.
59. Von Brocke, A., Wistuba, D., Gfrorer, P., Stahl, M., Schurig, V., Bayer, E., *Electrophoresis* **2002**, 23, 2963-2972.
60. Schurig, V., Mayer, S., *J. Biochem. Biophys. Methods* **2001**, 48, 117-141.
61. Mayer, S., Wachs, T., Henion, J.D. in *46th ASMS Conference on Mass Spectrometry and Allied Topics*. 1998. Orlando, FL, USA.
62. Que, A.H., Novotny, M.V., *Anal. Chem.* **2002**, 74, 5184-5191.
63. Que, A.H., Mechref, Y., Huang, Y., Taraszka, J.A., Clemmer, D.E., Novotny, M.V., *Anal. Chem.* **2003**, 75, 1684-1690.
64. Que, A.H., Novotny, M.V., *Anal. Bioanal. Chem.* **2003**, 375, 599-608.
65. Fu, H., Huang, X., Jin, W., Zou, H., *Current Opinion in Biotechnology* **2003**, 14, 96-100.

66. Lim, C.-K., Lord, G., *Pharm. Bull.* **2002**, 25, 547-557.
67. Cahours, X., Cherkaoui, S., Rozing, G., Veuthey, J.-L., *Electrophoresis* **2002**, 23, 2320-2326.
68. Krull, I.S., Sebag, A., Stevenson, R., *J. Chromatogr. A* **2000**, 887, 137-163.
69. Hearn, M.T.W., *Biologicals* **2001**, 29, 159-178.
70. Stahl, M., Jakob, A., Von Brocke, A., Nicholson, G., Bayer, E., *Electrophoresis* **2002**, 23, 2949-2962.
71. Gaspari, M., Gucek, M., Walhagen, K., Vreeken, R.J., Verheij, E.R., Tjaden, U.R., Van der Greef, J., *J. Microcol. Sep.* **2001**, 13, 243-249.
72. Colon, L.A., Maloney, T.D., Fermier, A.M., *Packed bed column*, in *Capillary Electrochromatography*, Z. Deyl and F. Svec, Editors. 2001, Elsevier: Amsterdam, pp. 113-164.
73. Chen, Y., Gerhardt, G., Cassidy, R., *Anal. Chem.* **2000**, 72, 610-615.
74. Schmid, M., Bauml, F., Kohne, A.P., Welsch, T., *J. High Resolut. Chromatogr.* **1999**, 22, 438-442.
75. Chen, J.-R., Dulay, M.T., Zare, R.N., Svec, F., Peters, E., *Anal. Chem.* **2000**, 72, 1224-1227.
76. Choudhary, G., Horvath, C., Banks, J.F., *J. Chromatogr. A* **1998**, 828, 469-480.
77. Behnke, B., Johansson, J., Zhang, S., Bayer, E., Nilsson, S., *J. Chromatogr. A* **1998**, 818, 257-259.
78. Carney, R.A., Robson, M.M., Bartle, K.D., Myers, P., *J. High Resolut. Chromatogr.* **1999**, 22, 29-32.
79. Yang, C., El Rassi, Z., *Electrophoresis* **1998**, 19, 2061-2067.

80. Zhang, M., Yang, C., El Rassi, Z., *Anal. Chem.* **1999**, 71, 3277-3282.
81. Smith, N., Evans, M.B., *J. Chromatogr. A* **1999**, 832, 41-54.
82. Walhagen, K., Unger, K.K., Olsson, A.M., Hearn, M.T.W., *J. Chromatogr. A* **1999**, 853, 263-275.
83. Zhang, M., El Rassi, Z., *Electrophoresis* **1998**, 19, 2068-2072.
84. Colon, L.A., Maloney, T.D., Fermier, A.M., *J. Chromatogr. A* **2000**, 887, 43-53.
85. Robson, M.M., Roulin, S., Shariff, S.M., Raynor, M.W., Bartle, K.D., Clifford, A.A., Myers, P., Euerby, M.R., Hohnson, C.M., *Chromatographia* **1996**, 43, 313-321.
86. Tang, Q., Xin, B., Lee, M.L., *J. Chromatogr. A* **1999**, 837, 35-50.
87. Fermier, A.M., Colon, L.A., *J. Microcol. Sep.* **1998**, 10, 439-447.
88. Maloney, T.D., Colon, L.A., *Electrophoresis* **1999**, 20, 2360-2365.
89. Inagaki, M., Kitagawa, S., Tsuda, T., *Chromatogr.* **1993**, 14, 55R-60R.
90. Stol, R., Mazereeuw, M., Tjaden, U.R., van der Greef, J., *J. Chromatogr. A* **2000**, 873, 293-298.
91. Pesek, J.J., Matyska, M.T., *Open tubular approaches to capillary electrochromatography*, in *Capillary Electrochromatography*, Z. Deyl and F. Svec, Editors. 2001, Elsevier: Amsterdam, pp. 241-270.
92. Swart, R., Kraak, J.C., Poppe, H., *Chromatographia* **1995**, 40, 587-593.
93. Tang, Q., Lee, M.L., *Trends Anal. Chem.* **2000**, 19, 648-663.
94. Pesek, J.J., Matyska, M.T., Menezes, S., *J. Chromatogr. A* **1999**, 853, 151-158.
95. Malik, A., *Electrophoresis* **2002**, 23, 3973-3992.
96. Liu, Z., Zou, H., Ni, J.Y., Zhang, Y., *Anal. Chim. Acta* **1999**, 378, 73-76.



97. Liu, Z., Wu, R., Zou, H., *Electrophoresis* **2002**, 23, 3954-3972.
98. Sawada, H., Jinno, K., *Electrophoresis* **1999**, 20, 24-30.
99. Šwart, R., Kraak, J.C., Poppe, H., *Trends Anal. Chem.* **1997**, 16, 332-342.
100. Constantin, S., Freitag, R., *J. Chromatogr. A* **2000**, 887, 253-263.
101. Hayes, J.D., Malik, A., *Anal. Chem.* **2001**, 73, 987-996.
102. Svec, F., Peters, E.C., Sykora, D., Frechet, J.M.J., *J. Chromatogr. A* **2000**, 887, 3-29.
103. Svec, F., *Capillary column technology: Continuous polymer monoliths*, in *Capillary Electrochromatography*, Z. Deyl and F. Svec, Editors. 2001, Elsevier: Amsterdam, pp. 183-240.
104. Hilder, E.F., Svec, F., Frechet, J.M.J., *Electrophoresis* **2002**, 23, 3934-3953.
105. Ericson, C., Hjerten, S., *Anal. Chem.* **1999**, 71, 1621-1627.
106. Hoegger, D., Freitag, R., *J. Chromatogr. A* **2001**, 914, 211-222.
107. Xiong, B.H., Zhang, L.H., Zhang, Y.K., Zou, H.F., Wang, J.D., *J. High Resolut. Chromatogr.* **2000**, 23, 67-72.
108. Zhang, S.H., Zhang, J., Horvath, C., *J. Chromatogr. A* **2001**, 189-200,
109. Yu, C., Xu, M.C., Svec, F., Frechet, J.M.J., *J. Polym. Sci., Part A: Polym. Chem.* **2002**, 40, 755-769.
110. Remcho, V.T., Tan, Z.J., *Anal. Chem.* **1999**, 71, 248A-255A.
111. Schewitz, L., Andersson, L.I., Nilsson, S., *Chromatographia* **1999**, 49, S93-S94.
112. Tan, Z.J., Remcho, V.T., *Electrophoresis* **1998**, 19, 2055-2060.

## CHAPTER II

### SILICA-BASED MONOLITHS FOR CAPILLARY ELECTROCHROMATOGRAPHY.

#### BACKGROUND AND RATIONALE FOR THE INVESTIGATION

##### Introduction

In Chapter I, the various column technologies utilized in CEC were introduced. While all have proven useful in their own right, each method has several disadvantages associated with it that prevent it from completely dominating the field. While providing high sample capacity and separation efficiency, packed columns suffer major difficulties associated with bubble formation resulting from the retaining frits. Frits introduce non-uniformity to the separation bed that exhibit different electroosmotic properties. This leads to a syringe effect that causes bubble formation, resulting in current breakdown. In addition, frits are difficult to reproduce and add to the fragility of the column. Open tubular columns, on the other hand, are very robust and easy to fabricate. However, they lack the surface area required for high sample capacity and retention. In addition, the relatively small optical path-length of the capillary limits the detection sensitivity. Incorporating thicker coatings of the bonded phase can enhance retention, but these films have proven difficult to reproduce [1].

In surveying the disadvantages associated with packed (p-CEC) and open tubular columns (OT-CEC), the need for column configurations that combined the strengths of these two methods became apparent. The best of both approaches would combine the high loading capacity of p-CEC with the high efficiency of OT-CEC without the need for fragile retention frits that can lead to bubble formation. All of these sound features could be combined in monolithic columns.

As previously mentioned in Chapter I, monolithic columns can be classified as either inorganic or organic polymer-based. Organic polymer monoliths have generated high separation efficiencies, but since polymerization is initiated using a free radical, they are somewhat difficult to reproduce. Furthermore, the presence of micropores within the polymer lead to a decrease in efficiency for small molecules [2] and extra care must be taken to prevent these monoliths from drying to eliminate solvent swelling effects.

Inorganic monoliths have been generated by the fusion of stationary phase particles, polymerization of transition metal alkoxide precursors using the sol-gel process and by cross-linking/entrapping particles in a packed bed using sol-gels. The following sections will provide a thorough background on the design and applications of these monoliths. Now, while monoliths have been generated using other transition metal oxide-based materials (e.g. zirconia [3, 4] and titania [5, 6]), silica-based monoliths comprise the bulk of interest for CEC separations, and therefore, will be the primary focus of this chapter.

## Silica-Based Monoliths

Silica-based monoliths include any column that incorporates one continuous piece (or rod) of porous silica. These can be generated by the polymerization of sol-gel precursors (sol-gel monoliths) [7] or by the immobilization of silica particles (particle-fixed monoliths) [8, 9]. The popularity of silica monoliths can be linked to the wide variety of highly characterized packing materials available, in addition to the availability of different chemistries that can be used for surface modification and ligand attachment. In this chapter, research reports on silica monolith design and their application to the separation of various compounds are first reviewed, and then the rationale of the investigation in this dissertation is presented.

### Particle-Fixed Monoliths

A valid approach to generating continuous silica bed columns has involved cementing bare or functionalized silica microparticles used as packing material in  $\mu$ -HPLC and CEC. Like traditional packed columns, these capillaries possess characterized silica particles that offer high phase ratio and narrow pore size distribution leading to high retention and separation efficiency, respectively. More importantly, immobilization of the microparticles stabilizes the separation bed and eliminates the need for retaining frits, thereby minimizing the difficulties associated with bubble formation. These columns are fabricated in exactly the same way as a packed capillary but with an additional immobilization step. This immobilization of the packed bed is usually

achieved by either thermal treatment or incorporation of sol-gel chemistry. Depending on the analysis, the resulting monolith may require sequential deactivation or functionalization steps.

Agglomeration of silica microparticles by thermal treatment Fabricating continuous beds by thermal treatment of packing materials involves the fusion of the porous silica particles at high temperatures (e.g., > 250 °C) in the presence of water. Usually an additive (e.g., NaHCO<sub>3</sub>) is included to facilitate the agglomeration of the microparticles. Sintering temperatures must be high enough to partially dissolve the silica particles, but low enough to prevent changes in the pore characteristics of the packing material [10]. Formation of the monolith is achieved when the grain boundaries of particles and the capillary wall are joined together after deposition of the previously dissolved silica upon cooling [11]. The resulting porous matrix provides a higher surface than its sol-gel counterpart without requiring the problematic frits used in traditional packed columns.

Despite the apparent advantages of these continuous bed columns, few papers have been published concerning this method. This may be due, in part, to the elaborate procedure involved. Asiaie *et al.* fabricated monolithic columns for CEC and  $\mu$ -HPLC by sintering octadecyl-silica in the presence of sodium bicarbonate, followed by rejuvenation of the octadecyl surface [8]. Sodium bicarbonate aids in agglomeration by wetting and partially dissolving the silica surface [10, 12]. Surface tension pulls the particles together to form interparticle boundaries that facilitate neck growth when thermally treated. Monoliths were generated by sintering at 260 °C and 360 °C without

and at 360 °C with sodium bicarbonate treatment. Particles were immobilized at 360 °C in both instances, and the presence of sodium bicarbonate greatly enhanced the stability of the packing material (2-3% variation in EOF velocity and 2% RSD for retention factor after 300 analyses). Columns were also fabricated by sintering bare silica instead of octadecyl-silica, followed by octadecylation. The retentive properties of each column were about the same, but, surprisingly, the columns made using bare silica displayed less stability and reproducibility than those made with octadecyl-silica. The authors suggest that the water binding ability of bare silica prevents it from being completely dehydrated during the drying step. During the sintering process, sudden bursts of water vapor could lead to bed rupture and concomitant gapping that destabilizes the monolith.

Electroosmotic and chromatographic properties were also investigated [8]. Electroosmotic mobility ( $\mu_{eo}$ ) increased with acetonitrile content at constant field strength for the octadecylated open capillaries and monoliths. However, for open bare silica capillaries an opposite trend was observed [8]. These findings indicate that EOF is not solely dependent on the properties of the bulk mobile phase (e.g., dielectric constant and viscosity). Rather, an organic modifier can have different effects on the accessibility of silanol groups located on bare and octadecylated silica surfaces. The octadecylated monolith achieved baseline separation of six polycyclic aromatic hydrocarbons (PAHs) in less than 6 min. In addition, six phenylthiohydantoin amino acids (PTH-AA) were separated in under 25 min at an acetonitrile concentration of 30% (v/v) [8].

The octadecylated monoliths were evaluated in both CEC and  $\mu$ -HPLC modes. Plots of the logarithmic retention factors for benzaldehyde and benzyl alcohol at the same conditions for both modes were almost identical, indicating that the presence of an

electric field had little or no effect on their retention [8]. Plots of the plate height versus the linear velocity showed that the  $A$  and  $C$  terms of the van Deemter equation were larger by a factor of 2.7 and 1.5 in  $\mu$ -HPLC than in CEC, respectively. Furthermore, the minimum plate height observed was twice as large for  $\mu$ -HPLC (16  $\mu\text{m}$  compared to 8  $\mu\text{m}$  for CEC) [8]. The van Deemter plots for different acetonitrile concentrations showed a decrease in slope with increasing concentration. Since the slope represents the  $C$  term of the van Deemter equation, this suggests that the intraparticle diffusion rate increases with decreasing viscosity.

A novel method for the immobilization of reversed-phase silica microparticles involving hydrothermal treatment with a moveable-heating coil has been introduced [9]. The process involves packing of the capillary, immobilization of the particles with a moveable-heating coil in the presence of water, and subsequent removal of the unbound particles. It is assumed that the temperature in the heated zone (ca. 300-400  $^{\circ}\text{C}$ ) partially dissolves the silica, causing it to become saturated. Immobilization occurs when the solution cools and silica is redeposited at the interstices between the particles and the capillary wall. The temperature and rate of movement of the heating coil are adjusted to insure that the polyimide layer on the outside of the capillary is unaffected and that any changes in the chromatographic properties are minimal. Two heating coil cycles were necessary to immobilize the particles, producing a separation efficiency of 220,000 plates/m for thiourea, but additional heating cycles increased peak tailing and lowered the efficiency (8 cycles: 160,000 plates/m) [9]. As a result of the EOF plug-flow profile, detection windows could be burnt at distances up to 4 cm from the packed bed without a significant loss in efficiency. In addition to maintaining retention time and plate number

over 300 injections, these columns were able to separate a mixture of 16 PAHs in about 20 min and a mixture of 11 herbicides in about 8 min [9].

Wistuba and Schurig [13] were able to achieve the separation of a variety of chiral compounds using a cyclodextrin-modified monolith. Bare silica microparticles were immobilized by sintering at 380 °C in the presence of Na<sub>2</sub>CO<sub>3</sub>, followed by polymer coating with a 5-10% solution of Chirasil-Dex at 235 °C. Chirasil-Dex is a permethylated β-cyclodextrin, and it is believed that immobilization is accomplished through reaction of its residual Si-H moieties with free silanol groups on the silica monolith. Due to the low electroosmotic velocity generated by the columns, analyses were performed with pressure support. A 12-bar pressure assisted analysis of mephobarbital enantiomers resulted in a substantial decrease in efficiency (from 88,400 to 50,600 plates/m) and a slight decrease in resolution (from 1.97 to 1.72) with no effect on the chiral separation factor ( $\alpha = 1.26$ ) [13]. Analyses performed under LC conditions (12 bar) resulted in elution times that were about 4.5 times longer with comparable separation and resolution factors illustrating the substantial contribution of EOF in the pressure assisted mode. At equivalent linear flow velocities, pressure assisted CEC exhibited a separation efficiency that was 2-2.5 times higher than the LC mode [13]. The monoliths displayed high stability (a 3% decrease in resolution of hexobarbital enantiomers after a 4-month operation period) as well as broad applicability for chiral compounds.

Entrapment/bonding of particles using sol-gels Immobilizing the packing material within a sol-gel matrix has also generated fixed particle monoliths. These



monoliths are referred to as “particle loaded” and can be accomplished by introducing the gelling reagents during or after the packing process. In the former case, slurry composed of stationary phase particles suspended in the sol-gel precursor is introduced into a capillary and allowed to cure, thereby entrapping the particles within the porous sol-gel network. Cavities within the network are large enough to allow the interaction of analytes with the sorbent particles, yet small enough to prevent movement of the particles themselves. In the latter case, the sol-gel solution performs more of a gluing function in immobilization by cross-linking the densely packed particles with the capillary wall and one another. In both instances, the presence of the particles alleviates the shrinking and cracking observed for columns generated by the sol-gel process alone, resulting in increased separation efficiency.

*Design and characterization* Dulay and coworkers [14] produced a particle loaded monolith by heating a capillary filled with a slurry composed of octadecylated silica (ODS) particles suspended in tetraethylorthosilicate (TEOS) and ethanol. Bare silica was also added to the solution to improve and stabilize EOF [15]. The presence of the ODS particles reduces fracturing of the matrix by decreasing pressure gradients in the pores. Slurries containing relatively high concentrations of ODS particles resulted in decreased selectivity due to inhomogeneities in the packing density. Analysis of a probe mixture was performed to compare columns containing only the sol-gel with columns made using 3 and 5  $\mu\text{m}$  diameter particles (Columns 1 and 2, respectively). No separation was observed for the column containing only sol-gel, whereas column 1 exhibited higher retention and separation efficiency than column 2 ( $k' = 0.40$  compared

to 0.15;  $N = 80,400$  compared to  $32,800$  plates/m for naphthalene). Difference in retention is a result of an increase in phase ratio for column 1. The authors attribute the overall modest separation efficiency of both columns to a “shielding” effect between the analytes and the ODS particles imbedded in the sol-gel network.

A thorough investigation of the permeability, band broadening and electrical properties of these kinds of columns has been reported by a separate group [16, 17]. Columns with an effective length of 21.5 cm and a total length of 30 cm were fabricated; each possessing different packed segments containing sol-gel bonded,  $3 \mu\text{m}$  ODS particles. The specific permeability  $B_0$  of the separation bed was almost 8 times greater than a column packed with  $3 \mu\text{m}$  particles alone ( $B_0 = 7.0 \times 10^{-14} \text{ m}^2$ ), thereby allowing pressures as low as 69 kPa to be applied for  $\mu\text{-LC}$  separations on columns 10 cm in length [16]. Resistivities of the packed segments were approximately 3 times greater than open segments ( $150 \Omega/\text{m}$  compared to  $52 \Omega/\text{m}$ ). The ratio of field strength for each open and packed segment was a constant 0.62, indicating the constant tendency for the accompanying increase in flow velocity of the packed bed ( $u = 0.16$  and  $0.09 \text{ cm/s}$  for packed and open segments, respectively). Optimum mobile phase velocities in terms of plate height were  $0.54 \text{ mm/s}$  for CEC (corresponding to 5 kV) and  $0.20 \text{ mm/s}$  for  $\mu\text{-LC}$ . The resulting plate heights were  $9.4$  and  $14.7 \mu\text{m}$ , respectively. Velocities exceeding these values led to a rapid decrease in efficiency attributed to a tortuosity effect in the inter- and intra-particle voids [17].

A thorough investigation on the effects of pH, buffer concentration, electric field strength and organic content on EOF for various particle loaded columns has been reported by Tang et al. [18-21]. In each instance, columns were packed with supercritical

CO<sub>2</sub> and subsequently immobilized with a sol solution containing both tetramethoxysilane (TMOS) and ethyltrimethoxysilane (ETMOS). ETMOS was used to end-cap the TMOS backbone with inert ethyl groups. This was possible because the rate of polycondensation was more rapid for TMOS than ETMOS. Incorporating ETMOS resulted in low asymmetry factors, thereby eliminating the need for post-deactivation or functionalization. Finally, separation beds were dried with supercritical CO<sub>2</sub> to prevent cracking resulting from capillary stress.

Columns loaded with either 7 μm ODS (4000 Å) [19, 20], 5 μm ODS (90 Å) [18, 21], 3 μm ODS (80 Å) [20], or 3 μm ODS/SCX (80 Å) [20, 21] particles were evaluated with PAHs and other small aromatic compounds. The mixed mode ODS/SCX particles were coated with octadecyl and propylsulfonic acid moieties [20, 21]. Columns fabricated with these particles produced a relatively constant EOF velocity in a pH range of 2-9 (approx. 1.9 mm/s at 884 V/cm), while the ODS particles of the same dimensions showed a steep decline in EOF velocity below pH 7 [20]. The van Deemter plots indicated an optimum EOF velocity of 0.92 mm/s (resulting in 175,000 plates/m) for the ODS/SCX particles [21], and in less than 6 min baseline separation was achieved for three corticosteroids [20].

The van Deemter plots were constructed for columns made with 3 and 7 μm ODS particles. While the 3 μm particles were able to furnish 180,000 plates/m, the 7 μm particles generated a maximum of 220,000 plates/m, not to mention an excess of 200,000 plates/m over a wide range of EOF velocities [20]. The large pores (4000 Å) present in the 7 μm particles were able to generate EOF, thereby eliminating stagnant mobile phase “pools” that can increase mass transfer resistance. Unfortunately, columns made with the

7- $\mu\text{m}$  particles exhibit one-tenth the retention compared to 3  $\mu\text{m}$  particles as a result of a decrease in surface area. However, baseline separation was achieved for 3 alkaloids on the 7  $\mu\text{m}$  ODS column in less than 12 min.

Comparisons were also made between packed and particle loaded columns made with 7  $\mu\text{m}$  particles [19]. The packed column was limited to field strengths  $< 400$  V/cm due to bubble formation. At equivalent field strengths, the sol-gel bonded separation bed possessed a 30% increase in EOF velocity with approximately one third of the current. In addition, the particle loaded column provided twice the maximum separation efficiency (220,000 plates/m) and a 30-60% increase in retention for equivalent analytes and conditions; indicating the sol-gel contributes to retention. The increase in efficiency for the sol-gel bed is a result of the partial filling of the interstitial space between the particles. This decrease in the interstitial space reduces mass transfer resistance in the mobile phase.

Chirica and Remcho produced silicate entrapped columns by rinsing packed columns with Kasil 2130 (pH 6) and heating gradually from 40  $^{\circ}\text{C}$  to 160  $^{\circ}\text{C}$  over a period of several days [22]. Particles were 5  $\mu\text{m}$  and were coated with either ODS or L-dansyl phenylalanine imprinted polymer. Analysis of PAHs on the ODS column resulted in capacity factors that were one third of those obtained for a non-entrapped column. This was due to pore occlusion and masking effects resulting from the sol solution. An enantiomeric separation of dansyl-phenylalanine was achieved with the MIP, resulting in a faster and more efficient analysis than the corresponding HPLC method. Overall, the particle loaded columns provided a higher EOF velocity and separation efficiency over those that were non-entrapped. The former is attributed to an increase in surface charge

density resulting from the silicate-entrapped matrix. The latter is attributed to a combination of decreased inter-particle channels that reduce Eddy diffusion, increased homogeneous charge distribution that minimizes diffusion in the radial direction and decreased retention that reduces diffusion and kinetic effects resulting from the stationary phase.

Chiral separations and non-aqueous CEC The monolithic stationary phases described above have been developed for use in reversed-phase CEC using hydro-organic mobile phases (e.g., mixtures of ACN-water). CEC is also useful for the separation of chiral species provided that the adequate chiral stationary phases are available. In this regard, Kato *et al.* modified their previous method of column fabrication [14] to obtain a high density of packing particles for the enantiomeric separation of amino acids [23]. Silica microparticles (5- $\mu\text{m}$ ) modified with (S)-*N*-3,5-dinitrobenzoyl-1-naphthyglycine (particle 1) or (S)-*N*-3,5-dinitrophenylaminocaronyl-valine (particle 2) were combined with 1  $\mu\text{m}$  bare silica particles and bonded by the sol-gel procedure. Thirteen amino acids and three non-protein amino acids were derivatized with 4-fluoro-7-nitro-2,1,3-benzoxadiazole and subsequently analyzed on columns made with particles of each type. All amino acids were baseline separated (except glutamic acid, Glu) on particle 1 at 5 mM phosphate (pH-2.5) in 70% acetonitrile, resulting in resolutions between 1.14 and 4.45. Resolution and plate height are superior to previously reported HPLC studies using the same particles [24]. Extended retention time and lowered resolution exhibited by Glu is attributed to an increase in nonsterioseleective interactions between unmodified amino groups on the particles and an additional carboxyl group located on Glu. Separations

involving particle 2 displayed substantially lower retention times under the same conditions. Even at optimal conditions, columns made with particle 2 displayed a significant decrease in performance when compared to columns fabricated with particle 1 because the moiety on particle 2 does not possess an electron-rich aromatic group that can form  $\pi$ - $\pi$  interactions with the amino acid label.

Not all species that can be separated by reversed-phase CEC can dissolve in hydro-organic mobile phases. This is the case of very hydrophobic compounds, such as retinyl esters, which require the use of non-aqueous mobile phases. To solve this separation problem, Roed *et al.* adopted Tang's method [19] of particle loading for the non-aqueous CEC separation of retinyl esters found in seal liver extract on columns loaded with endcapped 7  $\mu\text{m}$   $\text{C}_{18}$  [25] or 5  $\mu\text{m}$   $\text{C}_{30}$  particles [26]. An electric-field strength of 350 V/cm was selected to achieve optimum separation within a reasonable analysis time. The resulting EOF velocity (1 mm/s) allowed the use of longer columns for improved resolution [25]. Increasing the field strength led to a decrease in efficiency and resolution, while increasing the temperature from 40  $^{\circ}\text{C}$  to 60  $^{\circ}\text{C}$  resulted in higher separation efficiencies by reducing peak tailing [26]. In addition to an increased EOF velocity, these sol-gel bonded columns did not require time consuming conditioning steps necessary for their non-entrapped counterparts. Six trans-retinyl esters were baseline separated in less than 10 min using 2.5 mM lithium acetate in DMF-ACN-MeOH (2:7:1, v/v) on the  $\text{C}_{18}$  column. The  $\text{C}_{30}$  column achieved the same separation by increasing the temperature from 30  $^{\circ}\text{C}$  to 60  $^{\circ}\text{C}$ . While the  $\text{C}_{18}$  column provided better separation efficiency (reduced plate height = 1.9 compared to 3.9 for  $\text{RC}_{18:1}$ ), the  $\text{C}_{30}$  column

exhibited higher selectivity resulting in twice the resolution. In fact, the C<sub>30</sub> phase was able to achieve separation for cis-trans isomers of RC<sub>16:0</sub>.

### Sol-Gel Monoliths

Silica monoliths generated by the sol-gel process usually involves the catalytic hydrolysis, condensation and subsequent polycondensation of silica alkoxide precursors (e.g., tetramethoxysilane [TMOS], tetraethoxysilane [TEOS]) to form a macroporous gel network. These reactions can be catalyzed by acids [27, 28], bases [29, 30], ions [31, 32] or light [33, 34] and often incorporate the use of additives (e.g., polyethylene glycol, PEG) to manipulate phase separation and thus control macro-pore size and volume. Monoliths thus formed generally possess high throughpore-to-skeleton size ratios that can lead to a 10-fold improvement in column permeability as compared to packed columns in addition to providing high separation efficiency.

Figure 1 shows the reaction schemes involved in the sol-gel process using a silica alkoxide precursor in aqueous media [1]. First, the silica alkoxide is catalytically hydrolyzed whereby the alkoxide substituents are replaced with hydroxyl groups (1). These hydrolyzed products can undergo alcohol condensation with alkoxide moieties (2), or water condensation with other hydroxyl groups (3). The condensation and polycondensation reactions occur in parallel with the hydrolysis reaction at numerous sites in solution forming silica oligomers. These silica oligomers formed grow in size until they become sub-micron colloidal particles (i.e., sol) at which point they begin to impinge on one another and link together through random bonds. The gelation point is reached once

a single cluster expands throughout the sol. This “spanning cluster” coexists with the sol phase containing smaller clusters that eventually combine to form the macromolecular gel network [35].

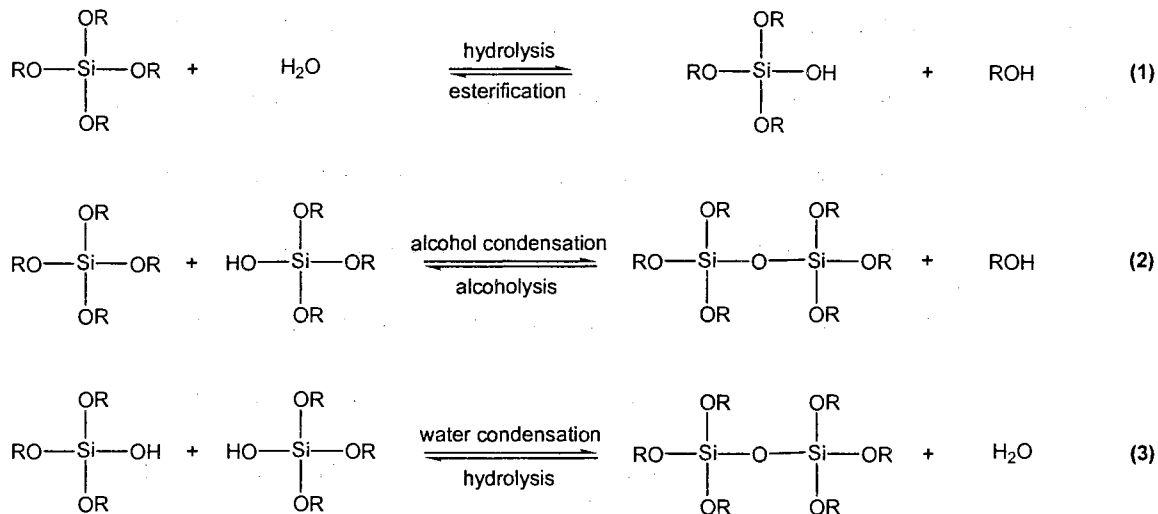


**Figure 1.** Hydrolysis and condensation reactions involved in the sol-gel process. Adapted from Ref. [1].

There are a variety of factors that influence the kinetics of reactions 1-3 and, ultimately, the morphology of the resulting gel. These include (but do not exclude): temperature, nature and concentration of catalyst, nature and concentration of solvent and type of alkoxide precursor [36]. One particular method of interest is the incorporation of additives in the sol mixture to induce phase separation (e.g., water soluble polymers and surfactants) [37]. For example, PEG forms strong hydrogen bonds with the silanols of the growing oligomers, thereby decreasing their solubility in solution. Macropore size can be manipulated by altering the PEG/silica ratio, while macropore volume can be independently manipulated by controlling the volume fraction of the solvent phase. For a more rigorous look into this concept, the reader is referred to the review written by Tanaka et al. [37].



The following is a brief overview of a typical procedure involved in generating these sol-gel monoliths. A pre-prepared sol solution is introduced into a pretreated fused-silica capillary. Pretreatment can be done hydrothermally, or by promoting ionization of the silanols using a basic rinse. The pretreatment is done to increase the surface concentration of reactive silanols to promote a high degree of cross-linking between the monolith and the capillary, thereby stabilizing the separation bed. After the gelation point is reached, the monolith is allowed to age in its pore liquid. At this time, the surface area of the sol-gel begins to decrease as a result of selective dissolution and precipitation. This is known as coarsening or “Ostwald ripening” and results from the fact that convex surfaces are more soluble than concave surfaces [38]. Many times this process is accelerated by exchanging the fluid phase of the gels in the “wet state” with solvents at  $\text{pH} > 8$  (i.e., pore tailoring) [39]. After aging, the gels are subsequently dried by evaporation (xerogel) or supercritical fluid (aerogel). Finally, the monoliths are stabilized by heat treatment at elevated temperature, making them ready for surface modification (i.e., stationary phase attachment).

#### Nonpolar sol-gel monoliths for reversed-phase CEC

*Design and characterization* Comparison of monolithic silica characteristics and performance in rod and capillary formats have been reported [40], in addition to evaluation of the capillary monoliths in pressure and electro-driven modes [40, 41]. These monoliths were formed by acetic acid catalysis of TMOS in the presence of PEG. Gelation was allowed to occur overnight, and the resulting monoliths were subsequently rinsed with aqueous  $\text{NH}_4\text{OH}$  to control mesopore size, dried with ethanol, and heat

treated at 330 °C. The size of the silica skeleton of the capillary monolith was  $\sim 2.2 \mu\text{m}$  with through-pore size of  $\sim 8 \mu\text{m}$  [41]. This resulted in through-pore size/skeleton size ratios in the range of 3-5, compared to 1-1.5 for silica rods and 0.25-0.40 for columns packed with  $5 \mu\text{m}$  particles [41]. The observed increase of this ratio is attributed to a lack of shrinkage caused by attachment to the capillary wall. Furthermore, the capillary monoliths were much more porous (total porosity = 96% of column volume), exhibited lower phase ratio (0.02-0.03, compared to 0.06 and 0.19 for a silica rod and particle packed column, respectively), and generated substantially lower back pressure at equivalent mobile phase velocities [40, 41]. As expected the capillary monolith provided much better separation efficiency in CEC mode compared to  $\mu$ -HPLC (80,000 and 24,000 plates/m for hexylbenzene, respectively). A steep slope in the van Deemter plot, in addition to a strong dependence of separation efficiency on retention for  $\mu$ -HPLC mode, indicated a slow mobile phase mass transfer resulting from the large through-pores of the monolith [41].

Kobayashi et al. [42] presented further evaluation of these kinds of columns in the CEC mode using a slightly modified preparation procedure. Instead of performing an  $\text{NH}_4\text{OH}$  rinse after gelation, urea was added to the sol solution. Mesopores were then modified in the presence of ammonia formed upon heating of the gel. Solutions of octadecyldimethyl-*N,N*-diethylaminosilane or octadecyltrichlorosilane reacted for 240 min (MS- $\text{C}_{18}$ (I)), 120 (MS- $\text{C}_{18}$ (II)), 60 (MS- $\text{C}_{18}$ (III)) and 30 min (MS- $\text{C}_{18}$ (IV)) were used to introduce various surface coverage of  $\text{C}_{18}$  ligand to the monolith. Separation efficiency and EOF velocity decreased with an increase in surface coverage of the bonded phase. For instance, the retention factor ( $k'$ ) for hexylbenzene on column MS-

C<sub>18</sub> (I) was 0.7, but only generated a separation efficiency of 72,000 plates/m at a linear velocity of 0.4 mm/s. Conversely, column MS-C<sub>18</sub> (III) generated a separation efficiency of 224,000 plates/m at 1.7 mm/s, but only provided a retention factor of 0.25 for hexylbenzene. Reaction with octadecyltrichlorosilane yielded an efficiency of 180,000 plates/m at 0.8 mm/s with a  $k' = 0.6$  for hexylbenzene. The van Deemter plots for each column displayed a decrease in plate height with an increase of linear velocity up to the upper limit of the instrument (30kV). The maximum plate count obtained was 240,000 plates/m for column MS-C<sub>18</sub> (IV) at ca. 1.4 mm/s. Column MS-C<sub>18</sub> (II) was able to separate 9 alkyl phthalates in less than 8 min at 20 kV assisted by a pressure of 20 psi. The pressure-assisted mode resulted in a 40% decrease in analysis time compared to the CEC mode, and a considerable improvement in separation efficiency compared to using pressure alone.

Fujimoto [43] implemented a slightly modified version of Tanaka's method [40] for fabricating capillary monoliths by using more concentrated NH<sub>4</sub>OH at longer reaction times and lower temperature. The resulting monolith was functionalized with C<sub>18</sub> ligands by reaction with dimethyloctadecylchlorosilane. The column exhibited high permeability (linear velocity of 0.63 mm/s at 1 atm) and an EOF velocity of 1.0 mm/s at a field strength of 546 V/cm. Methyl-, ethyl- and propylparaben were separated in less than 14 min at separation efficiencies of 112,800, 102,200 and 79,600 plates/m, respectively. Despite good run-to-run reproducibility (RSD = 0.2% for retention time of acetophenone), column efficiency was cut in half after 40 injections.

Meanwhile, Allen and El Rassi [44] thoroughly investigated several parameters in column fabrication to enhance column performance for the separation of neutral and

charged species (e.g., anilines, phenylthiohydantoin amino acids (PTH-AA) and dinitrophenyl amino acids (DNP-AA)). These investigations are the subject of chapter 3 of this dissertation, and are summarized here as follows. Systematic studies were performed to determine optimal conditions for pore tailoring and octadecyl bonding. For the C<sub>18</sub> coating step, it was determined that addition of 2,6-lutidine as an acid scavenger enhanced the coating process and that a reaction time of 4 hrs was all that was needed for maximum surface coverage. Optimization of the pore tailoring step involved examining columns fabricated at different reaction times with NH<sub>4</sub>OH. It was determined that an increase in reaction time first increased retention for the ABs up to 1.5 hrs and then gradually decreased the retention for these solutes up to 6 hrs, at which point retention drastically decreased as a result of a decrease in surface area. The van Deemter studies indicated that a reaction of 4.5 hrs was optimal in terms of maximum separation efficiency (160,000 plates/m) and overall separation efficiency over a wide range of mobile phase velocities. Thirteen out of 14 PTH-AAs injected could be separated on the monolithic column. PTH-arginine was the only species that possessed a positive charge and, therefore eluted before  $t_0$ . The remaining PTH-AA eluted in order of increasing hydrophobicity as expected for RPC.

A mix of 5 anilines and 16 DNP-AA were selected as test compounds for evaluating column performance for charged species. At acidic pH (~3.5) all anilines (except 3,4-dichloroaniline) were positively charged and eluted before  $t_0$  as a result of their co-directional electromigration with the EOF. To evaluate electrophoretic and chromatographic retention of a charged species, the authors [44] calculated the CEC retention parameters as described by Rathore and Horvath [45]. The retention parameters

were  $k_{cc}^*$ ,  $k_e^*$  and  $k^*$  which denote elution order, the contribution of electrophoretic mobility on the separation and chromatographic retention of the solutes, respectively. A sample containing 16 DNP-AA was also analyzed using negative potential at low pH (~4.5), whereby the analytes migrated towards the outlet end by overcoming the counter-directional EOF towards the inlet. Although chromatographic retention was evident in the separation (differences in elution order as compared to CZE mode), CEC retention factors could not be calculated as before since the analysis did not provide a value for  $t_0$  due to the reversal of EOF. Therefore, the authors introduced a mobility moduli expression where a decrease in value between the range of 0 and 1 would indicate increased chromatographic retention for the charged species.

Hayes and Malik applied the use of a quaternary amine sol-gel precursor to generate a silica-based monolith that exhibited electroosmotic flow reversal [46]. Trifluoroacetic acid catalyzed the sol-gel reaction of the precursors *N*-octadecyldimethyl- $\{3\text{-(trimethoxysilyl)propyl}\}$ ammonium chloride and TMOS. Since the resulting monolith possessed a positive charge on the surface, phenyldimethylsilane was added as a deactivating agent to the reaction mixture to end-cap any residual silanols that could interfere with the anodal EOF. In addition, analyses were run at acidic conditions (pH 2.34) to suppress the ionization of any silanols still present on the surface of the monolith. Electroosmotic mobility increased with an increase of organic modifier in the mobile phase, with a maximum mobility at ca.  $3.75 \times 10^{-4} \text{ cm}^2/\text{Vs}$  in 80% acetonitrile (v/v). A van Deemter plot was constructed for a range of mobile phase velocities corresponding to a potential range of  $-3$  to  $-19$  kV resulting in relatively flat curves for anthracene and naphthalene. Optimum linear velocity was 0.75 mm/s generating a plate

height of  $\sim 8$   $\mu\text{m}$ . Columns were evaluated with PAHs (145,000 plates/m for naphthalene), ABs (163,000 plates/m) and a mixture of aldehydes and ketones.

Sol-gel monoliths generated by photopolymerization of a silica monomer (3-trimethoxysilylpropylmethacrylate) in the presence of a catalyst (HCl) and a porogen (toluene) using a photoinitiator (Irgacure 1800) has been reported [34]. The photoinitiator was dissolved in toluene and subsequently added to a stock solution consisting of monomer and HCl. A stripe of polyimide coating is removed along a desired length of fused-silica capillary, and the sol solution is introduced. Upon irradiation with UV (365 nm), the photopolymerized sol-gel (PSG) is formed at the “unmasked” locations along the capillary corresponding to the stripe. No pre-treatment of the capillary is necessary and, since high temperatures are avoided, crack formation is minimal. In addition, an investigation on the effect of column length indicated that the PSG had little to no influence on conductance providing homogeneous field strength in open and packed segments and minimizing band broadening effects due to variations in EOF velocities [34].

The effects of altering HCl concentration and monomer to porogen ratio on monolith characteristics were investigated [47]. Increasing HCl concentration in the sol solution increased retention and column rigidity, which improved separation efficiency for test compounds. At concentrations of 0.001 M and 0.01 M not enough silanols were produced during hydrolysis to form the network. Increasing the monomer to porogen ratios decreased through-pore size, thereby increasing skeleton density and decreasing permeability. A 5% monomer solution only succeeded in coating of the walls of the capillary and was insufficient for the separation of the test solutes, while an 18%

monomer solution was the limit for columns that could still be rinsed by a syringe. A 10% monomer solution produced the fastest elution times (as a result of increased permeability) but exhibited lower retention than monoliths made with 15 and 18% monomer solutions. Despite a higher PSG content, the monolith made with 18% monomer solution provided similar retention to that of the monolith made with a 15% monomer solution, indicating similar surface areas. Sol-gels made with 10, 15 and 18% monomer solutions produced average separation efficiencies of 162,000, 149,000 and 37,000 plates/m, respectively, for a test mix composed of naphthalene, toluene and ethylbenzene. The authors then concluded that the 10 and 15% monomer solutions produced the best monoliths based on permeability, retention and separation efficiency [47].

Dulay et al. [48] introduced bonded-phases on the surface of their PSG for applications toward the separation of nucleosides and cationic peptides. Bonded phases of pentafluorophenylpropyldimethyl (PFPPDM), pentafluorophenyl (PFP), 3,3,3-trifluoropropyl ( $C_3F_3$ ), n-octadimethyl ( $C_8$ ), perfluorohexyl ( $CF_{13}$ ) and aminopropyl ( $NH_2$ ) were introduced by continuous rinsing at room temperature for no more than 90 min. Columns PSG- $C_3F_3$ , PSG- $CF_{13}$ , PSG-PFP, PSG- $C_8$  and PSG-PFPPDM all showed an improvement in resolution for APKs, compared to PSG alone. Column PSG-PFPPDM exhibited the most retention, while column PSG- $C_8$  provided a high level of retention and rapid EOF velocity. A study on the effect of silanization reaction time for the PSG- $C_8$  column indicated that a reaction time of 60 min was optimal in terms of resolution and selectivity. A mix of four nucleosides was separated by RPC in less than 14 min on column PSG- $NH_2$ . Analysis was performed in reverse polarity mode because the

monolith sustained a positive charge on the surface at the running conditions. In addition, four cationic peptides were separated on column PSG-PFPDM in less than 15 min, and a mixture of taxol, baccatin III and acetylbaccatin were baseline separated in less than 8 min on column PSG-C<sub>3</sub>F<sub>3</sub>.

Chip format The above chemistry was investigated for potential use in electrochromatography on a chip [49] created on a borosilicate glass plate (500  $\mu\text{m}$  thick x 100 mm wide). Channels 90  $\mu\text{m}$  wide and 35  $\mu\text{m}$  deep are connected to sample and buffer reservoirs (1.2 mm in diameter). A cover plate of equal thickness was thermally bonded to the microfluidic plate, and borosilicate glass tubes (100-150  $\mu\text{L}$ ) were glued over each reservoir. After filling all channels and wells with the sol solution, sections that were not masked with electrical tape were photopolymerized with UV in a black box for 5 min at 365 nm. Unreacted reagents were rinsed out, and the reservoirs were subsequently filled with the separation buffer and capped to prevent evaporation. A combination of potentials was applied to the reservoirs for sample introduction and separation. A baseline separation of coumarin 314 and coumarin 510 ( $R_s = 1.01$ ) was achieved in less than 80 s at an effective length of 1.2 cm, generating separation efficiencies of 21,300 and 6,100 plates/m, respectively [49]. The observed RSD for retention time was 3.13% for coumarin 314 and 5.18% for coumarin 510, while the RSD for resolution was 5.12% over 5 runs.

Use of nonpolar sol-gel monoliths in on-line preconcentration The principle of on-line preconcentration of dilute samples in CEC, which was first introduced and



investigated by Yang and El Rassi [50, 51] and then Tegeler and El Rassi [52, 53] using capillary columns packed with ODS microparticles, was later evaluated with sol-gel monolithic capillary columns. Quirino et al. [54, 55] applied the use of their photopolymerized sol-gel (PSG) columns to the pre-concentration of various samples. The PSG provided increased detection sensitivity with increases in injection plug length for PAHs, APKs, peptides and steroids [54]. For PAHs, a 27.4 mm injection plug resulted in peak height improvements that were 50, 125 and 127 times greater than an injection plug of 0.1 mm for naphthalene, phenanthrene, and pyrene, respectively. Similar increases in injection plug length for APKs provided peak height improvements in the range of 13-32 times on PSGs modified with (3,3,3-trifluoropropyl)trichlorosilane. For both sets of compounds, the degree of peak height enhancement (and peak width narrowing) was higher for more retained compounds indicating more efficient accumulation at the column inlet. To further evaluate pre-concentration, injection plug lengths for two different concentrations of naphthalene were adjusted to introduce equal amounts on the PSG. The amounts were confirmed by comparison of the corrected peak areas (peak area/migration time) for the concentrated and dilute samples (0.0023 and 0.0025, respectively). In comparing the corresponding peak heights (0.0869 and 0.0937, respectively), it became evident that pre-concentration had occurred. Pre-concentration of charged solutes was possible with the analysis of 5 separate peptides on a (pentafluorophenylpropyl)trichlorosilane modified PSG, and analysis of "real world" samples were performed on urine samples spiked with steroids [54].

Effects of solvent gradients and sample stacking on pre-concentration were also investigated [55]. Increasing concentration of the non-eluting solvent in the sample

matrix improved peak heights for all APKs up to 80% water (v/v) on pentafluorophenyl-bonded PSG. However, it was established that maximum peak height improvement occurred at 70% (v/v) water for acetophenone and propiophenone and 60% (v/v) water for the remaining APKs. This was due to a decrease in solubility of the analytes in highly aqueous sample matrices. Decreasing the acetonitrile concentration in the sample from 60% to 30% (v/v) resulted in peak height improvements that were 24-38 times better for the APKs. Studies were also performed on the limits of injection plug length. Only a slight decrease in resolution was observed for sample plugs equal to 91.2 cm (356% of total column length), which resulted in peak height improvements of 1118 and 1104 times for decanophenone and pyrene, respectively. The authors also demonstrated the effects of using solvent and concentration gradient on sample stacking for cationic peptides. In this case, increasing organic content and lowering buffer concentration in the samples accomplished sample stacking.

Ionic sol-gel monoliths for ion-exchange CEC – Chip CEC Breadmore *et al.* [56] designed ionic sol-gel monoliths for ion exchange CEC on a chip. In their investigation for microchip suitable sol-gels, the authors [56] examined the effect of using a high molecular weight, water-soluble polymer (100 kDa polyethylene oxide, PEO) on various column characteristics. The resulting monolith was compared to columns fabricated using a method developed by Tanaka's research group [41], which used 10 kDa PEO as an additive for macropore formation. While both columns provided equal surface area, the 100 kDa PEO gel exhibited a more open structure with increases in pore volume and pore diameter that resulted in a substantial decrease in back-pressure making it an attractive

option for microchip application. In examining the EOF properties of the two monoliths, the 100 kDa gel showed a decrease in EOF mobility with an increase in ionic strength, while the 10 kDa gel showed increases in EOF mobility with an increase up to 40 mM Tris, at which point EOF decreased as would be expected in theory. The increase for 10 kDa is due to a reduction in double layer overlap in the pores resulting from its compression at increasing ionic strength. This is not observed for 100 kDa because the greater number of macropores minimizes the micropore contribution to column flow. Poly(diallyldimethylammonium chloride) (PDDAC) was evaluated as both a dynamic and adsorptive coating for ion-exchange chromatography using organic anions as analytes. Reducing PDDAC concentration in the background electrolyte (BGE) only resulted in minor decreases in the mobility of the ions, indicating PDDAC adsorption predominates over pseudo-phase formation. The semi-permanent coating showed weak stability, however, since mobile phases without PDDAC required surface regeneration after 2 hours of operation. The dynamically coated 10 kDa gel exhibited higher retention than the coated 100 kDa gel as a result of increased capacity stemming from its smaller pores and closed structure.

Breadmore *et al.* [57] improved on their previous investigation of potential microchip sol-gels [56] discussed above, by constructing highly stable polyelectrolyte multilayers (PEMs) of PDDAC and dextran sulfate (DS) on the surface of their monoliths. These alternating layers of oppositely charged polyelectrolytes greatly enhance coating stability compared to single-layer varieties. Columns coated with a single layer of PDDAC showed decreases in EOF and anion mobilities after 22 runs, while the PEM columns showed no significant change after 100 consecutive separations.

EOF changed direction according to the last layer deposited as a result of alternating surface charge, but magnitude remained relatively constant regardless of polymer type or layer number. However, the retention factors for a group of inorganic anions increased by a factor of 1.7-1.8 going from the 1<sup>st</sup> PDDAC layer to the 8<sup>th</sup>, indicating an increase in capacity with increasing layer thickness. Ions were less retained with additional layers, possibly due to filling of the mesopores within the sol-gel. Increasing ionic strength decreased both EOF (33%) and retention of peptides in cation-exchange mode (i.e., DS as the exposed layer). The performance of Poly(sodium styrene-p-sulfonate) (PSS) as a negatively charged component of the PEMs was compared with DS by analysis of several peptides in cation-exchange mode. PSS showed a substantial increase in retention for all peptides studied, in addition to providing a stronger EOF ( $\mu_{eo} = 13.8 \times 10^{-9}$  compared to  $20.1 \times 10^{-9} \text{ m}^2/\text{Vs}$  for DS and PSS, respectively). In pure aqueous conditions, peptides were separated based on hydrophobic interactions as well as cation-exchange mechanisms. In addition, it is anticipated that molecular size may have an effect on retention with smaller molecules being able to access a higher number of ion-exchange sites within pores while larger molecules are restricted to sites on the outer surface of the monolith.

Chiral sol-gel monoliths for enantiomeric separations by CEC Several enantiomeric compounds have been separated by CEC using protein encapsulated sol-gel monoliths [33, 58, 59]. Phosphate buffer solutions of bovine serum albumin (BSA) [33, 58, 59], or ovomucoid (OVM) [33] were added to hydrolyzed sol solutions of TMOS to provide chiral selectivity. Methacryloxypropyltrimethoxysilane (MTMS) was used for

capillary pre-treatment, and was added to the sol solutions to investigate its assistance in encapsulation. Its presence improved enantioselective power for BSA, while diminishing enantioselectivity for the OVM encapsulated gels. Increasing BSA concentration in the sol solution resulted in improved chiral separation of DL-tryptophan (DL-Trp) at the expense of a decrease in EOF velocity. BSA encapsulated columns were able to completely resolve the Trp enantiomers ( $\alpha' = 1.12$ ) at separation efficiencies of 57,000 plates/m and 6,400 plates/m for the D (1<sup>st</sup> peak) and L (2<sup>nd</sup> peak) enantiomers, respectively. OVM encapsulated columns were able to completely resolve benzoin enantiomers ( $\alpha' = 1.07$ ) at separation efficiencies of 72,000 plates/m and 28,000 plates/m. In addition, OVM obtained chiral separation for eperisone ( $\alpha' = 1.19$ ) and chlorpheniramine ( $\alpha' = 1.23$ ). Overall the columns exhibited low column-to-column reproducibility with moderate run-to-run repeatability (RSD = 1.23 and 1.89% for retention time of benzoin enantiomers) [33].

In investigating the loadability of the BSA encapsulated monolith [58], it was determined that increasing DL-Trp concentration in the sample decreased enantiomer resolution. Conversely, increasing concentration of the running buffer increased enantioselectivity as a result of a reduction in non-specific electrostatic interactions with silanol groups that interfere with the separation and increasing pH of the mobile phase improved enantioselectivity as a result of a stronger EOF. At pH 5, BSA undergoes conformational changes and therefore, no separation was observed.

In examining the effect of several parameters on BSA encapsulation conditions, it was determined that EOF mobility of the resulting monoliths decreased with increases in reaction pH, ionic strength, buffer to sol ratio and BSA concentration [59]. These trends

were a result of a decrease in unreacted silanols on the surface of the monolith indicated by ATR-FT-IR measurements. In addition, increasing reaction pH deteriorated enantioselectivity of the columns. Since BSA is negatively charged at  $\text{pH} \geq 6$ , electrostatic repulsion between BSA and ionized silanol groups prevented efficient encapsulation. Enantioselectivity was enhanced by increasing MTMS concentration up to a limit of 30%, at which point columns exhibited low reproducibility. Studies involving dynamic light scattering and ATR-FT-IR indicated that the presence of BSA during gelation had little effect on the resulting gel structure and that BSA maintains its conformation, respectively.

Liu *et al.* [60] examined the effects of several parameters on the physical adsorption of avidin to silica monoliths for application in enantiomeric separations. Monoliths generated were activated with ammonia and subsequently rinsed with solutions of avidin, where its adsorption was achieved through both electrostatic and hydrophobic interactions. The adsorption proved to be relatively strong, obtaining column lifetimes of approximately 2 weeks before regeneration was needed. The surface coverage of avidin on a 20 cm x 50- $\mu\text{m}$  I.D. segment of capillary was estimated to be  $9.4 \times 10^{-9} \text{ mol/m}^2$ , or approximately 14% of the total surface area available on the monolith. The relatively low value is due to the fact that avidin cannot enter pores less than 5 nm, thereby making it unavailable to many pores in the sol-gel. This resulted in a very weak ( $t_0 > 60 \text{ min}$ ) EOF due to the counterbalance of positively charged avidin and negatively charged silanols on the surface of the monolith, and, therefore, analyses in CEC mode were limited to basic and acidic compounds. These columns showed a significant improvement for the separation of flurbiprofen and 4-fluoromandelic acid enantiomers

when compared to their analysis in OT-CEC columns made by the same method. Also, in CEC mode, baseline separation of two pairs of chrysanthemic acid enantiomers was achieved in less than 4 min at separation efficiencies between 126,000-224,000 plates/m. The authors also used field-enhanced sample injection to pre-concentrate these chrysanthemic acid enantiomers exhibiting a 20-24 folds peak area improvement in CEC mode.

Silica monoliths coated with Chirasil- $\beta$ -Dex for enantiomeric separation of several chiral compounds have been reported [61]. The sol-gel monoliths were generated according to the method developed by Tanaka *et al.* [41] and then modified by immobilization of the cyclodextrin to the surface. A van Deemter plot generated by the analysis of hexobarbital produced very similar separation efficiencies over a relatively broad range of mobile phase velocities (up to 92,200 plates/m), while resolution decreased with an increase in flow rate. In addition, increasing buffer and methanol concentration decreased EOF velocity, which resulted in a decrease of resolution as well. Baseline separation of the enantiomers mephobarbital, hexobarbital, benzoin and carprofen were accomplished within 23, 20, 32 and 42 min, respectively.

Chen and Hobo were able to achieve chiral separation for dansyl amino acids (Dns-AA) [62, 63] and hydroxy acids [62] using enantioselective monoliths having the chiral selectors, L-prolinamide [62] and L-phenylalaninamide [63] immobilized to the surface of a sol-gel monolith. Ligand attachment was the result of their reaction with epoxide moieties previously introduced with 3-glycidoxypropyltrimethoxysilane. Both were conditioned with  $\text{CuSO}_4$  so that the resulting Cu(II)-ligand complexes could form Cu(II) complexes of differing stability with analytes as a result of ligand exchange,

thereby promoting their separation. The presence of the  $\text{Cu}^{2+}$  on the surface resulted in an anodal EOF. Since all analytes possessed a negative charge under the analysis conditions, the solutes exhibited co-directional mobilities with the EOF and eluted before  $t_0$  in reversed polarity mode. For both stationary phases, EOF mobility increased linearly with field strength, decreased with an increase in pH and decreased with an increase in acetonitrile content. In addition, EOF increased with an increase in Cu(II) concentration [63]. Altering pH provided both increases and decreases for the different sets of enantiomers, and therefore the authors suggested a working pH in the range of 5.5-7.5 to provide sufficient EOF [63]. Altering organic content gave mixed results as well. In some instances, slowing EOF by increasing acetonitrile content of the mobile phase resulted in an increase in separation factor due to longer interactions with the stationary phase. However, since increasing acetonitrile content also results in decreasing the polarity of the mobile phase, analytes with hydrophobic moieties (e.g., Dns groups) showed a decrease in interaction with the chiral selectors. Since the hydroxy acids do not possess any significant hydrophobic groups, this particular phenomenon was not observed [62]. The L-prolinamide-modified column was able to separate enantiomers of 8 separate chiral hydroxy acid pairs and 9 separate Dns-AA pairs with separation factors in the range of 1.00-1.23 and 1.00-2.00, respectively. With the exception of the pairs Dns-DL-Phe and Dns-DL-Trp, the L-phenylalaninamide-modified column obtained superior enantiomeric separation of the Dns-AA in terms of separation factor, but exhibited longer analysis times [63].



## Rationale of the Investigation

A critical evaluation of the above comprehensive review of the development of silica-based monoliths specially designed for CEC reveals that this area of research, which involves the heart of the chromatographic process, has witnessed some major activities in the design of nonpolar and chiral monoliths for use in reversed-phase and chiral CEC, respectively. Although these research activities brought about significant progress in the development of CEC, the exploitation of the full potential of the concept of silica monoliths in CEC separations is yet to come. Thus far, most of the studies have focused on the optimization of the silica monolith backbone in terms of porosity, stability, permeability and surface modification with nonpolar ligands. However, no systematic studies exist on pore tailoring, a process in which micropores are converted into mesopores, in order to yield monolithic columns with high separation efficiencies. Moreover, virtually none of the published studies on monolithic silica involved quantitative evaluation of the retention parameters of charged solutes. The present dissertation addresses these deficiencies in Chapter III by studying the pore tailoring reaction and evaluating the CEC retention parameters of weak acids and bases with well-characterized nonpolar sol-gel monoliths.

Most of the nonpolar monolithic silica columns bearing octadecyl ligands have relied on the residual, unreacted surface silanols to support the EOF necessary for moving the mobile phase across the monolithic capillary column bringing about differential migration of the partitioning solutes. However, the silanol groups are weak acids, and can only produce sufficient EOF at mobile phase  $\text{pH} > 5$ , a fact that limits the utility of

monolithic silica columns to a narrow pH range. Also, nonpolar monolithic silica columns are not ideal media for separating large proteins by a reversed phase mechanism, due to strong protein binding to the stationary phase by electrostatic interactions with the ionized silanol groups. To overcome both shortcomings, stationary phases that exhibit strong EOF and minimum electrostatic interactions with proteins are urgently needed. Besides one contribution that describes the preparation of a positively charged octadecyl sol-gel monolith [46], systematic studies on producing amphiphilic sol-gel monoliths with relatively strong EOF are lacking. Thus, it is the aim of Chapter IV to fill in the gap by describing 3 different ways to produce amphiphilic sol-gel monoliths bearing fixed positive charges and octadecyl ligands on their surface. In addition, Chapter IV reports for the first time the retention parameters of proteins in CEC.

Furthermore, an inspection of the comprehensive review provided in this chapter shows that polar silica sol-gel monoliths are not yet available for performing normal phase CEC (NP-CEC) for the separation of polar compounds by CEC. This lack of polar monolithic silica columns is addressed in Chapter V, which introduces two different methods to produce polar sorbents for NP-CEC of a wide range of polar solutes including mono- and oligosaccharides.

In summary, the present dissertation has addressed problems whose solution has been required for further progress in CEC. In addition to filling in some of the existing gaps, this investigation also demonstrated the potentials of CEC in some significant separations, namely anilines, derivatized amino acids, nucleic acid bases and nucleosides, mono- and oligosaccharides and proteins. This helped yield a better understanding of the electrochromatographic behaviors of neutral and charged species.

## Conclusions

This chapter has provided a comprehensive review of the advances made in the preparation and use of monolithic silica-based stationary phases in CEC separations. While some major progress has been made in developing the silica monolith backbone, there are still needs for investigating the attachment of specific ligands to the silica skeleton in order to yield novel stationary phases, which will eventually find use in solving many separation problems in the life sciences.

## References

1. Malik, A., *Electrophoresis* **2002**, *23*, 3973-3992.
2. Tanaka, N., Ebata, T., Hashizume, K., Hosoya, K., Araki, M., *J. Chromatogr. A* **1989**, *475*, 195-208.
3. Minesso, A., Genna, F., Finotto, T., Baldan, A., Benedetti, A., *J. Sol.-Gel Sci. Technol.* **2002**, *24*, 197-206.
4. Marinsek, M., Macek, J., Meden, T., *J. Sol.-Gel Sci. Technol.* **2002**, *23*,
5. Yusuf, M.M., Imai, H., Hirashima, H., *J. Sol.-Gel Sci. Technol.* **2002**, *25*, 65-74.
6. Yu, J., Ju, H., *Anal. Chem.* **2002**, *74*, 3579-3583.
7. Tanaka, N., Kobayashi, H., *Capillary electrochromatography on monolithic silica columns*, in *Capillary Electrochromatography*, Z. Deyl and Svec, F., Editors. 2001, Elsevier: Amsterdam. pp. 165-181.
8. Asiaie, R., Huang, X., Farnan, D., Horvath, C., *J. Chromatogr. A* **1998**, *806*, 251-263.
9. Adam, T., Unger, K.K., Dittmann, M.M., Rozing, G.P., *J. Chromatogr. A* **2000**, *887*,
10. German, R.M., *Ceramics and Glasses, Engineered Materials Handbook*. 1987, ASM International, p. 260.
11. Moulson, A.J. Herbert, J.M., *Electroceramics*. 1992, Chapman and Hall: London, p. 100.
12. German, R.M., *Liquid Phase Sintering*. 1985, Plenum Press: London.
13. Wistuba, D., Schurig, V., *Electrophoresis* **2000**, *21*, 3152-3159.

14. Dulay, M.T., Kaularni, R.P., Zare, R.N., *Anal. Chem.* **1998**, *70*, 5103-5107.
15. Dulay, M.T., Yan, C., Rakestraw, D.J., Zare, R.N., *J. Chromatogr. A* **1996**, *725*, 361-366.
16. Ratnayake, C.K., Oh, C.S., Henry, M.P., *J. High Resolut. Chromatogr.* **2000**, *23*, 81-88.
17. Ratnayake, C.K., Oh, C.S., Henry, M.P., *J. Chromatogr. A* **2000**, *887*, 277-285.
18. Tang, Q., Xin, B., Lee, M.L., *J. Chromatogr. A* **1999**, *837*, 35-50.
19. Tang, Q., Wu, N., Lee, M.L., *J. Microcol. Sep.* **1999**, *11*, 550-561.
20. Tang, Q., Lee, M.L., *J. High Resolut. Chromatogr.* **2000**, *23*, 73-80.
21. Tang, Q., Lee, M.L., *J. Chromatogr. A* **2000**, *887*, 235-275.
22. Chirica, G., Remcho, V.T., *Electrophoresis* **1999**, *20*, 50-56.
23. Kato, M., Dulay, M.T., Bennett, B., Chen, J.-R., Zare, R.N., *Electrophoresis* **2000**, *21*, 3145-3151.
24. Fukushima, T., Kato, M., Santa, T., Imai, K., *Biomed. Chromatogr.* **1995**, *9*, 10-17.
25. Roed, L., Lundanes, E., Greibrokk, T., *J. Chromatogr. A* **2000**, *890*, 347-353.
26. Roed, L., Lundanes, E., Greibrokk, T., *J. Microcol. Sep.* **2000**, *12*, 561-567.
27. Agren, P., Counter, J., Laggner, P., *J. Non-Cryst. Solids* **2000**, *261*, 195-203.
28. Van Beek, J.J., Seykens, D., Jansen, J.B., *J. Non-Cryst. Solids* **1992**, *146*, 111-120.
29. Friggeri, A., Gronwalk, O., van Bommel, K.J., Shinkai, S., Reinhoudt, D.N., *Chem. Commun.* **2001**, 2434-2435.

30. Yoda, S., Ohshima, S., Kamiya, K., Kawai, A., Uchida, K., Ikazaki, F., *J. Non-Cryst. Solids* **1996**, *208*, 191-198.
31. Boury, B.F., Corriu, R.J., Delord, P., Nobili, M., *Chem. Mater.* **2002**, *14*, 730-738.
32. Murakami, Y., Matsumoto, T., Takasu, Y., *J. Phys. Chem. B* **1999**, *103*, 1836-1840.
33. Kato, M., Sakai-Kato, K., Matsumoto, N., Toyo'oka, T., *Anal. Chem.* **2002**, *74*, 1915-1921.
34. Dulay, M.T., Quirino, J.P., Bennett, B., Kato, M., Zare, R.N., *Anal. Chem.* **2001**, *73*, 3921-3926.
35. Brinker, C.J., Scherer, G.W., *Sol-Gel Science: The Physics and Chemistry of Sol-Gel Processing*. 1990, Academic Press, Inc: San Diego, CA.
36. Hench, L.L., *Sol-Gel Silica: Properties, Processing and Technology Transfer*. 1998, Noyes Publications: Westwood, NJ.
37. Tanaka, N., Kobayashi, H., Nakanishi, K., Minakuchi, H., Ishizuka, N., *Anal. Chem.* **2001**, 421A-429A.
38. Iler, R.K., *The Chemistry of Silica*. 1979, New York, NY: Wiley.
39. Nakanishi, K., Shikata, H., Ishizuka, N., Koheiya, N., Soga, N., *J. High Resolut. Chromatogr.* **2000**, *23*, 106-110.
40. Tanaka, N., Nagayama, H., Kobayashi, H., Ikegami, T., Hosoya, K., Ishizuka, N., Minakuchi, H., Nakanishi, K., Cabera, K., Lubda, D., *J. High Resolut. Chromatogr.* **2000**, *23*, 111-116.

41. Ishizuka, N., Minakuchi, H., Nakanishi, K., Soga, N., Nagayama, H., Hosoya, K., Tanaka, N., *Anal. Chem.* **2000**, *72*, 1275-1280.
42. Kobayashi, H., Smith, C., Hosoya, K., Ikegami, T., Tanaka, N., *Anal. Sci.* **2002**, *18*, 89-92.
43. Fujimoto, C., *J. High Resolut. Chromatogr.* **2000**, *23*, 89-92.
44. Allen, D., El Rassi, Z., *Electrophoresis* **2003**, *24*, 408-420.
45. Rathore, A.S., Horvath, C., *Electrophoresis* **2002**, *23*, 1211-1216.
46. Hayes, J.D., Malik, A., *Anal. Chem.* **2000**, *72*, 4090-4099.
47. Kato, M., Sakai-Kato, K., Toyo'oka, T., Dulay, M.T., Quirino, J.P., Bennett, B., Zare, R.N., *J. Chromatogr. A* **2002**, *961*, 45-51.
48. Dulay, M.T., Quirino, J.P., Bennett, B., Zare, R.N., *J. Sep. Sci.* **2002**, *25*, 3-9.
49. Morishima, K., Bennett, B., Dulay, M.T., Quirino, J.P., Zare, R.N., *J. Sep. Sci.* **2002**, *25*, 1226-1230.
50. Yang, C., El Rassi, Z., *Electrophoresis* **1999**, *20*, 2337-2342.
51. Yang, C., El Rassi, Z., *Electrophoresis* **2000**, *21*, 1977-1984.
52. Tegeler, T., El Rassi, Z., *Anal. Chem.* **2001**, *73*, 3365-3372.
53. Tegeler, T., El Rassi, Z., *J. Chromatogr. A* **2002**, *945*, 267-279.
54. Quirino, J.P., Dulay, M.T., Bennett, B., Zare, R.N., *Anal. Chem.* **2001**, *73*, 5539-5543.
55. Quirino, J.P., Dulay, M.T., Zare, R.N., *Anal. Chem.* **2001**, *73*, 5557-5563.
56. Breadmore, M.C., Shrinivasan, S., Wolfe, K.A., Power, M.E., Ferrance, J.P., Hosticka, B., Norris, P.M., Landers, J.P., *Electrophoresis* **2002**, *23*, 3487-3495.

57. Breadmore, C.M., Shrinivasan, S., Karlinsey, J., Ferrance, J.P., Norris, P.M., Landers, J.P., *Electrophoresis* **2003**, *24*, 1261-1270.
58. Kato, M., Matsumoto, N., Sakai-Kato, K., Toyo'oka, T., *J. Pharm. Biomed. Anal.* **2003**, *30*, 1845-1850.
59. Sakai-Kato, K., Kato, M., Nakakuki, H., Toyo'oka, T., *J. Pharm. Biomed. Anal.* **2003**, *31*, 299-309.
60. Liu, Z., Otsuka, K., Terabe, S., Motokawa, M., Tanaka, N., *Electrophoresis* **2002**, *23*, 2973-2981.
61. Kang, J., Wistuba, D., Schurig, V., *Electrophoresis* **2002**, *23*, 1116-1120.
62. Chen, Z., Hobo, T., *Electrophoresis* **2001**, *22*, 3339-3346.
63. Chen, Z., Hobo, T., *Anal. Chem.* **2001**, *73*, 3348-3357.



## CHAPTER III

# CAPILLARY ELECTROCHROMATOGRAPHY WITH MONOLITHIC SILICA COLUMNS. PREPARATION OF SILICA MONOLITHS HAVING SURFACE-BOUND OCTADECYL MOIETIES AND THEIR CHROMATOGRAPHIC CHARACTERIZATION AND APPLICATIONS TO THE SEPARATION OF NEUTRAL AND CHARGED SPECIES\*

### Introduction

Thus far, major progress has been made in the fabrication of silica-based monoliths as summarized in two very recent review articles [1, 2] as well as in chapter II of this dissertation. However, more systematic studies on the surface modification and pore tailoring of the silica monoliths in CEC are still needed. Moreover, previous studies on monolithic silica for CEC [3-6] have focused mainly on the preparation aspects and physical characterization of these novel columns. Although these initial studies constituted solid contributions for advancing the use of silica-based monolithic capillaries in CEC, systematic studies on understanding the chromatographic behavior of neutral and charged species on these novel capillary columns are badly needed. Thus, the aim of this

---

\* *The content of this chapter has been published in Electrophoresis, 2003, 24, 408-420*

chapter is to contribute to the further improvement of surface modification and pore tailoring of silica monoliths as well as to the understanding of their retentive chromatographic properties toward neutral and charged species

## Experimental

### Instrumentation

The instrument used for CEC was a P/ACE 5010 CE system from Beckman Instrument (Fullerton, CA, USA) equipped with a UV detector and a data handling system comprised of an IBM personal computer and P/ACE software. For column fabrication, temperature programming was carried out using a Sigma 3 Gas Chromatograph from Perkin-Elmer (Norwalk, CT, USA). Constant temperature processes were done using an Isotemp Oven from Fisher Scientific (Pittsburgh, PA, USA).

### Chemicals and Materials

Sodium phosphate monobasic, phosphoric acid and ammonium hydroxide were purchased from Mallinckrodt (Paris, KY, USA). Molecular biology grade tris (hydroxymethyl)aminomethane, ammonium acetate, glacial acetic acid, hydrochloric acid, sulfuric acid, HPLC grade acetonitrile, methylene chloride, aniline and benzene were obtained from Fisher Scientific (Fair Lawn, NJ, USA). Sodium hydroxide was

purchased from EM Science (Cherry Hill, NJ, USA). Tetramethylorthosilicate (TMOS), poly (ethylene glycol) (PEG) MW = 10,000, 2,6-lutidine (99+%), 3-chloro-4-methylaniline (99+%), 4-chloroaniline (98%), 3,4-dichloroaniline (98%), all of the alkyl phenyl ketones (APK's), and all of the alkyl benzenes (AB's) were from Aldrich Chemical Co. Inc. (Milwaukee, WI, USA). 3-Methylaniline was from Fluka Chemika (Ronkonkoma, NY, USA). Ethanol was purchased from Pharmco (Brookfield, CT, USA). 2,4-Dinitrophenylamino acids (DNP-AA) and phenylthiohydantion amino acids (PTH-AA) were from Sigma (St. Louis, MO, USA). Dimethyloctadecylchlorosilane was from Huls Petrarch Systems (Bristol, PA, USA). Fused-silica capillaries with an internal diameter of 100  $\mu\text{m}$  and an outer diameter of 360  $\mu\text{m}$  were purchased from Polymicro Technologies (Phoenix, AZ, USA).

### Column Preparation

Columns were prepared by a method similar to the one previously described by Ishizuka et al. [5] with some modifications. A segment of 100- $\mu\text{m}$  I.D. fused-silica capillary of a desired length was pre-treated hydro-thermally [6]. The capillary was first rinsed with deionized water and then sealed at both ends using a propane torch and placed in a GC oven for thermal conditioning by raising the temperature at a rate of 1  $^{\circ}\text{C}/\text{min}$  from 40  $^{\circ}\text{C}$  (2 min hold time) to a final temperature of 250  $^{\circ}\text{C}$  where it was maintained for 60 min. After pre-treatment was complete, the sealed ends were cut-off and the capillary was injected with a mixture containing TMOS. This mixture was prepared by adding 500  $\mu\text{L}$  of TMOS to a solution that contained 0.1325 g of PEG in

1250  $\mu\text{L}$  of 0.010 M acetic acid, followed by stirring for 45 min at 0  $^{\circ}\text{C}$ . After the mixture was injected into the pre-treated capillary, the inlet and outlet ends of the capillary were joined together with a piece of Teflon tubing to form a circle. The capillary was heated at 40  $^{\circ}\text{C}$  and allowed to react overnight. The resulting monolithic silica was rinsed with 0.010 M ammonium hydroxide then heated at 120  $^{\circ}\text{C}$  for 60 min. This process was repeated three times. The capillary was then dried by rinsing the column with 200 proof ethanol, followed by purging with helium at 160 psi for 60 min. The final heat treatment was done in a GC oven by ramping the temperature at a rate of 2.5  $^{\circ}\text{C}/\text{min}$  from 30  $^{\circ}\text{C}$  (2 min hold time) to 180  $^{\circ}\text{C}$  (60 min hold time), then again ramped at 2.5  $^{\circ}\text{C}/\text{min}$  to a final temperature of 330  $^{\circ}\text{C}$  where it was held for 21 hrs. The stationary phase was attached to the silica skeleton by first filling the column with a solution consisting of 300  $\mu\text{L}$  of 10% (wt/v) dimethyloctadecylchlorosilane in  $\text{CH}_2\text{Cl}_2$  and 20  $\mu\text{L}$  of 2,6-lutidine [7], followed by heating for 1 hour at 50  $^{\circ}\text{C}$ . This step was repeated four times. Columns that were 27 cm long and free of voids were cut from the original capillary. The columns were rinsed with water and windows were formed 7 cm from the outlet end by placing that portion of the capillary in fuming sulfuric acid until the polyimide coating was removed. After subsequent rinses of acetonitrile and water, the capillaries were installed into the P/ACE cartridges and were ready to be used.

## Results and Discussion

### Optimization of Column Fabrication

The optimal conditions for column fabrication are summarized in the previous section. These conditions were determined by performing systematic studies on (i) the C<sub>18</sub> coating of the monolithic silica, and (ii) the pore tailoring of the column. Homologous series of alkylbenzenes (AB's) and alkyl phenyl ketones (APK's) were the test compounds used in the chromatographic evaluation of the various columns, and the results are discussed in the following sections.

Coating of the stationary phase After construction of the monolithic silica column was completed, the monolith was reacted with dimethyloctadecylchlorosilane to yield an octadecyl-silica (C<sub>18</sub>-silica) stationary phase that would exhibit reversed-phase chromatography (RPC) behavior. According to Kinkel and Unger [7], the presence of a base in the reaction mixture can enhance the reactivity of the monochlorosilane in the silanization reaction by forming a reactive intermediate in addition to acting as an acid scavenger. In this regard, the effect of 2,6-lutidine on the silanization reaction under investigation was examined. Figure 1 shows a comparison of an APK separation achieved on a monolithic C<sub>18</sub>-silica column that was prepared by reacting the silica monolith with dimethyloctadecylchlorosilane in the presence of 2,6-lutidine (Fig. 1b, Column B) and a monolithic C<sub>18</sub>-silica column that was prepared in the absence of 2,6-lutidine (Fig. 1a, Column A) while keeping all other parameters involved in the

fabrication of these columns identical. Column B showed a substantial increase in retention over column A. For instance, for column A, amylbenzene exhibited a retention factor,  $k'$ , of 0.33, whereas a  $k'$  of 0.51 was achieved for the same solute on column B (an increase of ~60%). In addition to increased retention, the average mobile phase linear velocities for columns A and B were 1.41 mm/s and 1.05 mm/s, respectively. These findings support the idea that 2,6-lutidine facilitates the reaction between dimethyloctadecylchlorosilane and the silanol groups on the surface of the siliceous monolith. Obviously, the increase in retention is a result of the higher number of surface-bound  $C_{18}$  moieties available for interaction with the solutes. Likewise, a decrease in the mobile phase linear flow velocity is observed as a result of a lower concentration of surface silanols available to drive the mobile phase through the separation channel by EOF. Fortunately, these improvements in retention were not at the expense of sacrificing

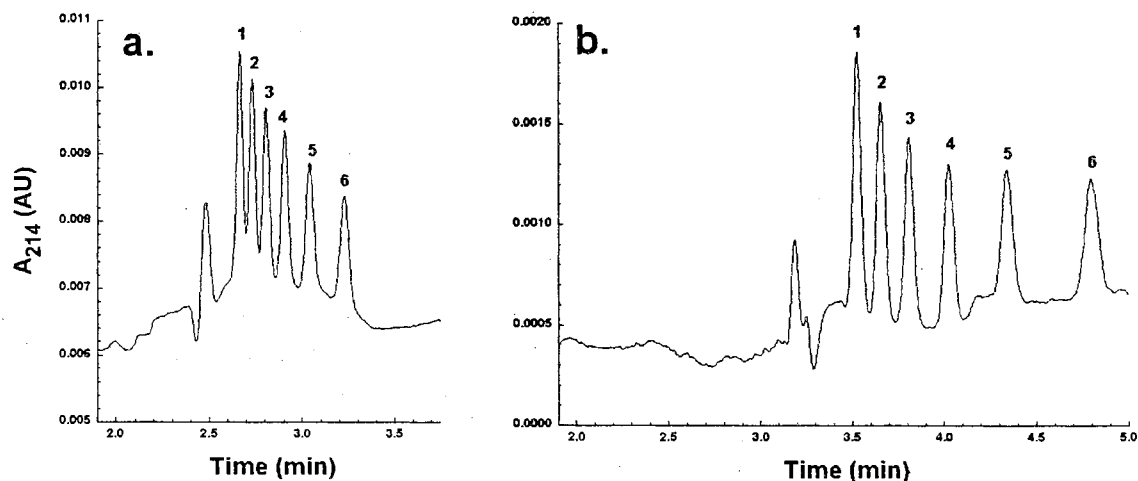


**Figure 1.** Typical electrochromatograms of APK's obtained on monolithic silica column bonded with octadecyl moieties in (a) the absence; (b) the presence of 2,6-lutidine in the silanization reaction with dimethyloctadecylchlorosilane. Conditions: monolithic  $C_{18}$ -silica capillary column, 20/27 cm x 100  $\mu$ m I.D.; hydro-organic mobile phase, 10 mM Tris (pH 8) at 75% (v/v) acetonitrile; voltage, 20 kV; wavelength, 214 nm; column temperature, 20°C. Solutes: 1, acetophenone; 2, propiophenone; 3, butyrophenone; 4, valerophenone; 5, hexanophenone; 6, heptanophenone.

separation efficiency. Column A exhibited a separation efficiency of 129,300 plates/m and column B gave almost identical results with an efficiency of 127,500 plates/m.

In another set of experiments, 5 identical bare monolithic columns were prepared, and subsequently reacted with dimethyloctadecylchlorosilane in the presence of 2,6-lutidine for 1, 2, 3, 5 and 6 hrs by refilling the column with a fresh dichloromethane solution containing dimethyloctadecylchlorosilane/2,6-lutidine for each additional reaction hour. This study was performed in order to determine the reaction time necessary to achieve maximum surface coverage with C<sub>18</sub> moieties and in turn enhance solute retention. Figure 2a shows the effect of reaction time on the k' values for the

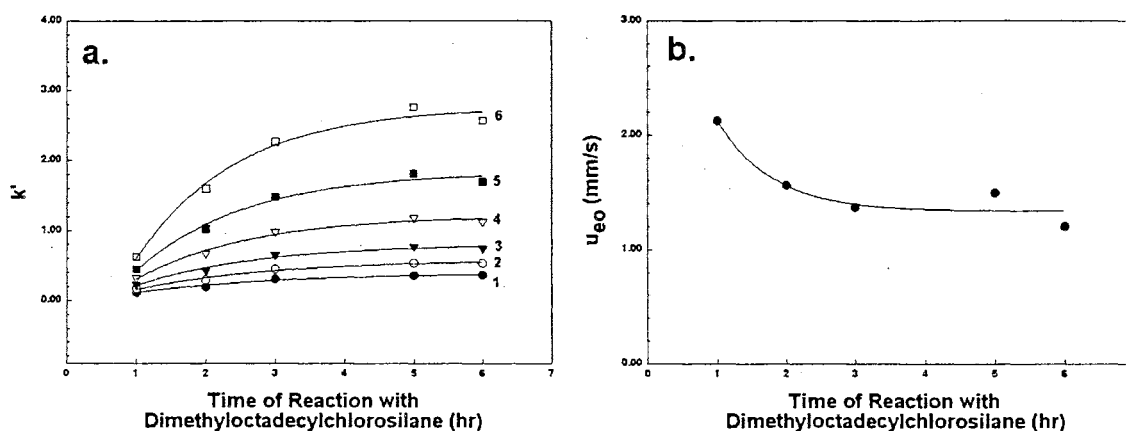


**Figure 2.** Effects of the reaction time between the silica monolith and dimethyloctadecylchlorosilane on (a) the retention factor,  $k'$ , of AB's; (b) the mobile phase flow velocity ( $u_{eo}$ ). Conditions: monolithic C<sub>18</sub>-silica capillary column, 20/27 cm x 100  $\mu$ m I.D.; hydro-organic mobile phase, 10mM Tris (pH 8) at 60% (v/v); voltage, 20kV; wavelength, 214 nm; column temperature, 30°C. Solutes: 1, benzene; 2, toluene; 3, ethylbenzene; 4, propylbenzene; 5, butylbenzene; 6, amylbenzene.

alkylbenzene homologous series. As can be seen in Fig. 2a,  $k'$  increased sharply between 1 and 3 hrs and then more or less stabilized after 4 to 5 hrs of reaction time. This indicates that a maximum surface coverage of the stationary phase with C<sub>18</sub> moieties is reached at or shortly after 4 hrs of reaction time in the presence of 2,6-lutidine. This is

further confirmed by the plot of the EOF velocity versus the reaction time shown in Fig. 2b whereby the EOF velocity drops sharply between 1 and 3 hrs and then more or less plateaus at longer reaction time. The drop in EOF velocity is an indication of fewer unreacted silanols on the surface of the stationary phase as the reaction time with dimethyloctadecylchlorosilane is increased.

Pore-tailoring After gelation of the silica monolith is complete, further tailoring of the pores is usually performed while the monolith is in the wet state by exchanging the fluid phase [8, 9]. The macroporous gel domains (i.e., through-pores) are formed during gelation while pore tailoring affects only the internal pore structure of the silica monolith. Therefore, the macroporous structure (i.e., through-pores) and mesopores of silica monoliths can be designed independently. Solvent exchange can be done with solutions that possess a  $\text{pH} > 8$  to convert micropores into mesopores of ca. 10 nm average pore diameter [8, 9]. A schematic of the silica monolith pore tailoring is illustrated in Fig. 3. In this investigation, an aqueous solution of 0.010 M  $\text{NH}_4\text{OH}$  was used as the pore

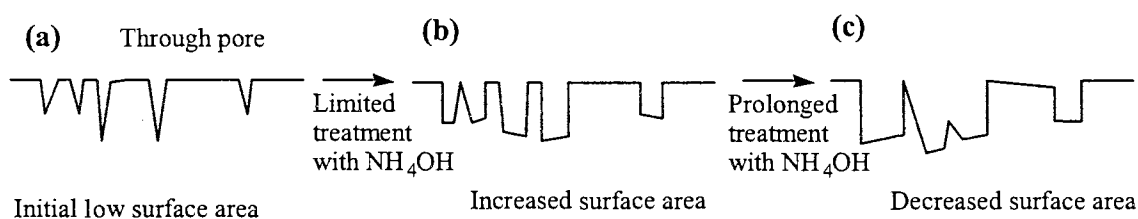


**Figure 3.** Schematic illustration for converting micropores to mesopores within the monolithic silica skeletons by treatment of the monoliths with a solution of  $\text{NH}_4\text{OH}$ . The schematic illustration represents one side of the through-pore which shows (a) the initial micropores that offer low surface area, (b) the mesopores obtained after treatment with  $\text{NH}_4\text{OH}$  for a limited period of time that increases the surface area of the monolith, and (c) the mesopores obtained after treatment with  $\text{NH}_4\text{OH}$  for a prolonged period of time that leads to increased pore diameter and subsequently decreased surface area.



tailoring medium. To study the effects of  $\text{NH}_4\text{OH}$  on the CEC properties (e.g., retention, EOF, separation efficiency) of the monoliths, five identical monolithic columns were prepared, and subsequently treated with 0.010 M  $\text{NH}_4\text{OH}$  for 0, 90, 180, 270 and 360 min. All five monolithic columns thus obtained were later reacted with dimethyloctadecylchlorosilane for four hours in the presence of 2,6-lutidine. Figure 4a shows the effect that  $\text{NH}_4\text{OH}$  pore tailoring time has on the retention factor of the alkyl benzenes. When the  $\text{NH}_4\text{OH}$  treatment step was replaced with water (0 min), very little retention was observed because the pores were not properly developed (i.e., the initial microporous gel skeleton was not reorganized into mesopores by simply treating the monolith with water), and most likely the specific surface area of the monolith was relatively low. This may have caused the column to have a very low phase ratio (i.e., a low  $k'$ ). A reaction time of 90 min is all that is necessary to circumvent the problem of low phase ratio as illustrated by the graphs in Fig. 4a. As can be seen in Fig. 4a,  $k'$  of

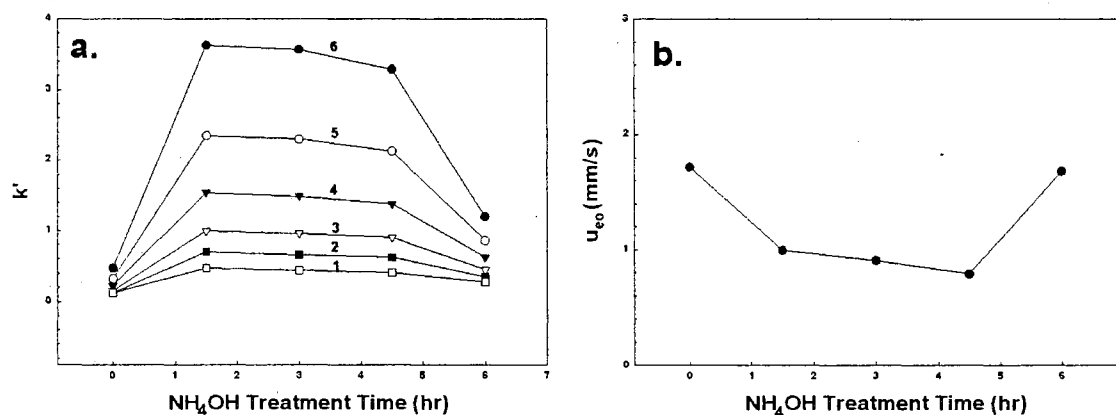


**Figure 4.** Effect of pore tailoring on (a)  $k'$  of AB's; (b) mobile phase flow velocity. Conditions are the same as Fig. 2.

amyl benzene was increased from 0.47 to 3.63 (almost 8 fold) as a result of this 90 min treatment with 0.010 M  $\text{NH}_4\text{OH}$ . However, as the  $\text{NH}_4\text{OH}$  treatment time periods were

lengthened, retention began to decline. This can be attributed to the overall loss of surface area available for reaction with dimethyloctadecylchlorosilane as a consequence of increasing the average pore diameter of the mesopores at excessively longer treatment time [8]. For illustration of mesopore enlargement and concomitant decrease in surface area, see Fig. 3. The decrease of  $k'$  for columns treated between 90 min to 270 min is minimal (9%), but this decrease becomes more significant when the monolithic column was treated for 360 min (a decrease of 64% in  $k'$  when compared to the 270 min treatment).

Figure 4b illustrates the effect of pore tailoring on the EOF velocity exhibited by the monolithic  $C_{18}$ -silica columns treated with  $NH_4OH$  at various amounts of time. The observed EOF velocity pattern seems to be more or less the mirror image of the retention pattern on the same  $C_{18}$  monolithic columns, Fig. 4a. Going from 0 to 90 min treatment with  $NH_4OH$  resulted in a decrease in EOF velocity from 1.72 to 1.00 mm/s. This sharp decrease in EOF can be attributed to the increased surface coverage with  $C_{18}$  moieties (i.e., decreased surface coverage in silanol groups to support the EOF). In other words, the higher retention exhibited by the monolith treated with  $NH_4OH$  for 90 min (see Fig. 4a) should be accompanied by a decrease in EOF velocity resulting from the lower fraction of unreacted silanols. By prolonging the pore tailoring from 90 min to 270 min, the EOF velocities get progressively slower. However, the  $k'$  values exhibited by the columns treated for 180 min and 270 min were slightly lower than those obtained with the column treated for 90 min, as shown above. This can be attributed to the loss in surface area available for stationary phase attachment due to the progressive increase of the average pore diameter of the mesopores and concomitantly the decrease in the

concentration of unreacted silanols to support the EOF as the  $\text{NH}_4\text{OH}$  treatment time was increased from 90 min to 270 min. In other words, longer  $\text{NH}_4\text{OH}$  treatment times will be accompanied by a decrease in surface area that ultimately results in a slight decrease in retention as well as the EOF. Of course, there is a limit to this trend as exhibited by the column treated with  $\text{NH}_4\text{OH}$  for 360 min where the EOF increases very sharply indicating that the pores become so large leading to a better orientation between the interconnected through-pores and the capillary axis. At a 360 min treatment, EOF velocity is increased, but retention is decreased due to the low phase ratio. Figure 5 shows a comparison of the separations of AB's achieved by these columns.

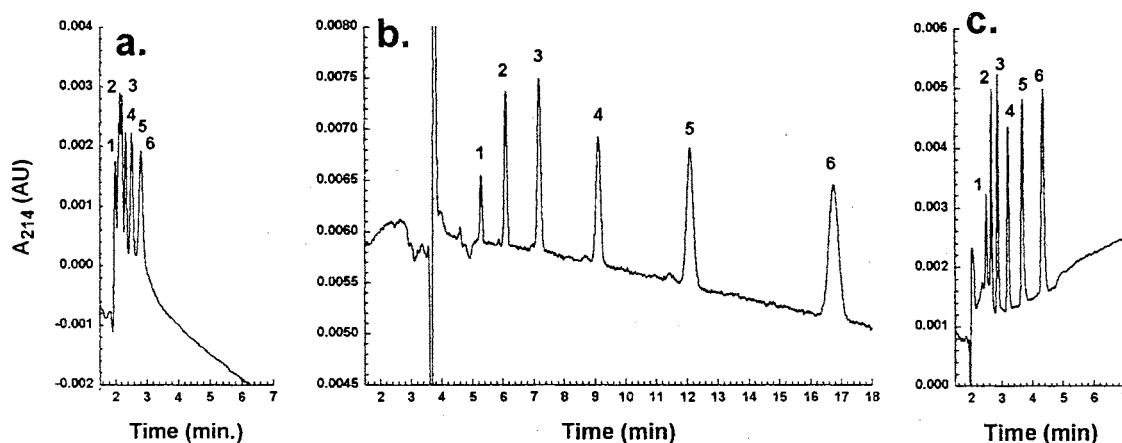


**Figure 5.** Comparison of electrochromatograms of AB's obtained on monolithic  $\text{C}_{18}$ -silica capillary columns previously treated with  $\text{NH}_4\text{OH}$  for (a) 0 minutes, (b) 180 minutes and (c) 360 minutes. Conditions and peak designations are the same as Fig. 2.

The separation efficiency exhibited by the various monolithic  $\text{C}_{18}$ -silica columns treated by  $\text{NH}_4\text{OH}$  is also an important variable that needs to be assessed. In this regard, the separation efficiencies of the various columns were evaluated at different EOF velocities by increasing the voltage from 6 kV to 30 kV in 3 kV increments to establish the van Deemter plots for the columns under investigation. Figure 6a shows an overlay

of these plots for columns treated for 90, 180, 270 and 360 min with  $\text{NH}_4\text{OH}$  prior to the silanization reaction. Columns treated for 90 min and 180 min behaved very similarly, providing minimum plate heights ( $H_{\text{min}}$ ) of 7.8  $\mu\text{m}$  and 7.7  $\mu\text{m}$ , respectively. This corresponds to a separation efficiency of almost 130,000 plates/m under these conditions. In addition, these columns exhibited this level of efficiency over a relatively wide range of linear velocities (i.e.,  $u_{\text{opt}}$  in the range 0.69-1.4 mm/s) giving them more flexibility to separation conditions. The column treated for 270 min performed equally well on the

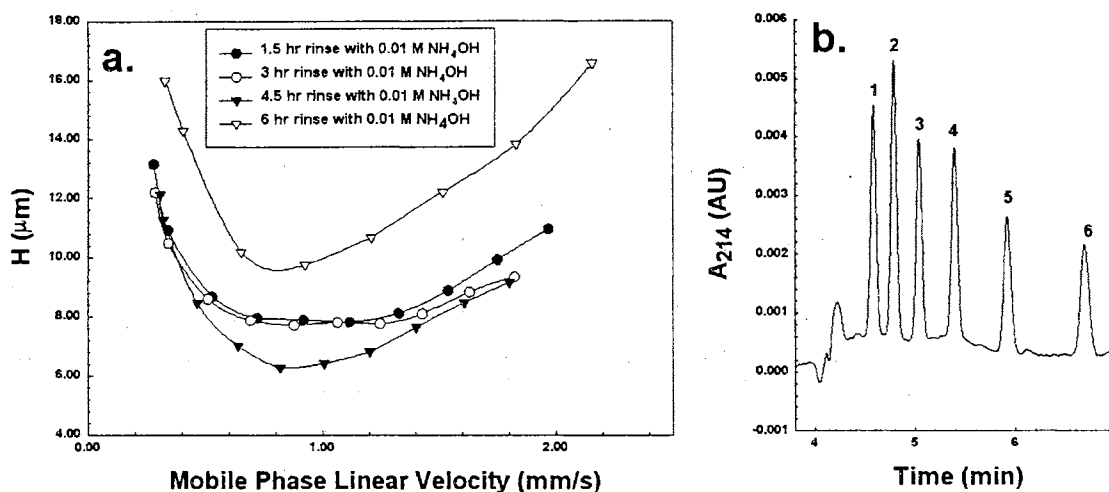


**Figure 6.** (a) The van Deemter plots obtained on monolithic  $\text{C}_{18}$ -silica capillary columns previously treated by  $\text{NH}_4\text{OH}$  for different time periods using APK's; (b) a typical electrochromatogram of the APK's obtained on the column treated with  $\text{NH}_4\text{OH}$  for 270 min obtained at  $u_{\text{opt}}$ . Conditions: monolithic  $\text{C}_{18}$ -silica capillary column, 20/27 cm x 100  $\mu\text{m}$  I.D.; hydro-organic mobile phase, 10mM Tris (pH 8) at 75% (v/v) acetonitrile; voltage was varied between 6-30kV; wavelength, 214 nm; column temperature, 20°C. Solute designations as in Fig. 1.

high and low ends of the mobile phase linear velocity scale, but actually performed better in the middle range providing an  $H_{\text{min}}$  of 6.3  $\mu\text{m}$  (160,000 plates/m) at a  $u_{\text{opt}}$  of 0.82 mm/s. Figure 6b shows a typical electrochromatogram obtained at this  $u_{\text{opt}}$  of 0.82 mm/s with a separation efficiency comparable to that obtained on capillaries packed with 3  $\mu\text{m}$

C<sub>18</sub>-silica microparticles with the advantages that the monolithic column offers, which are, among other things, high permeability and virtually no bubble formation. The column treated for 360 min failed to reach this level of performance (see van Deemter plot in Fig. 6a).

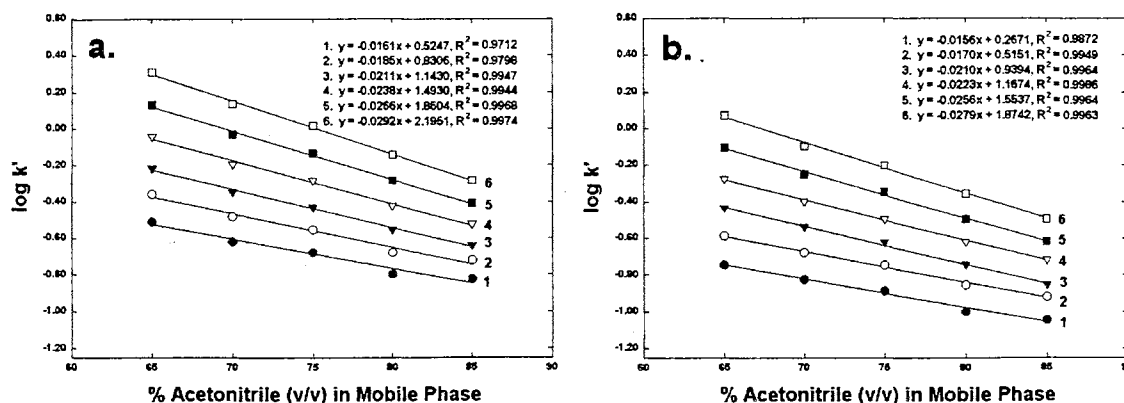


**Figure 7.** Plots of  $\log k'$  for (a) AB's; (b) APK's versus percent acetonitrile (v/v) in the mobile phase. Conditions: monolithic C<sub>18</sub>-silica capillary column, 20/27 cm x 100  $\mu$ m I.D.; hydro-organic mobile phase, 10mM Tris (pH 8) at different proportions of acetonitrile and water; other conditions as in Fig 1. Lines in (a): 1, benzene; 2, toluene; 3, ethylbenzene; 4, propylbenzene; 5, butylbenzene; 6, amylbenzene. Lines in (b): 1, acetophenone; 2, propiophenone; 3, butyrophenone; 4, valerophenone; 5, hexanophenone; 6, heptanophenone.

### Evaluation of the Chromatographic Retention

Neutral solutes Figure 7a and b show the linear dependence of the  $\log k'$  on the percent acetonitrile (v/v) in the mobile phase at a column temperature of 20 °C for AB's and APK's, respectively. These retention data are indicative of a truly RPC behavior towards neutral solutes over a wide range of mobile phase compositions. As expected, the APK's, which are more polar compounds than the AB's homologous series, are less retained in the range of percent acetonitrile (v/v) studied. For both homologous series, an

acetonitrile content of 80% (v/v) in the mobile phase appeared to give the best overall separation as far as retention, separation efficiency, and analysis time are concerned. At values lower than 80% acetonitrile (v/v), the viscosity of the mobile phase increased while the eluent strength decreased, thus lowering the mobile phase flow velocity and increasing solute retention, respectively. The net result is an increase in solute longitudinal diffusion and mass transfer resistance in the porous structures causing band broadening which lowers efficiency. Above 80% acetonitrile (v/v) both homologous series were not effectively separated.

To further gain insight into the retentive properties of the C<sub>18</sub>-silica monoliths under investigation, a set of relatively polar compounds were investigated for their retention behavior on the C<sub>18</sub>-monolithic column, namely a group of 5 anilines including aniline (pK<sub>a</sub> = 4.70), 3-methylaniline (pK<sub>a</sub> = 4.91), 4-chloroaniline (pK<sub>a</sub> = 4.06), 3-chloro-4-methylaniline (pK<sub>a</sub> = 4.05) and 3,4-dichloroaniline (pK<sub>a</sub> = 3.33). These weak bases were chosen for their ability to behave as neutral compounds at pH > 6 and as positively charged species at pH ≤ pK<sub>a</sub>. Figure 8 shows the electrochromatograms of the 5 anilines at pH 7 obtained with a mobile phase at 50% (v/v) acetonitrile (Fig. 8a) and 40% (v/v) acetonitrile (Fig. 8b). The elution order is that expected for RPC (i.e., chloro-substituted anilines are more retained than methyl-substituted anilines and disubstituted anilines are more retained than mono-substituted anilines). The k' values for aniline, 3-methylaniline, 4-chloroaniline, 3-chloro-4-methylaniline and 3,4-dichloroaniline were 0.19, 0.25, 0.29, 0.42 and 0.46, respectively, at 50% acetonitrile in the mobile phase. Going to lower acetonitrile content (40% v/v), the elution order stayed the same and baseline resolution was achieved for the 5 anilines with only a 1 min increase in the

analysis time (see Fig. 8b). The  $k'$  values of the solutes increased except for aniline which stayed the same. The values were 0.19, 0.32, 0.42, 0.71 and 0.84 for aniline, 3-methylaniline, 4-chloroaniline, 3-chloro-4-methylaniline and 3,4-dichloroaniline, respectively, at 40% (v/v) acetonitrile in the mobile phase. The constancy of retention for aniline at 40% and 50% (v/v) acetonitrile in the mobile phase may be indicative of some polar interaction (e.g., hydrogen bonding) between aniline and the surface silanols in

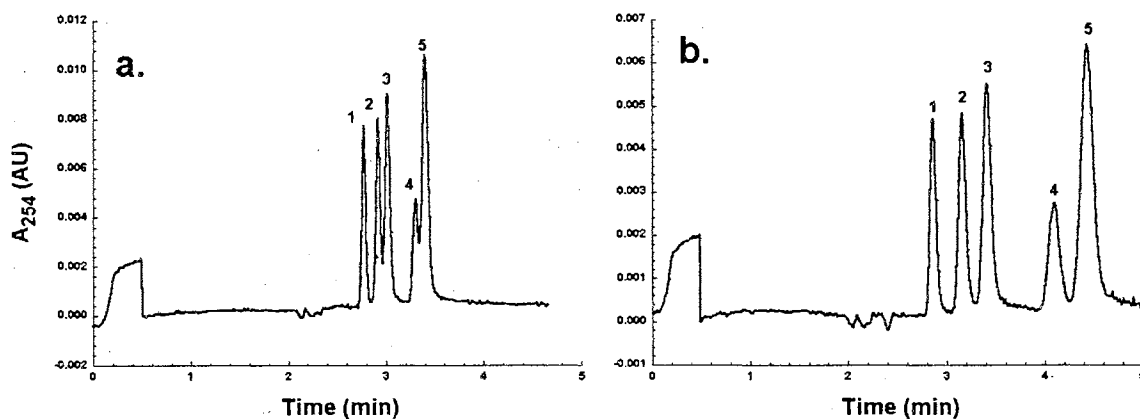


**Figure 8.** *Electrochromatograms of anilines. Conditions: hydro-organic mobile phase, 5mM sodium phosphate monobasic (pH 7) at (a) 50% v/v acetonitrile and (b) 40% v/v acetonitrile; wavelength, 254 nm; other conditions as in Fig. 7. Solutes: 1, aniline; 2, 3-methyl-aniline; 3, 4-chloroaniline; 4, 3-chloro-4-methylaniline; 5, 3,4-dichloroaniline.*

addition to the non-polar interaction that occurs with the  $C_{18}$  moieties of the stationary phase. Decreasing the mobile phase pH from 7.0 to 5.0 but keeping its organic content the same at 40% (v/v) acetonitrile almost doubled the analysis time (due to a decrease in the mobile phase velocity at pH 5.0) without significantly improving resolution. In addition,  $k'$  values remained constant indicating that the aniline species are still neutral at pH 5.0 in the presence of 40% acetonitrile in the mobile phase. This was verified by performing a CZE run in an open tube under the same mobile phase conditions and running voltage. These conditions did not yield any separation and the solutes co-eluted at the time of the EOF.

The retentive properties of the monolithic C<sub>18</sub>-silica columns were also evaluated with some PTH-AA (Fig. 9). Figure 10 shows the best separation achieved for 14 of these analytes. PTH-arginine was the only species in the mix that possessed a positive charge at the given conditions and therefore eluted before t<sub>0</sub>. The remaining PTH amino acids eluded in order of increasing hydrophobicity as expected in RPC. PTH-asparagine,

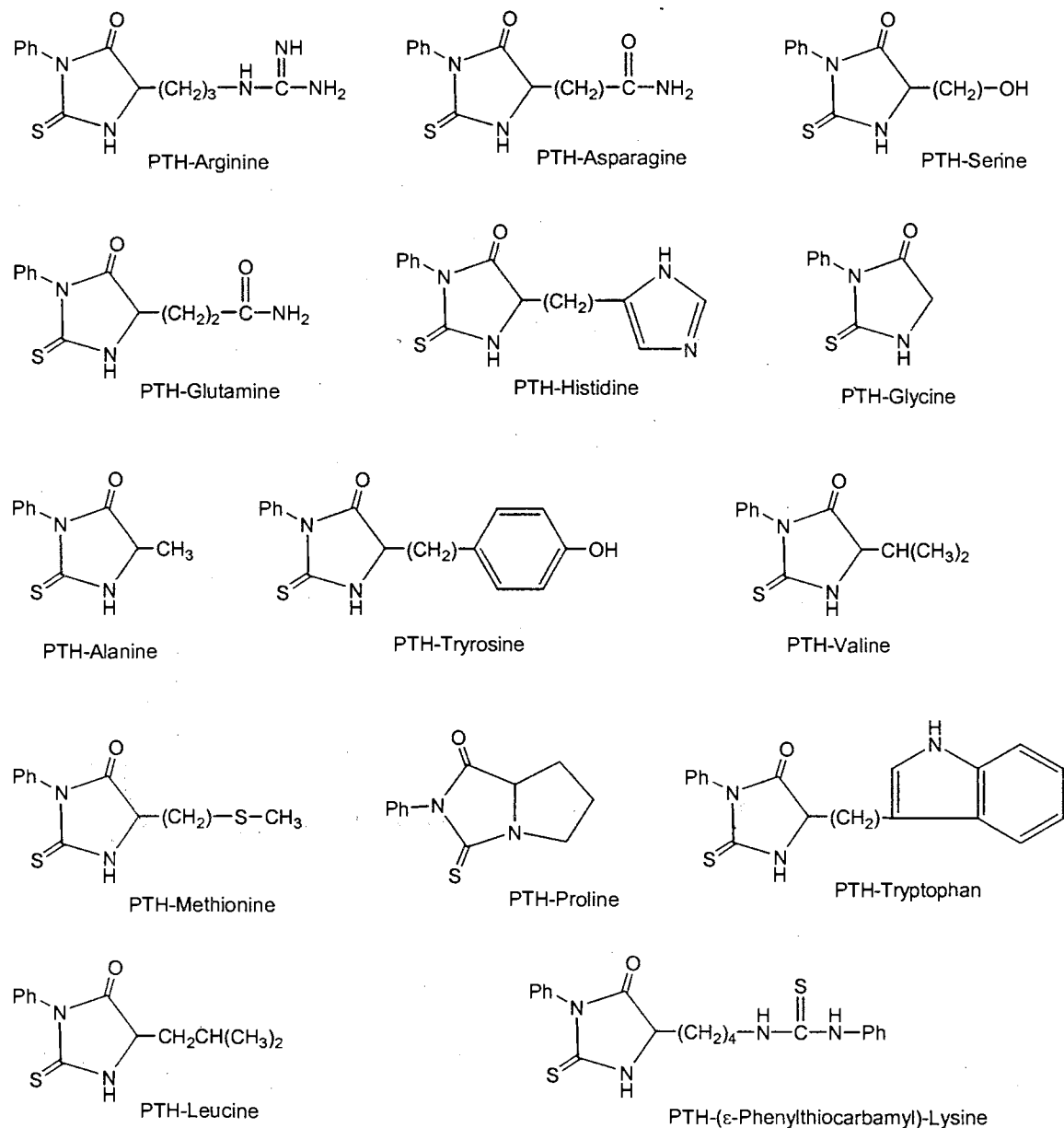


**Figure 9.** Structures of the phenylthiohydantoin amino acids (PTH-AA).



PTH-serine, PTH-glutamine and PTH-histidine were the most difficult to separate due to their polar side chains and baseline separation was not achieved. In addition, PTH-valine and PTH-methionine behaved very similarly and only a slight separation was observed. However, PTH-amino acids with non-polar side chains appeared to separate very well. For instance, PTH-glycine and PTH-alanine were separated by 1.49 minutes ( $k'$  equal to

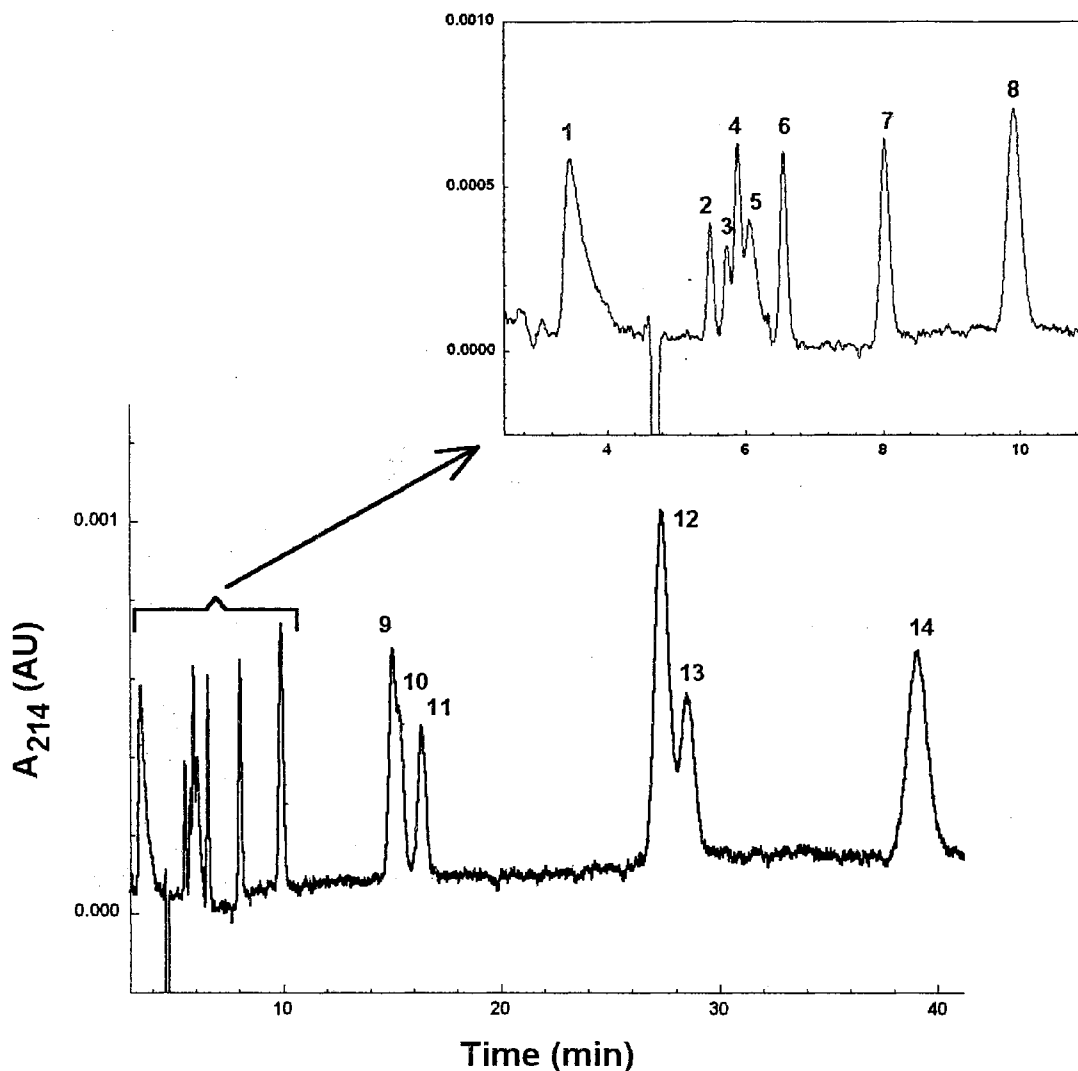


**Figure 10.** Electrochromatogram of PTH-amino acids. Conditions: hydro-organic mobile phase, 5mM sodium phosphate monobasic (pH 6) at 25% (v/v) acetonitrile; other conditions as in Fig. 7. Solutes: 1, PTH-arginine; 2, PTH-asparagine; 3, PTH-serine; 4, PTH-glutamine; 5, PTH-histidine; 6, PTH-glycine; 7, PTH-alanine; 8, PTH-tyrosine; 9, PTH-valine; 10; PTH-methionine, 11, PTH-proline; 12, PTH-tryptophan; 13, PTH-leucine; 14, PTH-( $\epsilon$ -phenylthiocarbamyl)-lysine.

0.40 and 0.72, respectively) and PTH-valine and PTH-leucine were separated by 13.53 min ( $k'$  equal to 2.22 and 5.11, respectively). PTH-aspartic acid and PTH-glutamic acid were not analyzed because both are acidic and the EOF velocity was not high enough to elute them in a reasonable amount of time.

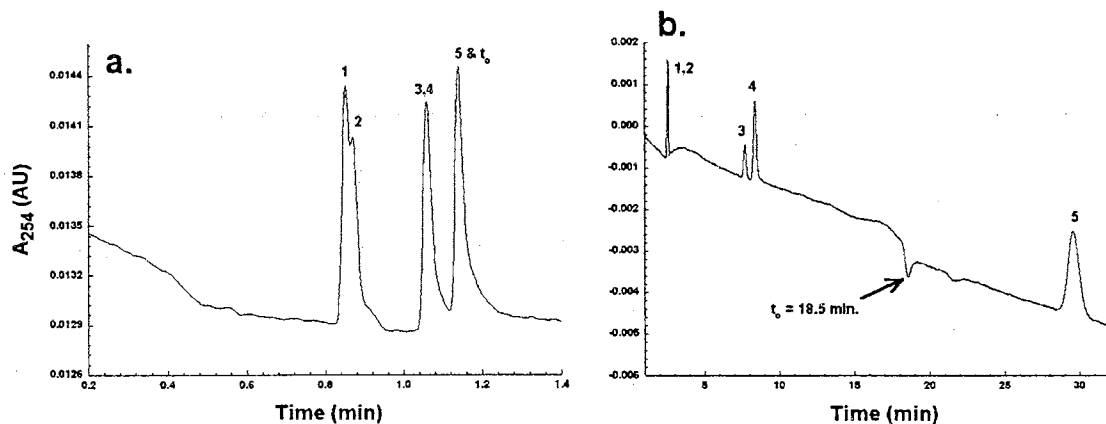


**Figure 11.** Comparison of aniline separations by (a) CZE and (b) CEC. Conditions: (a) open tube capillary; (b) monolithic  $C_{18}$ -silica capillary column, capillary dimensions, 20/27 cm x 100  $\mu$ m I.D.; hydro-organic mobile phase, 5mM sodium phosphate monobasic (pH 3.5) at 40% (v/v) acetonitrile; voltage, 20kV; wavelength, 254 nm; column temperature, 20°C. Peak designations as in Fig. 8.

Ionizable species Anilines, which were first investigated under mobile phase compositions that confer to them neutrality (see above section), were examined again under the same conditions except with a mobile phase of pH 3.5 where the anilines were positively charged. Figure 11 shows a comparison of the separations achieved by open tube (i.e., CZE) and CEC. As revealed from Fig. 10a, 3,4-dichloroaniline ( $pK_a = 3.33$ ) was not charged at these conditions and co-eluted with  $t_0$  (peak 5 in Fig. 10a). The remaining anilines were positively charged and eluted before  $t_0$ .

TABLE 1.

VALUES OF RETENTION PARAMETERS FOR ANILINES OBTAINED WITH A  
MOBILE PHASE CONSISTING OF 5mM SODIUM PHOSPHATE  
MONOBASIC (pH 3.5) AT 40% (v/v) ACETONITRILE

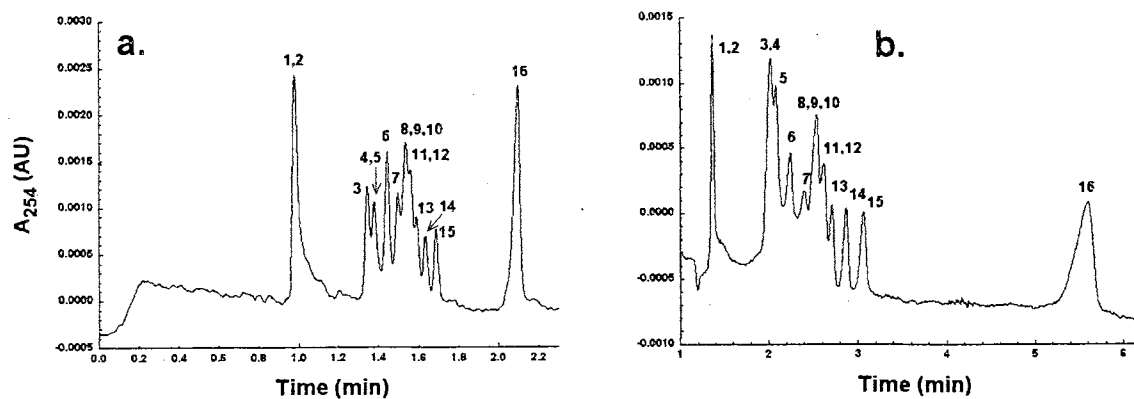
Solutes	$k_{cc}^*$	$k_e^*$	$k^*$
Aniline	-0.86	3.21	-0.41
3-Methylaniline	-0.86	3.48	-0.38
4-Chloroaniline	-0.58	0.78	-0.26
3-Chloro-4-methylaniline	-0.55	0.78	-0.19
3,4-Dichloroaniline	$k' = 0.59$	0.00	$k' = 0.59$

Table 1 lists the dimensionless values of  $k_{cc}^*$ ,  $k_e^*$  and  $k^*$  obtained for anilines. These retention/migration parameters were defined previously in chapter I (Refs. [10, 11]). All anilines displayed a positive  $k_e^*$  value except for 3,4-dichloroaniline which yielded a  $k_e^* = 0$  because it was not charged at the given conditions. The positive value of  $k_e^*$  indicates that the electrophoretic velocities of the solutes are co-directional with the electroosmotic velocity. The magnitude of  $k_e^*$  correlates well with the strength of the electrophoretic migration of the solutes. The  $k_{cc}^*$  expression serves as a useful peak locator, thus indicating the elution order of the solute peaks. Since 4 out of the 5 anilines eluted before the  $t_0$  of the CEC column, their values of  $k_{cc}^*$  are negative. Therefore, the smallest negative  $k_{cc}^*$  value is associated with the more retarded species. The  $k^*$  values for the anilines should indicate the overall solute retardation in terms of electrophoresis

and chromatography. An increase in the value of  $k^*$  (in the present case, a decrease in the negative value of  $k^*$ ) would symbolize an increase in the overall retardation. Since all of the anilines except 3,4-dichloroaniline yield negative values, this indicates that they all eluted before  $t_0$ . Furthermore, since 3,4-dichloroaniline does not possess a charge, its  $k^*$  and  $k_{cc}^*$  values are equal to its  $k'$  value.

As negatively and/or positively charged solutes, DNP-amino acids (DNP-AA) were selected as the model solutes. Figure 12 compares the separations achieved by CZE and CEC modes at 5 mM Tris (pH 8) in 60% water and 40% (v/v) acetonitrile. Although the CEC analysis time is over 3 min longer than that in CZE, the separations are almost identical indicating little or no retention of these charged species. The elution order is exactly the same as well as the co-elution patterns. In this mixture of DNP-AA, two derivatives are amphoteric with zwitterionic properties, namely N $\epsilon$ -DNP-lysine and O-DNP-tyrosine, while the other 14 DNP-amino acids are negatively charged. At the pH of the experiment (pH 8.0), the N $\epsilon$ -DNP-lysine and O-DNP-tyrosine migrated at the time of EOF in CZE (see Fig. 11a) indicating that their net charge is zero (i.e., zwitterions). In fact, the N $\epsilon$ -DNP-lysine and O-DNP-tyrosine are slightly retained in CEC but not separated with a  $k'$  of 0.14. For the other 14 negatively charged DNP-AA, they were fully ionized, a condition that prohibited any substantial interaction with the stationary phase and therefore, provided only an electrophoretic separative component. In this case, the presence of the C<sub>18</sub> moieties only succeeded in acting as an EOF suppressant that resulted in a longer analysis time in CEC than in CZE.

In an attempt to lessen the charge on the DNP-AA and promote interaction with the stationary phase, a mobile phase of lower pH than in the preceding section consisting



**Figure 12.** Comparison of DNP-AA separation by (a) CZE; (b) CEC. Conditions: (a) open tube; (b) monolithic  $C_{18}$ -silica capillary columns; hydro-organic mobile phase, 5mM Tris (pH 8) at 40% v/v acetonitrile; other conditions as in Fig. 10. Solutes, 1, DNP-tyrosine; 2, DNP-lysine; 3, di-DNP-tyrosine; 4, di-DNP-histidine; 5, di-DNP-lysine; 6, DNP-tryptophan; 7, DNP-phenylalanine; 8, DNP-isoleucine; 9, DNP-leucine; 10, DNP-methionine; 11, DNP-threonine; 12, DNP-valine; 13, DNP-serine; 14, DNP-alanine; 15, DNP-glycine; 16, di-DNP-cystine.

of 10 mM ammonium acetate (pH 4.5) in 70% (v/v) water and 30% acetonitrile was utilized instead. Unfortunately, the drop in pH resulted in the electrophoretic mobilities of the analytes becoming greater than the electroosmotic mobility of the mobile phase. This imbalance in mobility was used for the advantage of separation by applying a negative potential in the CEC analysis. This generated a reversal in EOF with counter-directional movement of the analytes towards the outlet end (i.e., the detection point).

Figure 13 compares the CEC separation with the CZE separation under the same conditions, except with a positive potential in CZE equal in magnitude to the negative potential in CEC. By inspecting both separations, it is evident that chromatographic interaction is occurring in CEC as manifested from the change in the elution order with respect to CZE. The di-DNP-histidine and di-DNP-lysine reversed their elution order in CEC, as well as two other pairs of analytes, namely DNP-threonine/DNP-methionine and DNP-serine/DNP-alanine. In addition, some of the solutes that co-eluted in CZE were

well separated in CEC (e.g., DNP-methionine, DNP-threonine, DNP-valine, DNP-phenylalanine, and DNP-leucine as well as di-DNP-tyrosine and di-DNP-histidine). O-DNP-tyrosine and N $\epsilon$ -DNP-lysine could not be eluted because they are positively

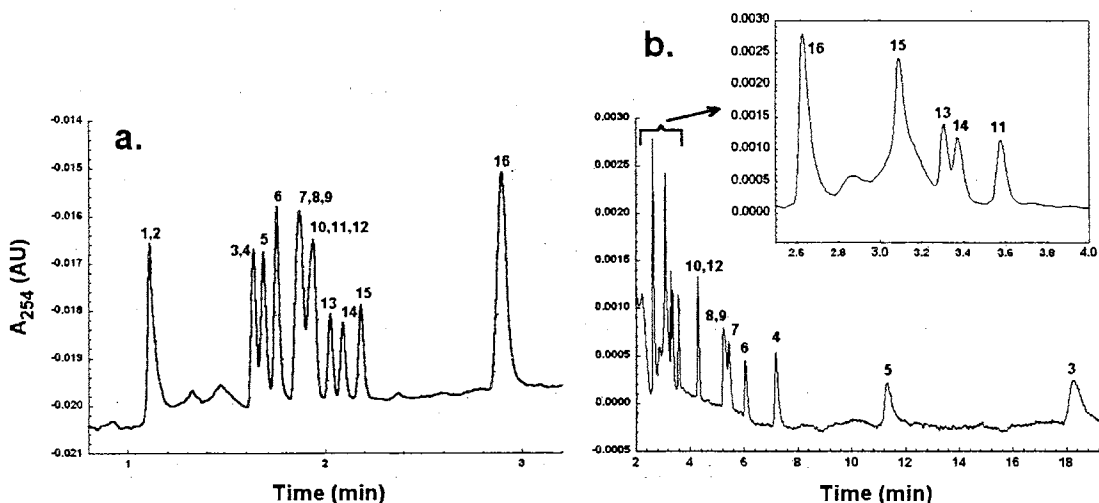


**Figure 13.** Comparison of DNP-AA separation by (a) CZE; (b) CEC. Conditions: (a) open tube capillary at 20 kV; (b) monolithic C<sub>18</sub>-silica capillary at -20 kV; hydro-organic mobile phase, 10mM ammonium acetate (pH 4.5) at 30% (v/v) acetonitrile. Other conditions and peak designations as in Fig. 11.

charged at pH 4.5. Unfortunately, the CEC retention factor proposed by Rathore and Horváth [12] (see chapter I) could not be used, due to the nature of the conditions. Since the EOF was in the reverse direction and the counter-directional mobility of the analytes was greater than that of the electroosmotic mobility of the mobile phase, the separation did not provide a  $t_0$  term. The magnitude of the flow velocity could be measured by making injections at the outlet end with an inert tracer, but obviously this tracer would never elute if injected at the inlet end with the other sample components. It then became necessary to introduce the following dimensionless expression

$$\eta = \frac{\mu_{\text{CEC}}}{\mu_{\text{ep,CZE}}} \quad (1)$$

where  $\eta$  is the mobility moduli,  $\mu_{ep,CZE}$  is the electrophoretic mobility in CZE and  $\mu_{CEC}$  is the adjusted apparent mobility (i.e., the apparent mobility minus the electroosmotic mobility) in CEC. In the absence of chromatographic partitioning in CEC, the value of  $\mu_{CEC}$  should approach that of  $\mu_{ep,CZE}$  obtained in CZE under the same electrolyte and running conditions, and  $\eta$  should approach unity. This assumes that the presence of chromatographic packing in the CEC column does not constitute an obstacle for the electrophoretic mobility of a charged “non interactive” species. “Non interactive” species denotes that the species does not interact with the stationary phase in the CEC column. On the other hand, the stronger the chromatographic partitioning of the charged solute (i.e., the negatively charged DNP-AA), the smaller the value of  $\mu_{CEC}$  and the greater its deviation from the  $\mu_{ep,CZE}$ , and consequently, the smaller the value of the moduli and  $\eta < 1$ . Therefore, the value of  $\eta$  should be  $0 < \eta \leq 1$ .

Table 2 lists the  $k_e^*$  and  $\eta$  values of the various DNP-AA. Ranking the analytes in order of increasing mobility moduli should in principle correlate to decreasing interaction with the stationary phase. From Table 2 the order of increasing mobility moduli is as follows: di-DNP-tyrosine < di-DNP-lysine < DNP-phenylalanine < DNP-isoleucine = DNP-leucine < DNP-tryptophan < di-DNP-cystine = di-DNP-histidine < DNP-methionine = DNP-valine < DNP-alanine < DNP-glycine < DNP-threonine = DNP-serine. This order seems to correlate more or less with the decreasing hydrophobicity of the solutes. For instance, while di-DNP-tyrosine and di-DNP-lysine are the most hydrophobic solutes (i.e., low  $\eta$  value) due to the presence of 2 dinitrophenyl groups, singly DNP tagged amino acids with bulky, non-polar side chains (e.g., DNP-phenylalanine, DNP-isoleucine, DNP-leucine and DNP-tryptophan) are next

TABLE 2.

VALUES OF  $k_e^*$  AND THE MOBILITY MODULI  $\eta$  FOR DNP-AA OBTAINED WITH A MOBILE PHASE CONSISTING OF 10 mM AMMONIUM ACETATE (pH 4.5) AT 30% ACETONITRILE (v/v).

Solutes	$k_e^*$	$\eta$
<i>N,O</i> -di-DNP-tyrosine	-1.77	0.61
<i>N,N</i> -di-DNP-lysine	-1.88	0.68
<i>N</i> -DNP-phenylalanine	-2.26	0.82
<i>N</i> -DNP-isoleucine	-2.26	0.84
<i>N</i> -DNP-leucine	-2.26	0.84
<i>N</i> -DNP-tryptophan	-2.02	0.86
<i>N,N</i> -di-DNP-histidine	-1.77	0.89
<i>N,N</i> -di-DNP-cystine	-3.39	0.89
<i>N</i> -DNP-valine	-2.36	0.91
<i>N</i> -DNP-methionine	-2.36	0.91
<i>N</i> -DNP-alanine	-2.58	0.98
<i>N</i> -DNP-glycine	-2.70	0.99
<i>N</i> -DNP-threonine	-2.36	1.02
<i>N</i> -DNP-serine	-2.49	1.02

on the hydrophobic scale (medium  $\eta$  value) and singly DNP tagged amino acids with polar side chains (e.g., DNP-threonine and DNP-serine) are the least hydrophobic (high  $\eta$  value). As expected, the elution order of the DNP-AA is a reflection of both the extent



of chromatographic interaction and the magnitude of charge-to-mass-ratio. For instance, di-DNP-cystine, which exhibits about the same  $\eta$  value (i.e., about the same interaction with the stationary phase) as DNP-methionine, eluted first because di-DNP-cystine is a doubly negatively charged solute (i.e., high charge-to-mass ratio) while DNP-methionine is a singly negatively charged solute (i.e., low charge-to-mass ratio). In fact, the  $k_e^*$  of di-DNP-cystine is 1.4 times greater in absolute value than that of DNP-methionine (see Table 2).

### Conclusions

Optimum conditions for the fabrication of monolithic silica capillary columns have been determined. Pore tailoring performed with 0.010 M  $\text{NH}_4\text{OH}$  for 270 min at 120 °C after gelation provided the best results in terms of both retention and separation efficiency. This pore-tailoring step (i) allowed sufficient surface coating with  $\text{C}_{18}$  moieties thus providing enhanced retention and (ii) eliminated the microporosity which, in turn, narrowed the pore size distribution, which increased separation efficiency.

The presence of 2,6-lutidine in the silanization reaction between the silica monolith and dimethyloctadecylchlorosilane facilitated the extent of this reaction and enhanced the surface coverage of the  $\text{C}_{18}$  moieties. The monolithic  $\text{C}_{18}$ -silica columns thus generated provided relatively high retention and separation efficiency. These columns yielded sufficient mobile phase flow velocities, yielding relatively rapid analysis time. The van Deemter studies showed that a wide range of flow velocities could be used without a significant drop in separation efficiency.

The monolithic C<sub>18</sub>-silica columns were applied to the separation of both neutral and charged analytes including PTH-AA, DNP-AA and anilines. A mobility moduli expression has been introduced, and some insights regarding the retention behavior of charged species have been described.

## References

1. Tanaka, N., Kobayashi, H., Nakanishi, K., Minakuchi, H., Ishizuka, N., *Anal. Chem.* **2001**, 73, 420A-429A.
2. Tanaka, N., Kobayashi, H., *Capillary electrochromatography on monolithic silica columns*, in *Capillary Electrochromatography*, F. Svec, Editor. 2001, Elsevier: Amsterdam, pp. 165-181.
3. Tanaka, N., Nagayama, H., Kobayashi, H., Ikegami, T., Hosoya, K., Ishizuka, N., Minakuchi, H., Nakanishi, K., Cabrera, K., Lubda, D., *J. High Resolut. Chromatogr.* **2000**, 23, 111-116.
4. Fujimoto, C., *J. High Resolut. Chromatogr.* **2000**, 23, 89-92.
5. Ishizuka, N., Minakuchi, H., Nakanishi, K., Soga, N., Nagayama, H., Hosoya, K., Tanaka, C.K., *Anal. Chem.* **2000**, 72, 1275-1280.
6. Hayes, J.D., Malik, A., *Anal. Chem.* **2000**, 72, 4090-4099.
7. Kinkel, J.N., Unger, K.K., *J. Chromatogr.* **1984**, 316, 193-200.
8. Nakanishi, K., Shikata, H., Ishizuka, N., Koheiya, N., Soga, N., *J. High Resolut. Chromatogr.* **2000**, 23, 106-110.
9. Nakanishi, K., Minakuchi, H., Ishizuka, N., Soga, N., Tanaka, N., *Monolithic HPLC column via sol-gel route*, in *Sol-Gel Synthesis and Processing*, S. Komarneni, Editor. 1998, American Ceramic Society: Westerville, pp. 139-150.
10. Rathore, A.S., Horvath, C., *Electrophoresis* **2002**, 23, 1211-1216.
11. Rathore, A.S., Wen, E., Horvath, C., *Anal. Chem.* **1999**, 71, 2633-2641.
12. Rathore, A.S., Horvath, C., *Electrophoresis* **2002**, 23, 1211-1216.

## CHAPTER IV

# CAPILLARY ELECTROCHROMATOGRAPHY WITH MONOLITHIC-SILICA COLUMNS. PREPARATION OF AMPHIPHILIC SILICA MONOLITHS HAVING SURFACE-BOUND CATIONIC OCTADECYL MOIETIES AND THEIR CHROMATOGRAPHIC CHARACTERIZATION AND APPLICATION TO THE SEPARATION OF PROTEINS AND OTHER NEUTRAL AND CHARGED SPECIES\*

### Introduction

Both polymer-based [1-3] and silica-based [4-6] monoliths have been introduced to CEC. The majority of polymer-based monoliths have been prepared by an *in situ* polymerization, whereby at least one of the monomers involved carries a fixed charge to support a relatively strong electroosmotic flow (EOF) [7]. On the other hand, for silica-based monoliths, the charge necessary for EOF is furnished by the ionization of existing silanol groups on the surface of the monolith [5, 8]. Due to the weak acidity of silanols, the resulting silica monolith can only produce sufficient EOF at  $\text{pH} > 5.0$ , a fact that can put some limits on the utility of such phases over a wide range of mobile phase pH. Furthermore, to successfully perform reversed-phase CEC (RP-CEC) of

---

\* The content of this chapter has been published in *The Analyst*, 2003, 128, 1249-1256

proteins with little or no electrostatic interactions (i.e., minimum solute binding), it is preferred that the surface charge supporting the EOF be positive.

It is therefore the aim of this contribution to design monolithic silica stationary phases for RP-CEC possessing octadecyl ligands for retention and selectivity and fixed positive charges to support a relatively strong EOF for mobile phase pH < 5.0. These kinds of phases are referred to as amphiphilic stationary phases to reflect the presence of both hydrophobic moieties and polar charged functions on the surface of the monolith.

## Experimental

### Instrumentation

The instrument used for CEC was a P/ACE 5510 CE system from Beckman Instrument (Fullerton, CA, USA) equipped with a diode-array detector and a data handling system comprised of an IBM personal computer and P/ACE software. For column fabrication, temperature programming was carried out using a Sigma 3 Gas Chromatograph from Perkin-Elmer (Norwalk, CT, USA). Constant temperature processes were done using an Isotemp oven from Fisher Scientific (Pittsburgh, PA, USA).

## Chemicals and Materials

Sodium phosphate monobasic, phosphoric acid and ammonium hydroxide were purchased from Mallinckrodt (Paris, KY, USA). Ammonium acetate, glacial acetic acid, hydrochloric acid, sulfuric acid, HPLC grade acetonitrile (ACN), aniline and benzene were obtained from Fisher Scientific (Fair Lawn, NJ, USA). Sodium hydroxide and *N,N*-Dimethylformamide (DMF) were purchased from EM Science (Cherry Hill, NJ, USA). Tetramethylorthosilicate (TMOS), poly (ethylene glycol) (PEG) MW = 10,000, 3-chloro-4-methylaniline (99+%), 4-chloroaniline (98%), 3,4-dichloroaniline (98%), [3-(trimethoxysilyl)propyl]octadecyldimethyl ammonium chloride (TODAC), octadecylamine, all of the alkyl phenyl ketones (APK's), and all of the alkyl benzenes (AB's) were from Aldrich Chemical Co. Inc. (Milwaukee, WI, USA). 3-Methylaniline was from Fluka Chemika (Ronkonkoma, NY, USA). Ethanol was purchased from Pharmco (Brookfield, CT, USA). Horse heart cytochrome c, bovine pancreas ribonuclease A, bovine milk  $\beta$ -lactoglobulin B, horse skeletal muscle myoglobin, bovine pancreas  $\alpha$ -chymotrypsinogen A, bovine erythrocyte carbonic anhydrase, chicken egg white lysozyme and the phenylthiohydantoin amino acids (PTH-AA) were from Sigma (St. Louis, MO, USA). ( $\gamma$ -Glycidoxypropyl)trimethoxysilane ( $\gamma$ -GPTS) was purchased from Huls America Inc. (Bristol, PA, USA). Chloropropyltrimethoxysilane (CPTS) was obtained from Dow Corning (Midland, MI, USA). *N,N*-Dimethyloctadecylamine (DMODA) was purchased from Acros Organics (New Jersey, USA). Fused-silica capillaries with an internal diameter of 100  $\mu$ m and an outer diameter of 360  $\mu$ m were from Polymicro Technologies (Phoenix, AZ, USA).

## Preparation of the Silica Backbone

Optimum conditions for fabricating the silica backbone was established in chapter III (Ref. [8]). This method was a modified version of the one previously described by Ishizuka *et al.* [4]. The following is a brief summary of the optimized procedure. A segment of 100- $\mu\text{m}$  I.D. fused-silica capillary of a desired length was pre-treated hydrothermally by rinsing with water and heating in a GC oven [9]. After pre-treatment was complete, the capillary was injected with a polymerizing mixture containing TMOS. This mixture was prepared by adding 500  $\mu\text{L}$  of TMOS to a solution that contained 0.1325 g of PEG in 1250  $\mu\text{L}$  of 0.010 M acetic acid followed by stirring for 45 min at 0  $^{\circ}\text{C}$ . After the mixture was injected into the pre-treated capillary, the inlet and outlet ends of the capillary were formed into a circle by joining them together with a piece of Teflon tubing. The capillary was heated at 40  $^{\circ}\text{C}$  and allowed to react overnight. The resulting monolithic silica was rinsed with 0.010 M ammonium hydroxide then heated at 120  $^{\circ}\text{C}$  for 90 min. This ammonium hydroxide treatment for 90 min was found optimum for pore tailoring whereby the micropores within the monolithic silica skeleton are converted to mesopores [8]. The capillary was then dried by rinsing the column with 200 proof ethanol followed by purging with helium at 160 psi for 60 min. The final heat treatment was done in a GC oven by ramping the temperature at a rate of 2.5  $^{\circ}\text{C}/\text{min}$  from 30  $^{\circ}\text{C}$  (2 min hold time) to 180  $^{\circ}\text{C}$  (60 min hold time), then again ramped at 2.5  $^{\circ}\text{C}/\text{min}$  to a final temperature of 330  $^{\circ}\text{C}$  where it was held for 21 hrs.

After the silica backbone was generated, stationary phase attachment was done by one of the procedures described in the following section. Columns that were 27 cm long

and free of voids were cut from the original capillary. The columns were rinsed with water and windows were formed 7 cm from the outlet end by placing that portion of the capillary in fuming sulfuric acid until the polyimide coating was removed. After subsequent rinses of ACN and water, the capillaries were installed into the P/ACE cartridges and were ready to be used.

#### Surface Modification of the Silica Monoliths – Formation of Bonded Phases

Figure 1 shows a schematic of the three reaction pathways investigated for the generation of the desired cationic C<sub>18</sub> stationary phase. These steps were performed after the final heat treatment discussed in the previous section. For path A, 100 μL of TODAC was dissolved in 100 μL of DMF. This solution was pushed through the column and reacted at 120 °C for 1 hr. This step was repeated 3 times. The resulting stationary phase is denoted C<sub>18</sub>-NQ1. The surface modification described in path A was originally introduced by Zhang and El Rassi [10] and then used by Yang and El Rassi [11] for the preparation of silica microparticles with surface bound cationic octadecyl ligands for use in HPLC and CEC, respectively. For path B, 100 μL of CPTS was dissolved in 100 μL of DMF. This solution was perfused through the column and reacted at 120 °C for 1 hr. This step was repeated 3 times. After rinsing with DMF followed by toluene, the column was filled with a solution consisting of 100 μL DMODA and 100 μL of toluene and reacted for 1 hr at 70 °C. This step was repeated an additional three times. This stationary phase is denoted C<sub>18</sub>-NQ2. For path C, 20 μL of γ-GPTS was dissolved in 200 μL of toluene. This solution was introduced into the column and reacted at 110 °C for



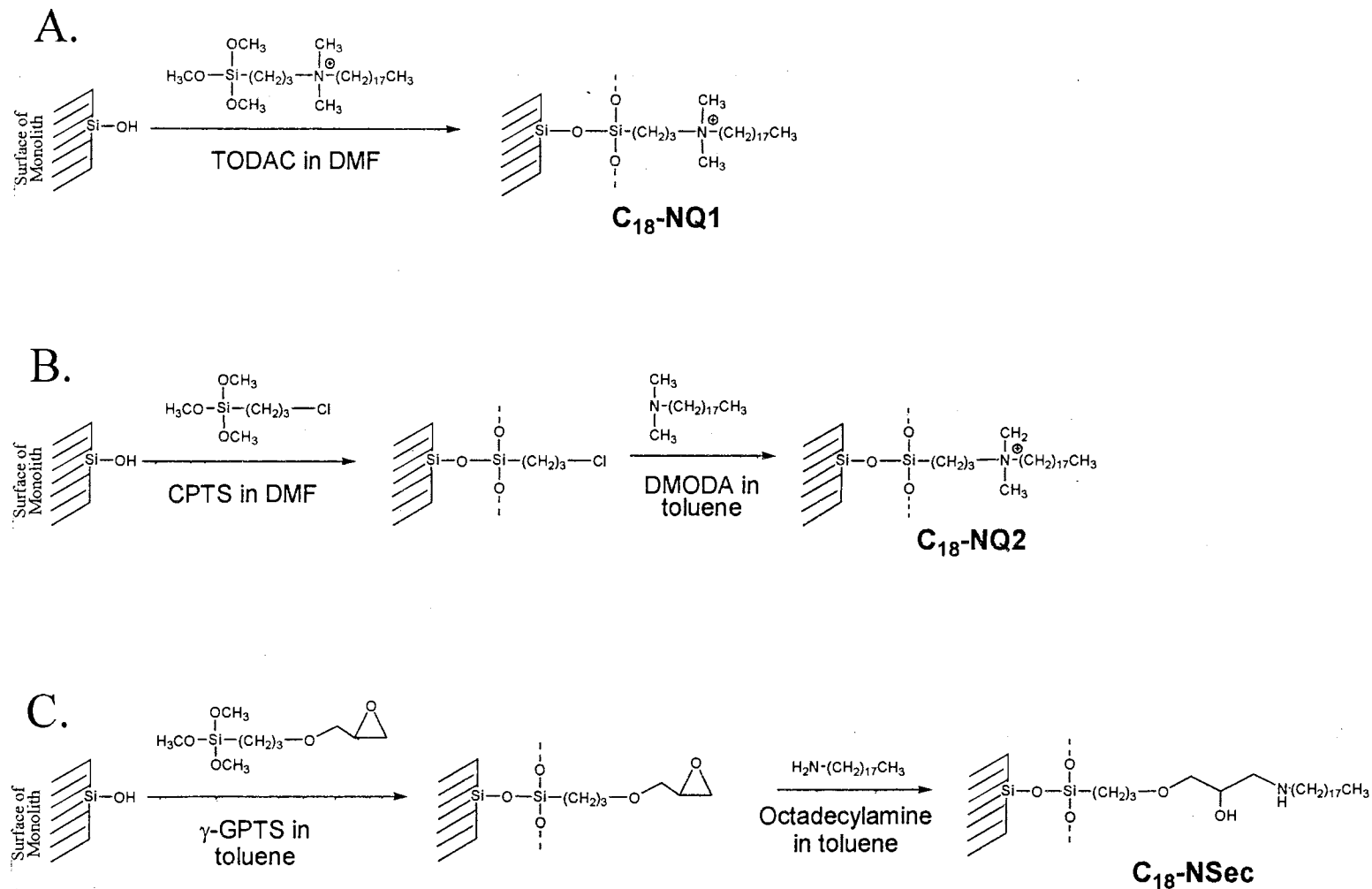


**Figure 1.** Schematic of the 3 reaction pathways investigated. (A) Reaction of TODAC in DMF at 120 °C. (B) Reaction of CPTS in DMF at 120 °C followed by reaction of DMOA in toluene at 70 °C. (C) Reaction of  $\gamma$ -GPTS in toluene at 110 °C followed by reaction with octadecylamine in toluene at 80 °C.

1 hr. This step was repeated 3 times. After rinsing with toluene the column was filled with a 5% octadecylamine solution (wt./v) in toluene and reacted at 80 °C for 1 hr. This step was repeated twice, and then the final reaction was done overnight. The resulting stationary phase is denoted C<sub>18</sub>-NSec.

## Results and Discussion

### Characterization of the Stationary Phases

As mentioned earlier, the focus of this research was to generate an amphiphilic stationary phase comprised of a fixed positive charge and a neutral ligand (C<sub>18</sub>). A stationary phase of this nature could provide a strong anodic EOF over a wide range of pH values while also exhibiting reversed-phase chromatography (RPC) retention behavior. Three separate methods are described for the fabrication of an alkyl amine ligand that exhibits such properties (see experimental). In an attempt to characterize the behavior and performance of these monoliths, the homologous series of alkyl benzenes (AB's) were used as model compounds, and the results are described in the following sections.

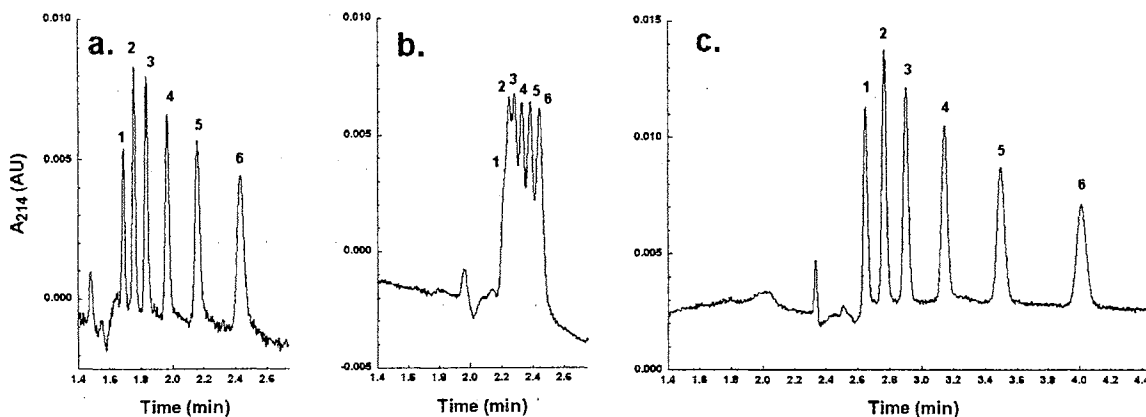
Table 1 shows a comparison of the retention factor  $k'$  and selectivity factor  $\alpha$  for AB's observed for the three cationic octadecyl columns generated by the 3 pathways shown in Fig. 1, and for an ODS monolithic column. Typical electrochromatograms for AB's obtained on the three cationic octadecyl monolithic stationary phases are shown in Fig. 2. Note that the ODS data were obtained at 65% (v/v) acetonitrile (ACN) rather than

TABLE 1.

RETENTION FACTOR ( $k'$ ) AND SELECTIVITY FACTOR ( $\alpha$ ) FOR AB'S  
OBTAINED WITH THE DIFFERENT C<sub>18</sub>-MONOLITHS AT 60% (v/v)  
ACETONITRILE (65% (v/v) FOR ODS COLUMN).

Analytes	C <sub>18</sub> -NQ1		C <sub>18</sub> -NQ2		C <sub>18</sub> -Nsec		ODS	
	$k'$	$\alpha$	$k'$	$\alpha$	$k'$	$\alpha$	$k'$	$\alpha$
Benzene	0.14		0.12		0.13		0.31	
		1.29		1.08		1.38		1.45
Toluene	0.18		0.13		0.18		0.45	
		1.33		1.15		1.33		1.40
Ethyl benzene	0.24		0.15		0.24		0.63	
		1.38		1.13		1.42		1.48
Propyl benzene	0.33		0.17		0.34		0.93	
		1.36		1.18		1.44		1.51
Butyl benzene	0.45		0.20		0.49		1.40	
		1.42		1.15		1.47		1.51
Amyl benzene	0.64		0.23		0.72		2.11	

60% (v/v) ACN. The ODS column exhibits substantially higher retention than any of the octadecyl amine columns, and may be due to the fact that the octadecyl moiety of the ODS stationary phase does not incorporate a fixed charge (i.e., it is more hydrophobic). This may also reflect a higher phase ratio for the ODS column. Columns C<sub>18</sub>-NQ1 and C<sub>18</sub>-Nsec show very similar retention and selectivity, indicating that they possess similar "hydrophobic" phase ratios. Column C<sub>18</sub>-NQ2 displayed very little retention compared to the other alkyl amine columns with benzene and toluene co-eluting (see Fig. 2). This may indicate that the reaction between the chloropropylsilyl-monolith and DMODA (see reaction scheme in Fig. 1) is sluggish and consequently did not yield a sufficient surface coverage with octadecyl ligands (i.e., low phase ratio) to ensure retention and selectivity.



**Figure 2.** Comparison of the separations of AB's achieved by columns (a)  $C_{18}$ -NQ1, (b)  $C_{18}$ -NQ2 and (c)  $C_{18}$ -NSec. Conditions: monolithic capillary column, 20/27 cm x 100  $\mu$ m I.D.; hydro-organic mobile phase, 10 mM sodium phosphate monobasic (pH 2.5) at 60% ACN (v/v); voltage, -20kV; wavelength, 214 nm; column temperature, 20  $^{\circ}$ C. Solutes: 1, benzene; 2, toluene; 3, ethylbenzene; 4, propylbenzene; 5, butylbenzene; 6, amylbenzene.

Separation efficiency for  $C_{18}$ -NQ1 and  $C_{18}$ -NSec are also very comparable despite the difference in flow velocity, which were about 2.2 mm/s for the former and 1.4 mm/s for the latter under the conditions stated in Fig. 2. The  $C_{18}$ -NQ1 column yielded 163,000 plates/m versus 157,000 plates/m for  $C_{18}$ -NSec column. Again, column  $C_{18}$ -NQ2 does not achieve this level of performance, and only 85,000 plates/m were obtained. This lower separation efficiency may be attributed to the suspected low phase ratio.

Once it was established that columns  $C_{18}$ -NQ1 and  $C_{18}$ -NSec were viable separation media, a van Deemter study was performed on each column to evaluate performance over a wider range of mobile phase velocities at pH 2.5. Figure 3 shows the results of the study in terms of plate height versus EOF velocity. Both columns generated relatively high separation efficiencies over a fairly wide range of mobile phase linear velocities. For a mobile phase velocity range of 0.76 mm/s to 2.17 mm/s (corresponding to an applied voltage range of -9 kV to -24 kV) column  $C_{18}$ -NSec exhibited an average

efficiency of 140,000 plates/m. For a mobile phase velocity range of 0.78 to 2.83 mm/s (corresponding to an applied voltage range of -9 kV to -27 kV) column C<sub>18</sub>-NQ1 exhibited an average separation efficiency of 169,000 plates/m.

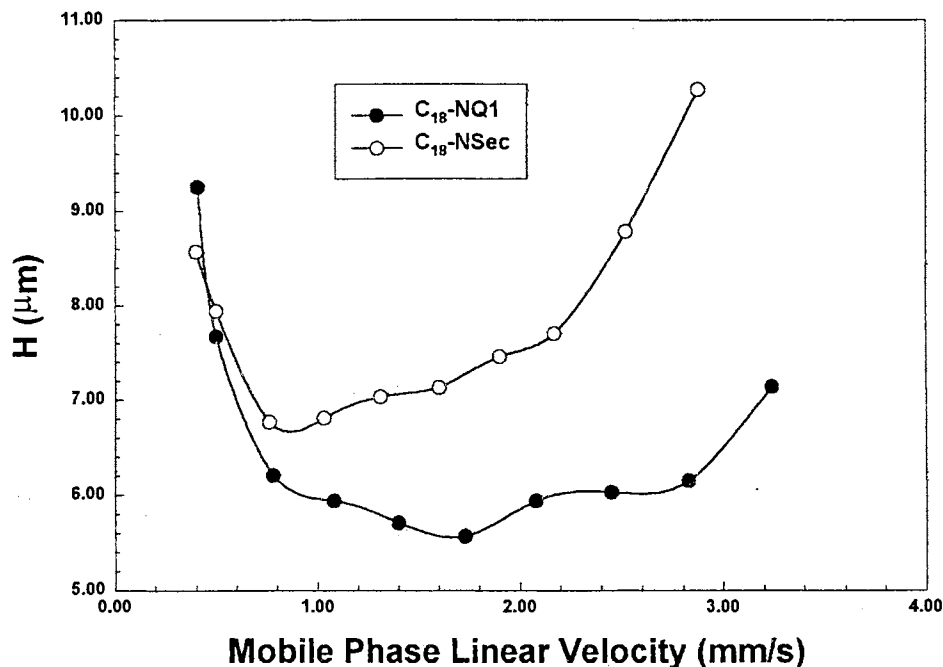


**Figure 3.** The van Deemter plots for columns C<sub>18</sub>-NQ1 and C<sub>18</sub>-NSec. Conditions: monolithic capillary column, 20/27 cm x 100 μm I.D.; hydro-organic mobile phase, 10 mM sodium phosphate monobasic (pH 2.5) at 60% ACN (v/v); voltage was varied between -5 and -30kV; wavelength, 214 nm; column temperature, 20 °C.

Figure 4 shows the effect of increasing mobile phase pH on the EOF velocities for both columns. In all instances, column C<sub>18</sub>-NQ1 exhibits a higher mobile phase linear velocity than column C<sub>18</sub>-NSec. Since both columns have similar retentive property toward AB's, they must have similar phase ratio, a condition that excludes attributing the lower mobile phase linear velocity obtained on C<sub>18</sub>-NSec to a lower phase ratio. Rather, since column C<sub>18</sub>-NQ1 incorporates a quaternary amine within the ligand, all molecules will contain a completely ionized nitrogen atom regardless of pH. However, column

$C_{18}$ -NSec possesses a secondary amine on its surface and, therefore, the degree of ionization is dependent upon an equilibrium at the pH of the mobile phase. The mobile

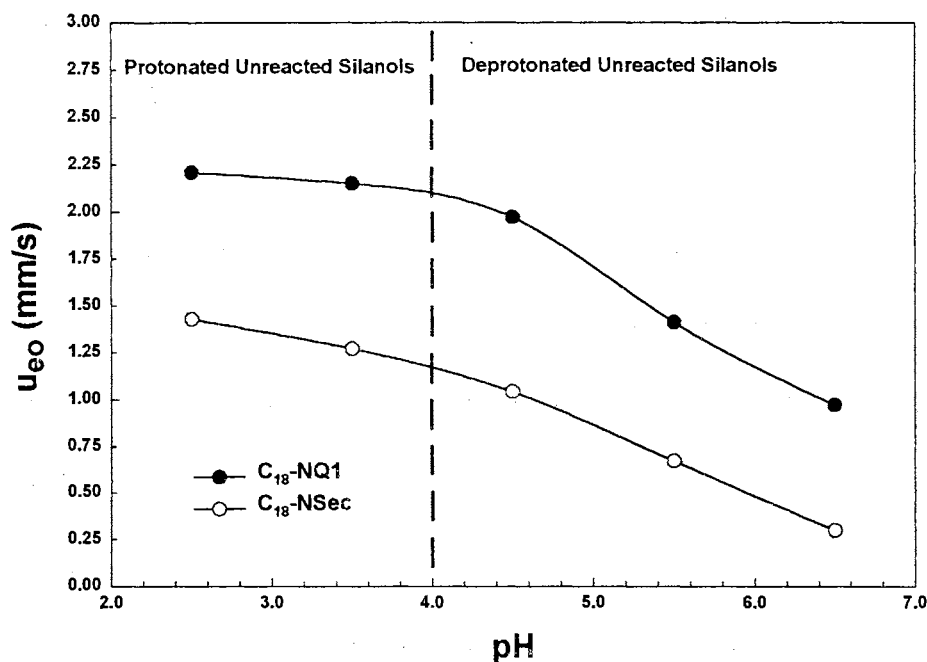


**Figure 4.** Plot of mobile phase velocity as a function of pH for columns  $C_{18}$ -NQ1 and  $C_{18}$ -NSec. Conditions: monolithic capillary column, 20/27 cm x 100  $\mu$ m I.D.; hydro-organic mobile phase, 10 mM sodium phosphate monobasic (pH varied between 2.5-6.5) at 60% ACN (v/v); voltage, -20kV; wavelength, 214 nm; column temperature, 20 °C.

phase velocities for both columns decrease with an increase in pH as a result of ionizing silanol groups that lead to the lowering of the net positive charge density of the monoliths. The dashed line in Fig. 4 divides the pH ranges that correspond to protonated and deprotonated unreacted silanol groups. Surprisingly, at pH values up to 6.5, column  $C_{18}$ -NSec still contains an excess of cationic secondary amine groups with respect to ionized silanol groups to support a relatively low anodic EOF.

## Evaluation of the Chromatographic Retention

Neutral and slightly polar solutes The retentive properties of the cationic C<sub>18</sub>-monoliths under investigation were evaluated with a group of five anilines including aniline (pK<sub>a</sub> = 4.70), 3-methylaniline (pK<sub>a</sub> = 4.91), 4-chloroaniline (pK<sub>a</sub> = 4.06), 3-chloro-4-methylaniline (pK<sub>a</sub> = 4.05) and 3,4-dichloroaniline (pK<sub>a</sub> = 3.33). To further gain insight into the retention mechanism, the results were compared to those obtained on the ODS monolith previously studied [8]. These weak bases were chosen for their ability to behave as neutral compounds at pH > 6 and as positively charged species at pH ≤ pK<sub>a</sub>. Table 2 compares the retention factors (k') for each analyte and the selectivity factor (α) on the ODS, C<sub>18</sub>-NQ1 and C<sub>18</sub>-NSec columns at pH 7.0. In all cases, the elution order is

TABLE 2.

RETENTION FACTOR (k') AND SELECTIVITY FACTOR (α) FOR ANILINES OBTAINED ON THE DIFFERENT C<sub>18</sub>-MONOLITHS USING 5 mM SODIUM PHOSPHATE MONOBASIC (pH 7.0) AT 40% (v/v) ACETONITRILE.

Analytes	ODS		C <sub>18</sub> -NQ1		C <sub>18</sub> -NSec	
	k'	α	k'	α	k'	α
Aniline	0.19		0.19		0.20	
		1.68		1.53		1.60
3-Methylaniline	0.32		0.29		0.32	
		1.31		1.55		1.66
4-Chloroaniline	0.42		0.45		0.53	
		1.69		1.51		1.66
3-Chloro-4-methylaniline	0.71		0.68		0.88	
		1.18		1.41		1.51
3,4-Dichloroaniline	0.84		0.96		1.33	

the same following what is expected for an RPC retention mechanism (i.e., chloro-substituted anilines are more retained than methyl-substituted anilines and disubstituted anilines are more retained than mono-substituted anilines). However, and as expected, the extent of solute retention differed from one type of C<sub>18</sub>-monolith to another. Column C<sub>18</sub>-NQ1 exhibited slightly less retention for 3-methylaniline and 3-chloro-4-methylaniline than the ODS column, with slightly more retention for 4-chloroaniline and 3,4-Dichloroaniline. In all instances, column C<sub>18</sub>-NSec provided retention that was greater than or equal to the ODS and C<sub>18</sub>-NQ1 columns for all the anilines. These differences may be attributed to the existing differences in the nature of charges and other functionalities on the surface of the different C<sub>18</sub>-monoliths. All three monoliths share the presence of the octadecyl ligand (i.e., main ligand responsible for RPC behavior) and some residual un-reacted silanols on the surface. In addition, C<sub>18</sub>-NQ1 possesses quaternary amine functions while C<sub>18</sub>-NSec has secondary amine functions, hydroxyl groups and ether linkages (see Fig.1 for structures). This may explain the higher retention exhibited by the C<sub>18</sub>-NSec column *via* additional polar interactions of the anilines with the existing polar groups of the stationary phase (e.g., hydroxyl and ether groups). Although the ODS column exhibited much higher retention towards the neutral, non-polar alkyl-benzenes (see Table 1) than the two cationic C<sub>18</sub>-monoliths, the neutral, slightly polar anilines can undergo polar and non-polar interactions with the stationary phases. Figure 5 shows the separation achieved for the anilines at pH 7.0 for column C<sub>18</sub>-NQ1. At pH 7.0, there is still a sufficient flow (1.27 mm/s) for column C<sub>18</sub>-NQ1 to complete the separation in less than 6 minutes. Column C<sub>18</sub>-NSec, however, only had a



mobile phase velocity of 0.35 mm/s and required almost 25 min to complete the separation.

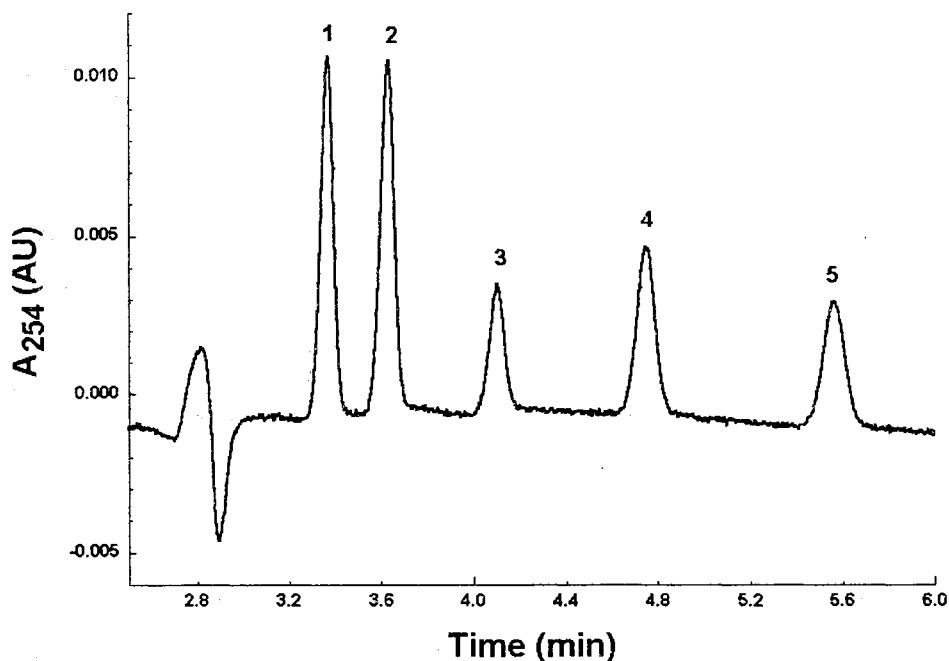


**Figure 5.** Separation of anilines on column  $C_{18}$ -NQ1. Conditions: monolithic  $C_{18}$ -NQ1 capillary column, 20/27 cm x 100  $\mu$ m I.D.; hydro-organic mobile phase, 5 mM sodium phosphate monobasic (pH 7.0) at 40% ACN (v/v); voltage, -20kV; wavelength, 254 nm; column temperature, 20 °C. Solutes: 1, aniline; 2, 3-methylaniline; 3, 4-chloroaniline; 4, 3-chloro-4-methylaniline; 5, 3,4-dichloroaniline.

The retentive properties of the cationic monolithic  $C_{18}$ -silica columns were also evaluated with some PTH-AA. Table 3 compares the retention factor ( $k'$ ) and selectivity factor ( $\alpha$ ) for the amino acids under investigation using ODS,  $C_{18}$ -NQ1 and  $C_{18}$ -NSec columns. While there is no difference in the elution order of the PTH-AA on the two cationic  $C_{18}$ -monoliths, many differences exist between the retention order of the two cationic monoliths and the ODS column. Figure 6 shows the separation achieved of the PTH-AA on column  $C_{18}$ -NQ1 in which 12 out of the 13 PTH-AA were separated. Peak

TABLE 3.

RETENTION FACTOR ( $k'$ ) AND SELECTIVITY FACTOR ( $\alpha$ ) FOR PTH-AA OBTAINED ON THE DIFFERENT C<sub>18</sub>-MONOLITHS USING 5 mM SODIUM PHOSPHATE MONOBASIC AT pH 6.0 (ODS) OR pH 2.5 (C<sub>18</sub>-NQ1 AND C<sub>18</sub>-NSec) AT 25% (v/v) ACETONITRILE.

<u>ODS</u>			<u>C<sub>18</sub>-NQ1</u>			<u>C<sub>18</sub>-NSec</u>		
<u>Analytes</u>	<u>k'</u>	<u><math>\alpha</math></u>	<u>Analytes</u>	<u>k'</u>	<u><math>\alpha</math></u>	<u>Analytes</u>	<u>k'</u>	<u><math>\alpha</math></u>
Asn	0.18		Gln	0.38		Gln	0.21	
		1.28			1.11			1.05
Ser	0.23		Asn	0.42		Asn	0.22	
		1.13			1.19			1.32
Gln	0.26		Ser	0.50		Ser	0.29	
		1.53			1.00			1.24
Gly	0.40		Gly	0.50		Gly	0.36	
		1.80			1.34			1.36
Ala	0.72		Ala	0.67		Ala	0.49	
		1.56			1.74			1.53
Tyr	1.12		Pro	1.17		Pro	0.75	
		1.98			1.07			1.13
Val	2.22		Tyr	1.25		Tyr	0.85	
		1.03			1.11			1.33
Met	2.28		Val	1.39		Val	1.13	
		1.10			1.18			1.11
Pro	2.50		Met	1.64		Met	1.25	
		1.98			1.53			1.65
Trp	4.96		Leu	2.51		Leu	2.06	
		1.03			1.95			1.82
Leu	5.11		Trp	4.90		Trp	3.75	
		1.44			1.93			1.58
Lys	7.36		Lys	9.45		Lys	5.92	

numbering is given on the basis of elution order for the ODS column. For C<sub>18</sub>-NSec, PTH-Gln, PTH-Pro, PTH-Leu, PTH-Gly and PTH-Ala have all shifted down in the elution order, while PTH-His, PTH-Tyr and PTH-Val have shifted up when compared to the ODS column. The cationic monoliths have higher retention factors for the PTH-AA

with polar side chains (i.e., the first to elute) whereas the ODS column gives higher retention factors for the PTH-AA with non-polar side chains (i.e., the last to elute) with the exception of PTH-Lys on column C<sub>18</sub>-NQ1. This is again another indication of the presence of some polar interactions (in addition to non-polar interactions) between the more polar solutes and the cationic C<sub>18</sub>-monoliths.

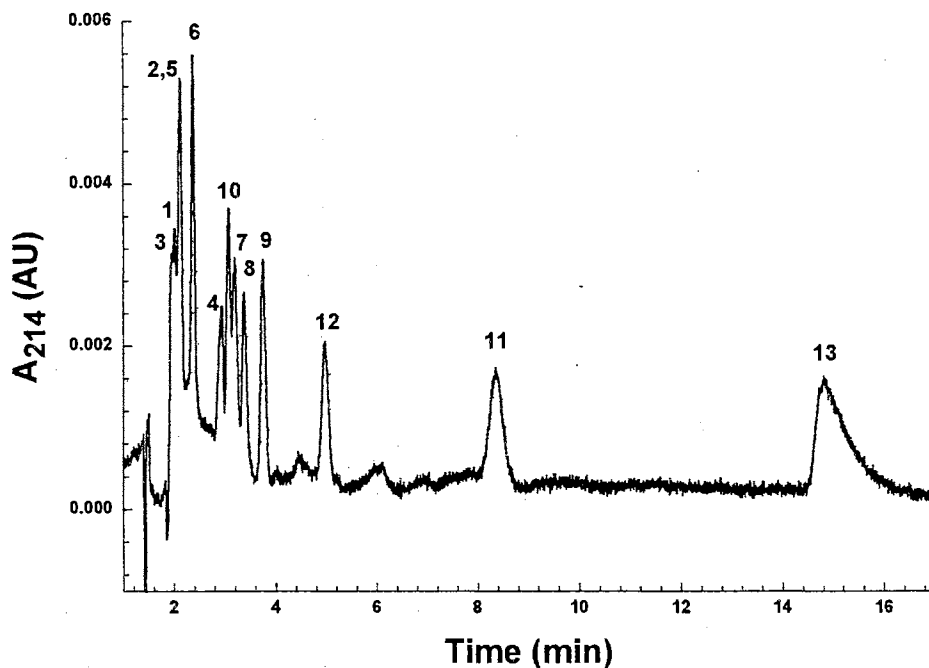


**Figure 6.** Separation of PTH-amino acids on column C<sub>18</sub>-NQ1. Conditions: monolithic C<sub>18</sub>-NQ1 capillary column 20/27 cm x 100  $\mu$ m I.D.; hydro-organic mobile phase, 5mM sodium phosphate monobasic (pH 2.5) at 25% (v/v) ACN; voltage, -20kV; wavelength, 214 nm; column temperature, 20 °C. Solutes: 1, PTH-asparagine; 2, PTH-serine; 3, PTH-glutamine; 4, PTH-histidine; 5, PTH-glycine; 6, PTH-alanine; 7, PTH-tyrosine; 8, PTH-valine; 9, PTH-methionine; 10; PTH-proline, 11, PTH-tryptophan; 12, PTH-leucine; 13, PTH-( $\epsilon$ -phenylthiocarbamyl)-lysine.

Ionizable species Once again the anilines were selected as analytes due to the fact that they are ionized at pH 3.5, with the exception of 3,4-dichloroaniline, which exhibited no electrophoretic mobility and migrated as a neutral species in CZE. Table 4 shows the values of  $k^*_{cc}$ ,  $k^*_e$  and  $k^*$  for the anilines when analyzed on ODS, C<sub>18</sub>-NQ1 and C<sub>18</sub>-

TABLE 4.

VALUES OF RETENTION PARAMETERS FOR ANILINES OBTAINED ON THE DIFFERENT STATIONARY PHASES USING 5 mM SODIUM PHOSPHATE MONOBASIC (pH 3.5) AT 40% (v/v) ACNITRILE.

Analytes	ODS			C <sub>18</sub> -NQ1			C <sub>18</sub> -NSec		
	k* <sub>cc</sub>	k* <sub>e</sub>	k*	k* <sub>cc</sub>	k* <sub>e</sub>	k*	k* <sub>cc</sub>	k* <sub>e</sub>	k*
Aniline	-0.86	3.21	-0.41	1.13	-0.33	0.43	0.65	-0.34	0.10
3-Methylaniline	-0.86	3.48	-0.38	1.39	-0.36	0.52	0.84	-0.37	0.16
4-Chloroaniline	-0.58	0.78	-0.26	0.47	-0.08	0.35	0.49	-0.08	0.37
3-Chloro-4-methylaniline	-0.55	0.78	-0.19	0.66	-0.08	0.52	0.75	-0.08	0.61
3,4-Dichloroaniline	k' = 0.59			k' = 0.77			k' = 1.02		

NSec columns. Recall, these retention/migration parameters were defined previously in chapter I ( Refs. [8, 12, 13]).

Negative  $k_{cc}^*$  and  $k^*$  values indicate elution of the analyte before  $t_0$ , and is observed with the ODS column. The more negative the values of  $k_{cc}^*$  and  $k^*$ , the earlier the elution of the peak occurs before the EOF marker. Negative  $k_e^*$  values indicate an electrophoretic mobility that is counter-directional to the EOF. This is the case for columns C<sub>18</sub>-NQ1 and C<sub>18</sub>-NSec. Columns C<sub>18</sub>-NQ1 and C<sub>18</sub>-NSec yielded almost identical  $k_e^*$  values for each aniline solute. Column C<sub>18</sub>-NQ1 exhibited higher  $k^*$  for aniline and 3-methylaniline than column C<sub>18</sub>-NSec, but column C<sub>18</sub>-NSec provided higher retention for the chloro-substituted anilines. The difference in elution order and extent of retention among the three C<sub>18</sub>-monoliths is again the result of the difference in charges and other functionalities on the surface of the three C<sub>18</sub>-monoliths.

Figure 7 compares the separations achieved for the anilines on the two cationic C<sub>18</sub>-monolithic columns. Figures 7a and b show the difference in elution order. For column C<sub>18</sub>-NSec (Fig. 7a), aniline is located between 4-chloroaniline and 3-chloro-4-methylaniline and 3-methylaniline is located between 3-chloro-4-methylaniline and 3,4-dichloroaniline. For column C<sub>18</sub>-NQ1 (Fig. 7b), aniline elutes after 3,4-dichloroaniline and 3-methylaniline is the last to elute. Figure 7c illustrates the effect of increasing the ionic strength of the mobile phase on the elution order. When the electrolyte concentration is increased from 5 mM to 20 mM, the anilines elute as if they were uncharged (i.e., in order of increasing hydrophobicity). Increasing the ionic strength results in screening of the positive charges of the solutes by the electrolyte counter ions, which leads to differences in electrophoretic mobility [14] among the various anilines and

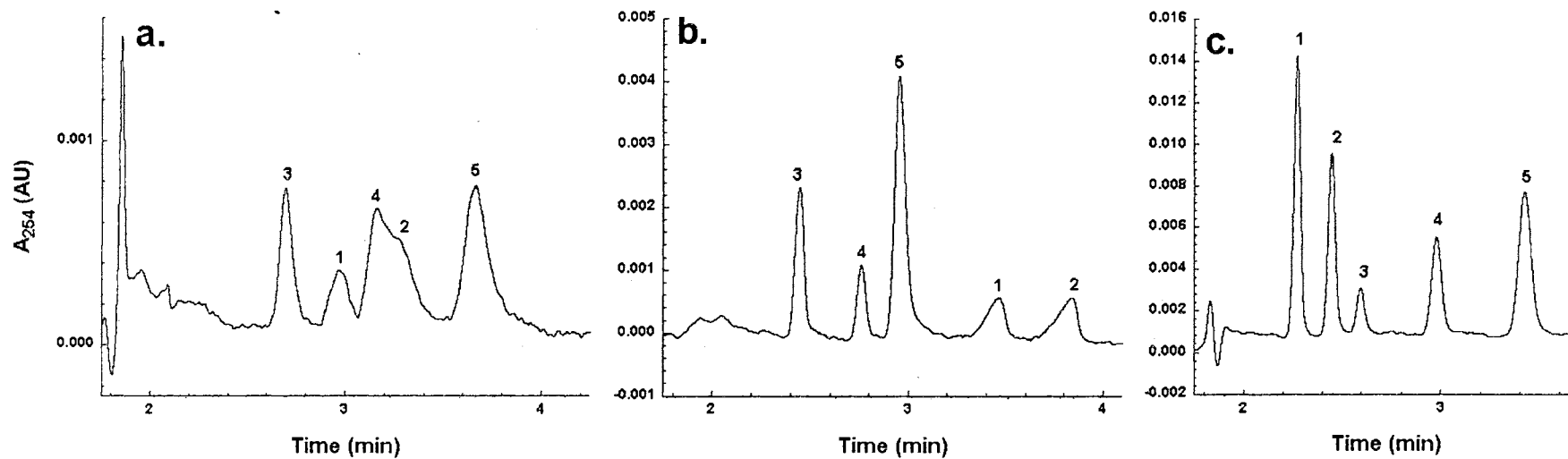


**Figure 7.** Comparison of aniline separations on column (a)  $C_{18}$ -NSec and (b and c)  $C_{18}$ -NQ1. Conditions: monolithic capillary column 20/27 cm x 100  $\mu$ m I.D.; hydro-organic mobile phase, (a and b) 5mM (c) 20mM sodium phosphate monobasic (pH 3.5) at 40% (v/v) ACN; voltage, -20kV; wavelength, 254 nm; column temperature, 20  $^{\circ}$ C. Peak designations the same as Figure 5.

to a decrease in electrostatic repulsion from the similarly charged stationary phase surface (i.e., increasing solute association with the stationary phase C<sub>18</sub> ligand). The net result is an elution order, which conforms to the hydrophobicity of the solute.

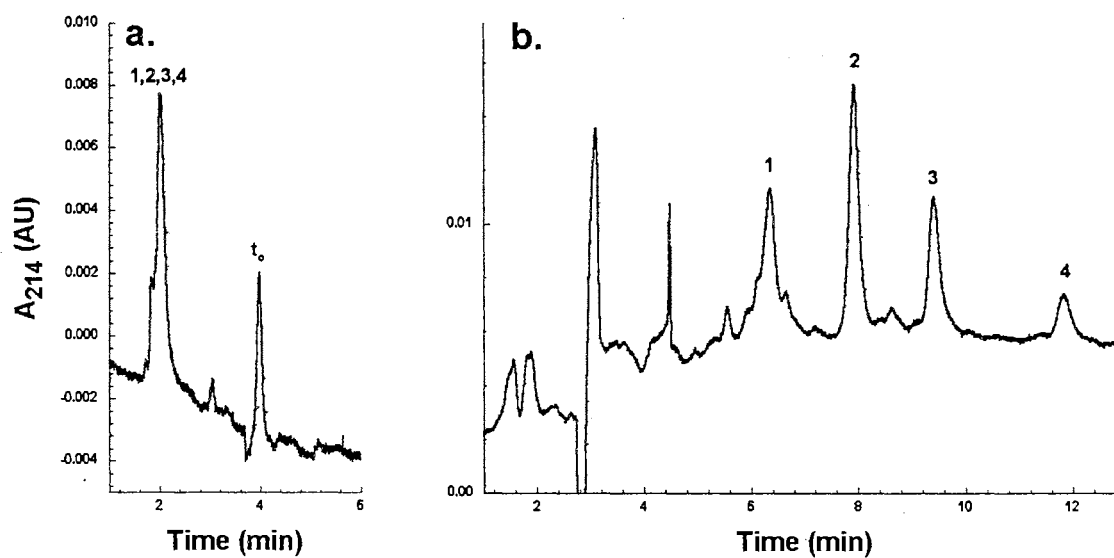
A group of seven standard proteins widely differing in pI values and molecular weight were also selected to study the retention behavior of charged solutes in CEC. Table 5 gives the values of  $k^*_{cc}$ ,  $k^*_e$  and  $k^*$  for each of the proteins analyzed on column C<sub>18</sub>-NSec. As can be seen in this table, the proteins exhibited similar velocity factor  $k^*_e$

TABLE 5.

VALUES OF RETENTION PARAMETERS OF SOME STANDARD PROTEINS  
OBTAINED ON C<sub>18</sub>-NSec COLUMN USING 20 mM SODIUM PHOSPHATE  
MONOBASIC (pH 2.5) AT 60% (v/v) ACETONITRILE.

Analytes	$k^*_{cc}$	$k^*_e$	$k^*$
Ribonuclease A	0.94	-0.14	0.67
Carbonic anhydrase	1.30	-0.17	0.91
Lysozyme	1.34	-0.17	0.93
$\alpha$ -Chymotrypsinogen A	1.34	-0.15	0.99
Cytochrome C	1.44	-0.17	1.03
Myoglobin	1.58	-0.18	1.12
$\beta$ -Lactoglobulin B	2.00	-0.18	1.48

because at pH 2.5 the proteins are mainly positively charged regardless on their pI values. This translates into little difference in migration times in CZE as shown in Fig. 8a. Figure 8b shows the separation of ribonuclease A, carbonic anhydrase, myoglobin and  $\beta$ -lactoglobulin B. Since all proteins under investigation displayed similar migration times in CZE (Fig. 8a), it can be stated that the electrophoretic component has little or no impact on the separation of these proteins in CEC and the resolution obtained in Fig. 8a can be totally attributed to differences in their association with the  $C_{18}$  ligands of the stationary phase.



**Figure 8.** Separation of proteins. Conditions: (a) CZE with open tubular fused silica column and (b)  $C_{18}$ -NSec monolithic capillary column 20/27 cm x 100  $\mu$ m I.D.; hydro-organic mobile phase, 20mM sodium phosphate monobasic (pH 2.5) at 60% (v/v) ACN; voltage, -20kV; wavelength, 214 nm; column temperature, 20  $^{\circ}$ C. Solutes: 1, ribonuclease A; 2, carbonic anhydrase; 3, myoglobin; 4,  $\beta$ -lactoglobulin B.



## Conclusions

Three different synthetic routes have been introduced and evaluated for the preparation of amphiphilic silica-based monoliths possessing surface-bound octadecyl ligands and positively charged groups (e.g., quaternary and secondary amines). These amphiphilic stationary phases yielded anodic electroosmotic flow (EOF) over a wide range of mobile phase pH, and allowed the rapid separation of neutral and charged species including anilines, PTH-amino acids and proteins. Although they exhibited RPC retention behavior, the amphiphilic monoliths exhibited different elution order and extent of retention towards slightly polar species (e.g., anilines and PTH-AA) when compared to ODS monoliths due to the presence of charged functionalities and other polar groups on the surface of the amphiphilic monoliths. The CEC retention factor  $k^*$  and velocity factor  $k_e^*$ , which reflects the contribution of the electrophoretic mobility, were evaluated for charged solutes such as anilines and proteins.

## References

1. Fujimoto, C., *Anal. Chem.* **1995**, *67*, 2050-2053.
2. Peters, E.C., Petro, M., Svec, F., Frechet, J.M.J., *Anal. Chem.* **1997**, *69*, 3646-3649.
3. Palm, A., Novotny, M.V., *Anal. Chem.* **1997**, *69*, 4499-4507.
4. Ishizuka, N., Minakuchi, H., Nakanishi, K., Soga, N., Nagayama, H., Hosoya, K., Tanaka, C.K., *Anal. Chem.* **2000**, *72*, 1275-1280.
5. Tanaka, N., Nagayama, H., Kobayashi, H., Ikegami, T., Hosoya, K., Ishizuka, N., Minakuchi, H., Nakanishi, K., Cabrera, K., Lubda, D., *J. High Resolut. Chromatogr.* **2000**, *23*, 111-116.
6. Tanaka, N., Kobayashi, H., *Capillary electrochromatography on monolithic silica columns*, in *Capillary Electrochromatography*, F. Svec, Editor. 2001, Elsevier: Amsterdam, pp. 165-181.
7. Hilder, E.F., Svec, F., Frechet, J.M.J., *Electrophoresis* **2002**, *23*, 3934-3953.
8. Allen, D., El Rassi, Z., *Electrophoresis* **2003**, *24*, 408-420.
9. Hayes, J.D., Malik, A., *Anal. Chem.* **2000**, *72*, 4090-4099.
10. Zhang, Y., El Rassi, Z., *J. Liq. Chromatogr.* **1995**, *18*, 3373-3396.
11. Yang, C., El Rassi, Z., *Electrophoresis* **2000**, *21*, 1977-1984.
12. Bedair, M., El Rassi, Z., *Electrophoresis* **2002**, *23*, 2938-2948.
13. Bedair, M., El Rassi, Z., *J. Chromatogr. A* **2003**, in press.
14. Mechref, Y., Ostrander, G.K., El Rassi, Z., *J. Chromatogr. A* **1997**, *792*, 75-82.

## CHAPTER V

# CAPILLARY ELECTROCHROMATOGRAPHY WITH MONOLITHIC SILICA COLUMNS. PREPARATION OF HYDROPHILIC SILICA MONOLITHS HAVING SURFACE-BOUND CYANO GROUPS: CHROMATOGRAPHIC CHARACTERIZATION AND APPLICATION TO THE SEPARATION OF CARBOHYDRATES, NUCLEOSIDES, NUCLEIC ACID BASES AND OTHER NEUTRAL POLAR SPECIES

### Introduction

Thus far, the vast majority of capillary electrochromatography (CEC) separations have been performed using reversed-phase (RP) mode (for typical references see [1-11]) by incorporating non-polar stationary phases (e.g., C<sub>18</sub> phases) and more polar hydro-organic mobile phases (e.g., acetonitrile-water, alcohol-water mixtures). This fact has often given the impression that CEC is simply a reversed-phase chromatography technique without moving parts (i.e., without pumps) whereby an electric field is applied to the capillary column to move the mobile phase across the capillary by the so-called electroosmotic flow (EOF). Although RP-CEC is the technique of choice for the separation of a wide range of hydrophobic to slightly polar compounds, the separation of very polar compounds (e.g., carbohydrates, nucleosides, amino acids) by RP-CEC

requires the use of plain aqueous electrolyte mobile phases to allow sufficient retention and selectivity for polar compounds. Unfortunately, the highly aqueous condition of the mobile phase combined with a non-wettable stationary phase usually leads to bubble formation in CEC and interruption of the separation process.

Normal-phase chromatography (NPC) employing polar stationary phases and less polar mobile phases (e.g., organic solvent mixtures) has proved to be very efficient for the separation of polar species by HPLC [12]. Since a wide variety of polar stationary phases (e.g., bare silica gels and silica bonded polar phases such as amino, polyamine, cyano, amide, hydroxylic, poly(2-hydroxyethyl aspartamide), cyclodextrin phases, ion-exchange resins, etc.) can be utilized to achieve NPC, the more generic term “hydrophilic interaction chromatography” was proposed in 1990 by Alpert [13] to cover all forms of chromatography driven by polar (hydrophilic) interactions. As in NP-HPLC, normal phase CEC (NP-CEC) is expected to yield better performance than RP-CEC for polar compounds. Despite this fact, only a few attempts have surfaced. These include the use of bare silica microparticles [14-16], cellulose-based packing materials [15], amino phases consisting of a macroporous polymer-based monolith [17, 18], strong cation-exchange silica based particles (e.g., poly(2-sulfoethyl-aspartamide)-silica) [19] and a hydrophilic macroporous weak anion-exchange polymer-based monolith [20]. All of these investigations are initial studies on NP-CEC and further research and development are needed in this area of CEC to enlarge the scope of applications using CEC.

Thus, it is the aim of this chapter to investigate NP-CEC with hydrophilic silica-based monoliths toward the separation of polar species. In this regard, two different

synthetic schemes have been investigated to produce hydrophilic silica monoliths with surface bound cyano groups.

## Experimental

### Instrumentation

The instrument used for CEC was a P/ACE 5510 CE system from Beckman Instrument (Fullerton, CA, USA) equipped with a diode-array detector and a data handling system comprised of an IBM personal computer and P/ACE software. For column fabrication, temperature programming was carried out using a Sigma 3 Gas Chromatograph from Perkin-Elmer (Norwalk, CT, USA). Constant temperature processes were done using an Isotemp Oven from Fisher Scientific (Pittsburgh, PA, USA).

### Chemicals and Materials

Sodium phosphate monobasic, phosphoric acid, thiourea and ammonium hydroxide were purchased from Mallinckrodt (Paris, KY, USA). Molecular biology grade tris (hydroxymethyl) aminomethane (Tris), ammonium acetate, glacial acetic acid, hydrochloric acid, sulfuric acid, methylene chloride, phenol (90%), resorcinol, catechol, hydroquinone, HPLC grade methanol and HPLC grade acetonitrile, were obtained from Fisher Scientific (Fair Lawn, NJ, USA). Sodium hydroxide, formamide and *N,N*-

dimethylformamide (DMF) were purchased from EM Science (Cherry Hill, NJ, USA). Toluene, triethylamine (TEA) (99+%), 3-hydroxypropionitrile (3-HPN) (97%), 2,6-lutidine (99+%), tetramethylorthosilicate (TMOS) (99+%), boron trifluoride (BF<sub>3</sub>) diethyl etherate, poly (ethylene glycol) (PEG) MW = 10,000, and all of the chlorophenols including 2-chlorophenol (2-CP), 2,4-dichlorophenol (2,4-DCP), 3,4,5-trichlorophenol (3,4,5-TCP) and 2,4,5-TCP were from Aldrich Chemical Co. Inc. (Milwaukee, WI, USA). Ethanol was purchased from Pharmco (Brookfield, CT, USA). Uracil, cytosine, adenine, uridine, adenosine, inosine and cytidine were from Sigma (St. Louis, MO, USA). The p-nitrophenyl (pNP) derivatives of mono and oligosaccharides including pNP *N*-acetyl- $\beta$ -D-glucosaminide (pNP- $\beta$ GlcNAc), pNP *N*-acetyl- $\beta$ -D-galactosaminide (pNP- $\beta$ GalNAc), pNP *N,N'*-diacetyl- $\beta$ -D-chitobioside (pNP- $\beta$ chitobiose), pNP  $\alpha$ -D-glucopyranoside (pNP- $\alpha$ Glc), pNP  $\beta$ -D-glucopyranoside (pNP- $\beta$ Glc), pNP  $\beta$ -D-galactopyranoside (pNP- $\beta$ Gal), pNP  $\alpha$ -D-maltoside (pNP-Mal), pNP  $\alpha$ -D-maltotrioside, pNP  $\alpha$ -D-maltotetraoside and pNP  $\alpha$ -D-maltopentaoside as well as the o-nitrophenyl (oNP) derivatives of monosaccharides including oNP *N*-acetyl- $\alpha$ -D-glucosaminide (oNP- $\alpha$ GlcNAc) and oNP *N*-acetyl- $\beta$ -D-galactosaminide (oNP- $\beta$ GalNAc) were from Sigma. 3-Cyanopropyltrimethoxysilane (3-CPDMS) and ( $\gamma$ -glycidoxypropyl)trimethoxysilane ( $\gamma$ -GPTS) were purchased from Huls America Inc. (Bristol, PA, USA). Pyrogallol was purchased from J.T. Baker Chemical Co. (Phillipsburg, NJ, USA). Thymine was purchased from Nutritional Biochemicals Corporation (Cleveland, OH, USA). Fused-silica capillaries with an internal diameter of 100  $\mu$ m and an outer diameter of 360  $\mu$ m were purchased from Polymicro Technologies (Phoenix, AZ, USA).

### Preparation of the Silica Backbone

Monolithic columns were prepared by a method described in chapters III and IV (Refs. [21, 22]). This method was a modified version of the one previously described by Ishizuka et al. [23]. Briefly, a segment of 100- $\mu\text{m}$  I.D. fused-silica capillary of a desired length was pre-treated hydro-thermally by rinsing with water and heating in a GC oven [24]. After pre-treatment was complete, the capillary was injected with a polymerizing mixture containing TMOS. This mixture was prepared by adding 500  $\mu\text{L}$  of TMOS to a solution that contained 0.1325 g of PEG in 1250  $\mu\text{L}$  of 0.010 M acetic acid followed by stirring for 45 min at 0  $^{\circ}\text{C}$ . After the mixture was injected into the pre-treated capillary, the inlet and outlet ends of the capillary were formed into a circle by joining them together with a piece of Teflon tubing. The capillary was heated at 40  $^{\circ}\text{C}$  and allowed to react overnight. The resulting monolithic silica was rinsed with 0.010 M ammonium hydroxide then heated at 120  $^{\circ}\text{C}$  for 90 min. This 90-min ammonium hydroxide treatment was found optimum for pore tailoring whereby the micropores within the monolithic silica skeleton are converted to mesopores [22]. The capillary was then dried by rinsing the column with 200 proof ethanol followed by purging with helium at 160 psi for 60 min. The final heat treatment was done in a GC oven by ramping the temperature at a rate of 2.5  $^{\circ}\text{C}/\text{min}$  from 30  $^{\circ}\text{C}$  (2 min hold time) to 180  $^{\circ}\text{C}$  (60 min hold time), then again ramped at 2.5  $^{\circ}\text{C}/\text{min}$  to a final temperature of 330  $^{\circ}\text{C}$  where it was held for 21 hrs.

After the silica backbone was generated, stationary phase attachment was done by one of the procedures described in the following section. Columns that were 27 cm long and free of voids were cut from the original capillary. The columns were rinsed with

water and windows were formed at 7 cm from the outlet end by placing that portion of the capillary in fuming sulfuric acid until the polyimide coating was removed. After subsequent rinses of acetonitrile and water, the capillaries were installed into the P/ACE cartridges and were ready to be used.

### Surface Modification of the Silica Monoliths – Formation of Bonded Phases

Figure 1 shows a schematic of the two reaction pathways investigated for the generation of the desired cyano or cyano/hydroxy stationary phases. These steps were performed after the final heat treatment described in section 2.3. For path A, 20  $\mu\text{L}$  of 3-CPDCS and 10  $\mu\text{L}$  of 2,6-lutidine were dissolved in 200  $\mu\text{L}$  of methylene chloride. This solution was perfused through the column and reacted at 50  $^{\circ}\text{C}$  for 1 hr. This step was repeated 3 times. The resulting stationary phase is denoted CN-monolith. For path B, 20  $\mu\text{L}$  of  $\gamma$ -GPTS was dissolved in 200  $\mu\text{L}$  of toluene. This solution was introduced into the column and reacted at 110  $^{\circ}\text{C}$  for 1 hr. This step was repeated 3 times. After rinsing with toluene and then DMF, the column was filled with a solution containing 200  $\mu\text{L}$  of DMF, 20  $\mu\text{L}$  of 3-HPN and 3  $\mu\text{L}$  of  $\text{BF}_3$ . The column was allowed to react at room temperature for 1 hr. This step was repeated twice, and then the final reaction was done overnight. The resulting stationary phase is denoted CN-OH-monolith.



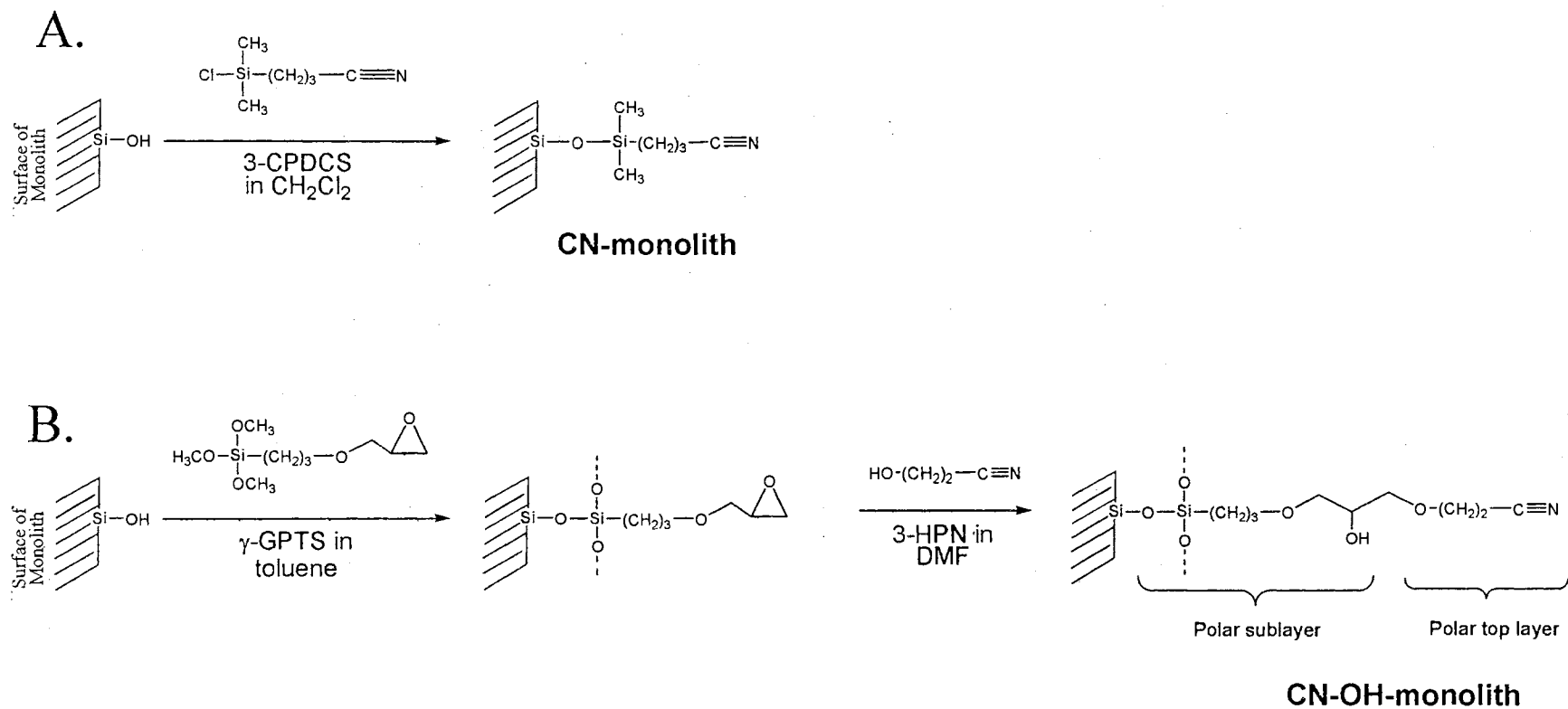


**Figure 1.** Schematic of the two reaction pathways investigated. (A) Reaction of 3-CPDCS catalyzed by 2,6-lutidine in methylene chloride at 50 °C. (B) Reaction of  $\gamma$ -GPTS in toluene at 110 °C followed by reaction of 3-HPN in DMF catalyzed by  $\text{BF}_3$  at room temperature.

## Results and Discussion

### Comparison of the Cyano Phases

Two different reaction schemes have been investigated for the preparation of cyano silica-based monolithic stationary phases. As can be seen in Fig. 1, path A yielded a cyano monolith (CN-monolith) in a single reaction step while path B gave a mixed ligand containing hydroxyl and cyano functions (i.e., CN-OH-monolith) in a two-step reaction. Although in path B, the treatment with  $\gamma$ -GPTS is aimed at providing a spacer arm for attaching the cyano ligand 3-HPN (i.e., the polar top layer), the spacer arm becomes a part of the interacting ligand by providing a hydrophilic sublayer containing polar hydroxyl groups. In addition, epoxide moieties that do not react with 3-HPN will yield diol ligands (i.e., silylpropyl glyceryl ether ligands).

Table 1 summarizes the retention factor ( $k'$ ), separation efficiency and EOF velocity obtained on the two cyano phases with a series of model solutes. The mobile phase velocity on the CN-monolith is ~17% higher than that on the CN-OH-monolith indicating more available silanol groups to support the EOF. This may reflect a lower phase ratio (i.e., lower surface coverage with polar ligands) for the CN-monolith or a better shielding of the silanols by the spacer arm (i.e., the polar sublayer) in the CN-OH-monolith. Both reasoning could explain the difference in EOF velocity of the cyano monoliths under investigation as well as the higher  $k'$  values obtained with the CN-OH-monolith. The CN-OH-monolith should yield a more polar stationary phase, thus

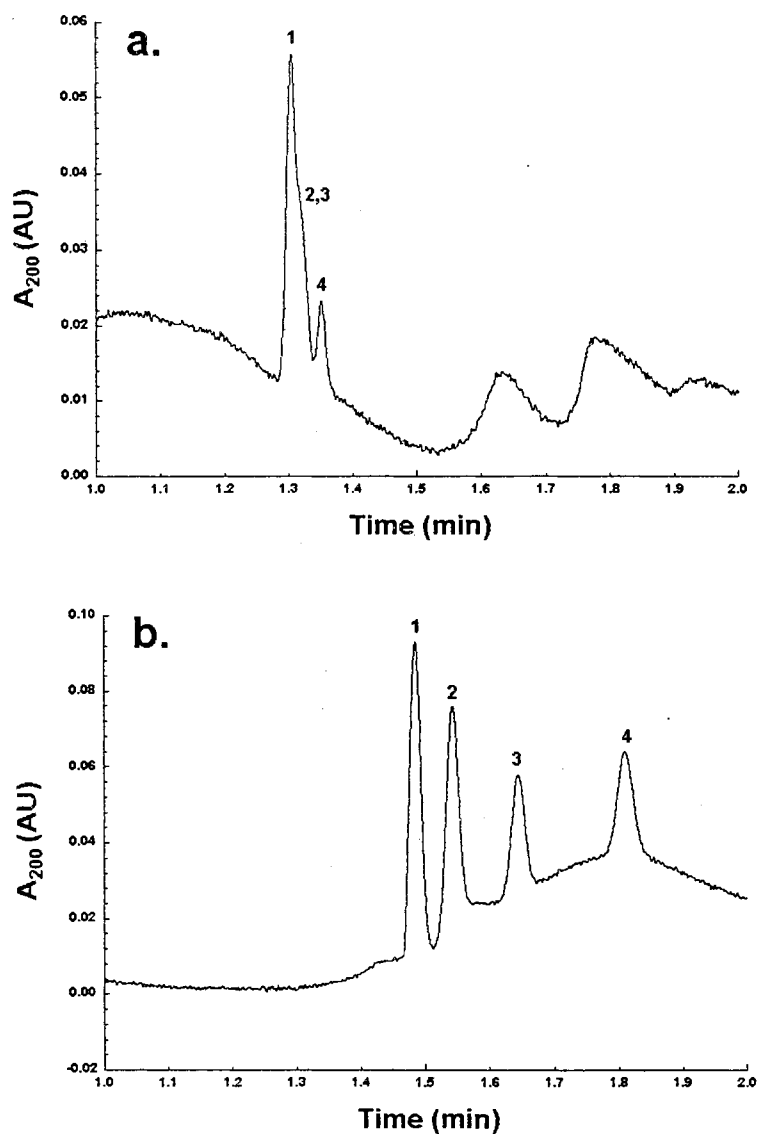
providing a higher “polar” phase ratio and consequently, stronger retention under equivalent mobile phase compositions.

TABLE 1.

COMPARISON OF CN-MONOLITH AND CN-OH MONOLITH USING  
5 mM TEAPO<sub>4</sub> (pH 6.5) AT 95% (v/v) ACETONITRILE.

Analytes	CN		CN-OH	
	k'	u <sub>eo</sub> (mm/s)	k'	u <sub>eo</sub> (mm/s)
DMF	~ 0	2.57	0.04	2.19
Formamide	0.018		0.11	
Thiourea	0.037		0.22	
2-CP	0.017	213,000 plates/m	0.049	199,000 plates/m
2,4-DCP	0.042		0.091	
3,4,5-TCP	0.091		0.14	
2,4,5-TCP	0.39		0.29	

On the basis of the above results, the cyano monolith obtained *via* path B (i.e., CN-OH-monolith) shown in Fig. 1B, is a promising hydrophilic monolith for normal-phase CEC (NP-CEC). In fact, a quick inspection of Fig. 2 reveals the superiority of CN-OH-monolith over CN-monolith in terms of retention and selectivity under the same elution conditions. The CN-OH-monolith was therefore used for the remainder of this investigation.



**Figure 2.** Electrochromatograms of some model compounds on cyano columns made by two different pathways. Conditions: capillary column (a) CN-monolith and (b) CN-OH-monolith, 20/27 cm x 100  $\mu$ m I.D.; hydro-organic mobile phase, 5 mM TEAPO<sub>4</sub> (pH 6.5) at 95% (v/v) ACN; voltage, 20kV; wavelength, 200 nm; column temperature, 20 °C. Solutes: 1, toluene; 2, DMF; 3, formamide; 4, thiourea.

### Characterization of the CN-OH-Monolith with Polar Solutes

Mobile phase composition As in all CEC modes, the mobile phase composition not only impacts retention and selectivity, but also the mobile phase flow velocity due to

the various effects of ions, organic solvent, pH and viscosity. Figure 3 shows typical electrochromatograms obtained for toluene, DMF, formamide and thiourea under four different mobile phase compositions. The results are summarized in Table 2 in terms of  $k'$ , average separation efficiencies and flow velocity. Toluene serves as the EOF marker [19]. While the mobile phase conditions in Fig. 4a, c and d (corresponding to mobile phases [a], [c] and [d] in Table 2) involve constant ACN concentration (i.e., 95% v/v) but different nature of electrolytes, the conditions in Fig. 4b (mobile phase [b] in Table 2) calls for different nature and content of organic modifiers and electrolytes. Small variations in  $k'$  were observed for the four different mobile phases tested, with mobile phase [b] giving the lowest  $k'$  values. The change in mobile phase flow velocity is the most significant and noticeable. Mobile phase [a] yielded an EOF velocity 3.5 times greater than that exhibited by mobile phase [d]. This may explain, in part, the lowest separation efficiency observed with mobile phase [d], whereby longitudinal molecular diffusion is contributing the most to band broadening. Another aspect of mobile phase composition is the contribution of the eluent component to baseline irregularities. Mobile phase irregularities in normal phase chromatography have been previously reported in HPLC [13] as well as in CEC [19]. Mobile phase [a] generated the best results in terms of separation efficiency and flow velocity, but produced the most irregular baseline, whereas mobile phase [c] ran cleaner with good separation efficiency and flow velocity.

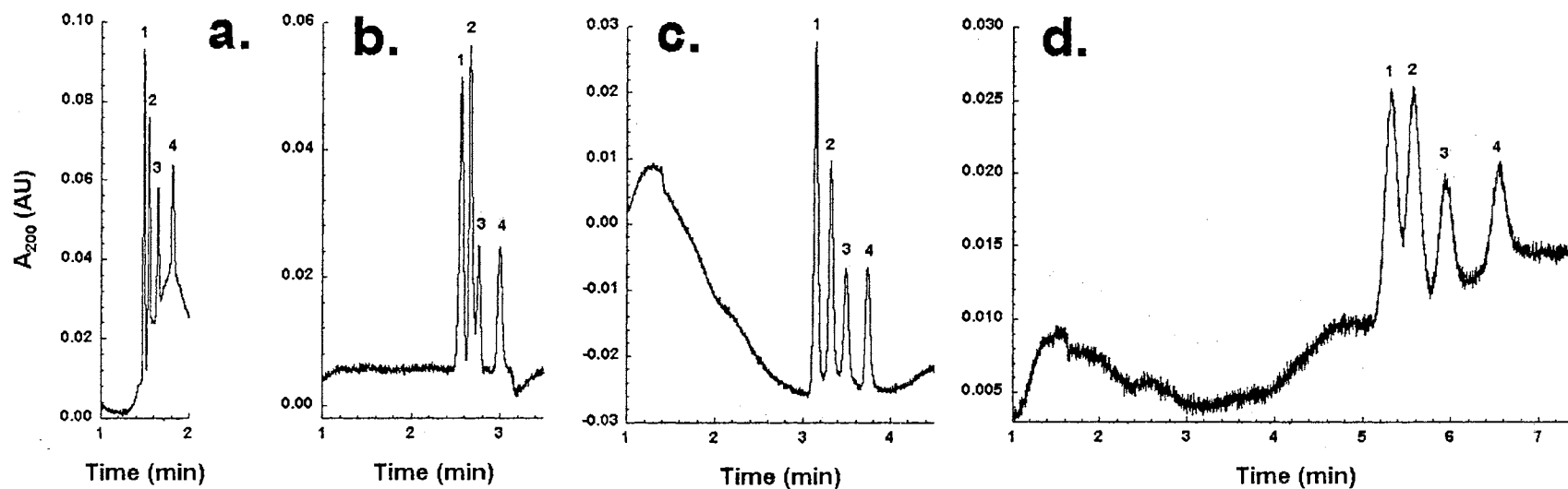


**Figure 3.** Comparison of mobile phase conditions for the separation of model compounds on the CN-OH-monolith column. Conditions: CN-OH-monolithic capillary column, 20/27 cm x 100  $\mu$ m I.D.; hydro-organic mobile phase, (a) 5 mM TEAPO<sub>4</sub> (pH 6.5) at 95% (v/v) ACN, (b) 92.65% ACN, 5% MeOH, 2.3% acetic acid, 0.05% (v/v) TEA, (c) 5mM NH<sub>4</sub>Ac (pH 4.5) at 95% (v/v) ACN, (d) 5mM Tris (pH 7.8) at 95% (v/v) ACN; voltage, 20kV; wavelength 200 nm; column temperature, 20 °C. Peak designations are the same as Figure 2

TABLE 2.

EFFECT OF THE MOBILE PHASE COMPOSITION ON THE BEHAVIOR OF THE CN-OH-MONOLITH COLUMN.

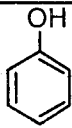
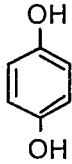
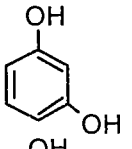
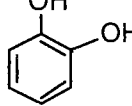
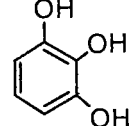
	Mobile phase composition	$u_{eo}$ (mm/s)	$k'$			$N_{avg}$ (plates/m)
			<i>DMF</i>	<i>Formamide</i>	<i>Thiourea</i>	
139	[a]: 5 mM TEAPO <sub>4</sub> (pH 6.5) @ 95% (v/v) ACN	2.21	0.039	0.11	0.22	161,000
	[b]: 92.65% (v/v) ACN, 5% (v/v) MeOH, 2.3% (v/v) acetic acid and 0.05% (v/v) TEA	1.30	0.040	0.077	0.17	117,000
	[c]: 5 mM NH <sub>4</sub> Ac (pH 4.5) @ 95% (v/v) ACN	1.06	0.054	0.11	0.19	120,000
	[d]: 5 mM Tris/HCl (pH 7.8) @ 95% (v/v) ACN	0.62	0.049	0.11	0.23	36,000

## Correlation of solute retention and structure

*Phenols* To further characterize the CN-OH-monolith under investigation, a series of phenols were electrochromatographed using mobile phase [a]. The calculated  $k'$  values are shown in Table 3. As expected for a hydrophilic monolith,  $k'$  increases with an increase in the number of hydroxyl groups within the molecule. Moreover, the extent of polar interactions depends on the position of the hydroxyl groups. This interaction is

TABLE 3.

RETENTION FACTOR ( $k'$ ) FOR PHENOLS OBTAINED ON CN-OH-MONOLITH USING 5.0 mM TEAPO<sub>4</sub> (pH 6.5) AT 95% (v/v) ACETONITRILE.

Phenols	Structure	$k'$
Phenol		0.037
Hydroquinone		0.070
Resorcinol		0.089
Catechol		0.093
Pyrogallol		0.43



stronger for catechol (ortho substituted phenol) and resorcinol (meta substituted phenol) than for hydroquinone (para substituted phenol). The hydroxyl group selectivity factor in the para position ( $\alpha_{\text{pOH}}$ ) can be obtained by taking the ratio between the retention factors for hydroquinone and phenol ( $\alpha_{\text{pOH}} = 1.89$ ). Similarly, the ratio of  $k'$  of resorcinol to that of phenol yields a value of 2.40 for the hydroxyl group selectivity factor in the meta position ( $\alpha_{\text{mOH}} = 2.40$ ). The ratio of  $k'$  of catechol to that of phenol gives the hydroxyl group selectivity factor in the ortho position ( $\alpha_{\text{oOH}} = 2.51$ ). Thus, the positional group selectivity factors in the order of decreasing values are  $\alpha_{\text{oOH}} > \alpha_{\text{mOH}} > \alpha_{\text{pOH}}$ .

Nucleic acid bases and their nucleosides Due to the multiplicity of their polar groups, the nucleic acid bases and nucleosides are important probes for evaluating the polarity of the stationary phases under investigation, and, in turn, the influence of functional groups on normal phase retention. As can be seen in Fig. 4a, the nucleic acid bases under investigation, namely uracil, thymine, cytosine and adenine, elute in order of increasing amine functions (particularly primary and secondary amines) and size. Upon conjugation of the bases with ribose to yield nucleosides, the interactions of the polar conjugates with the CN-OH-monolith increased for all analytes investigated except adenosine. The addition of ribose to uracil led to an increase in  $k'$  by a factor of  $\sim 2.6$ , and the  $k'$  value of cytidine increased by a factor of 1.3 with respect to the base cytosine. On the other hand, the  $k'$  value of adenosine decreased by a factor of  $\sim 1.7$  when compared with the  $k'$  value for adenine. The conjugation of adenine with a ribose residue to yield adenosine transforms a secondary amine to a tertiary amine group. The net result of these changes is a decrease in retention for adenosine when compared to that of

adenine. Therefore, it appears from these data that an amine group contributes much more to retention than the addition of a whole ribose moiety.

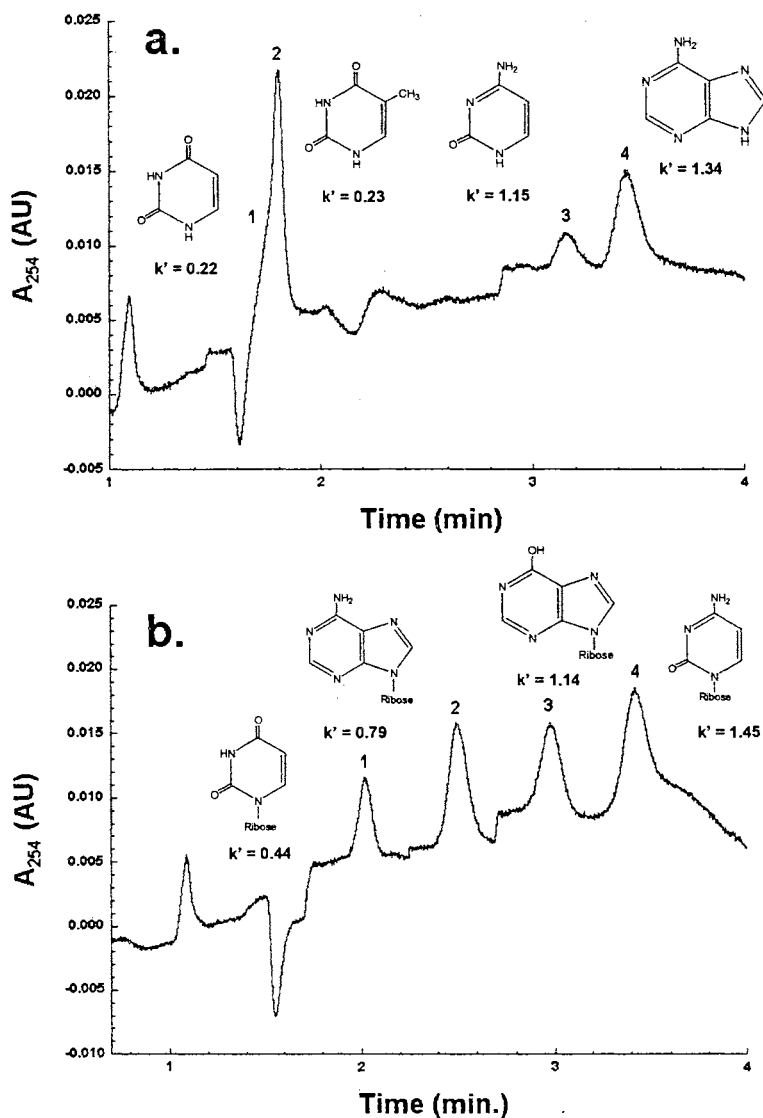


**Figure 4.** Electrochromatograms of (a) nucleic acid bases and (b) nucleosides on the CN-OH-monolith column. Conditions are the same as in Figure 2 except wavelength is 254 nm. Solutes: (a) 1, uracil; 2, thymine; 3, cytosine; 4, adenine (b) 1, uridine; 2, adenosine; 3, inosine; 4, cytidine.

Nitrophenyl derivatives of mono- and oligosaccharides. The retention of some ortho- and para-nitrophenyl (oNP and pNP, respectively) derivatives of mono- and oligosaccharides were examined on the CN-OH-monolith. Figure 5a shows the

separation of pNP-maltooligosaccharides up to a d.p. = 5 with a separation efficiency of 111,000 plate/m at a flow velocity of 1.0 mm/s. As expected for an NP-CEC retention

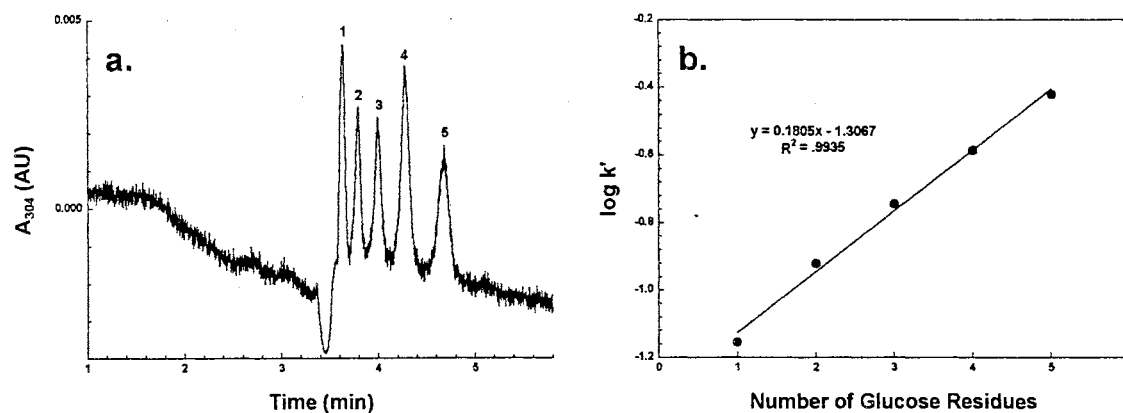
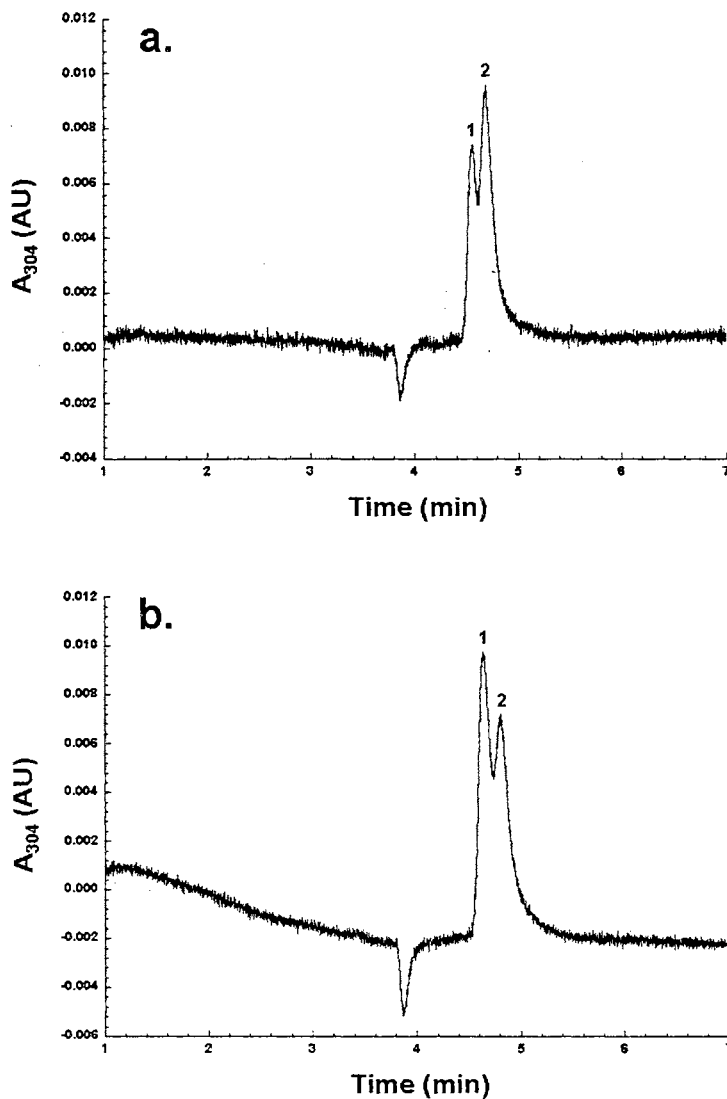


**Figure 5.** (a) Electrochromatogram of pNP-oligosaccharide homologous series and (b) plot of  $\log k'$  vs. number of glucose residues. Conditions: CN-OH-monolith capillary column, 20/27 cm x 100  $\mu$ m I.D.; hydro-organic mobile phase, 5mM NH<sub>4</sub>Ac (pH 4.5) at 80% acetonitrile (v/v); voltage, 20kV; wavelength, 304 nm; column temperature, 20 °C. Solutes: 1, pNP- $\alpha$ Glc; 2, pNP  $\alpha$ -D-maltoside; 3, pNP  $\alpha$ -D-maltotrioside; 4, pNP  $\alpha$ -D-maltotetraoside; 5, pNP  $\alpha$ -D-maltopentaoside.

mechanism, the oligomers retention increased with increasing d.p. since this results in an increase of the number of solute polar sites available for interaction with the fixed polar sites of the monolithic stationary phase. Also shown in Fig. 5b is the plot of  $\log k'$  of the pNP-maltooligosaccharides versus the number of glucose residues in the sugar molecule. The plot is linear with an  $R^2 = 0.9935$  and a slope, or glucosyl group selectivity factor ( $\alpha_{\text{Glc}}$ ) of 0.18 in log units (i.e., an  $\alpha_{\text{Glc}} = 1.51$ ). The y-intercept is equal to  $-1.3067$  corresponding to a retention factor contribution for the pNP-residue of  $k' = 0.049$ . This interaction can be considered negligible since the pNP confers a relatively non-polar property to the sugar derivatives.

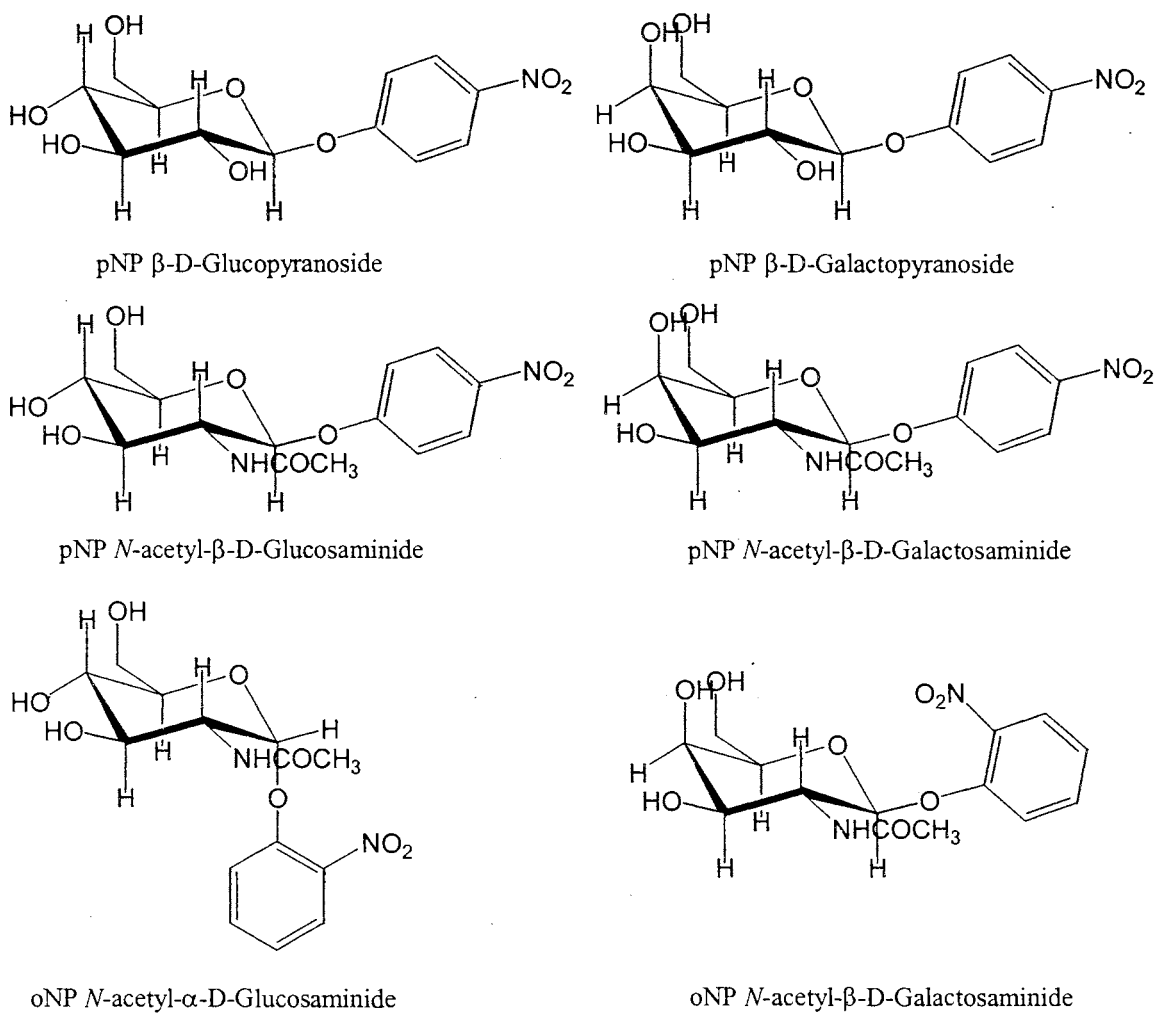
Upon increasing the acetonitrile content of the mobile phase from 80% to 95% (v/v), the glucosyl selectivity factor ( $\alpha_{\text{Glc}}$ ) increased from 1.51 to 3.94 as calculated from

the ratio of retention factors between pNP  $\alpha$ -D-maltoside and pNP- $\alpha$ Glc. Also, at 95% (v/v) ACN in the mobile phase, the  $\alpha$ <sub>GlcNAc</sub> (as calculated from the ratio of retention factors between pNP- $\beta$ chitobiose and pNP- $\beta$ GlcNAc) is relatively high, and equal to 8.35. These selectivity factors demonstrate the high discriminative power of the stationary phase under consideration.



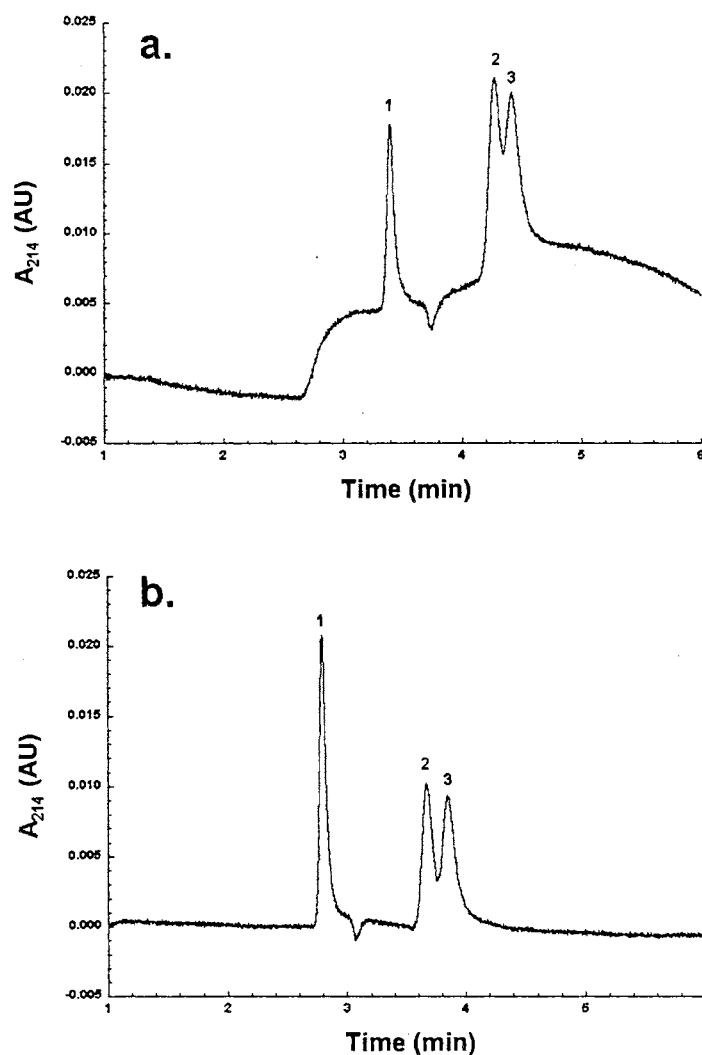
**Figure 6.** Electrochromatograms of (a) pNP monosaccharides and (b) pNP N-acetyl monosaccharides obtained on the CN-OH-monolith column. Conditions: monolithic capillary column, 20/27 cm x 100  $\mu$ m I.D.; hydro-organic mobile phase, 5mM  $\text{NH}_4\text{Ac}$  (pH 4.5) at 95% (v/v) ACN; voltage, 20kV; wavelength, 304 nm; column temperature, 30  $^\circ\text{C}$ . Solutes: (a) 1, pNP- $\beta$ Gal; 2, pNP- $\beta$ Glc and (b) 1, pNP- $\beta$ GalNAc; 2, pNP- $\beta$ GlcNAc.

Figure 6 further illustrates the discriminative power of the CN-OH-monolith, namely the separation of pNP- $\beta$ Gal and pNP- $\beta$ Glc (Fig. 6a) as well as that of pNP- $\beta$ GalNAc and pNP- $\beta$ GlcNAc. The solute pair pNP- $\beta$ Gal/pNP- $\beta$ Glc and the solute pair pNP- $\beta$ GalNAc/pNP- $\beta$ GlcNAc only differ in the orientation of their hydroxyl groups at the C4 position (Fig. 7). These sugar pairs, which differ in configuration at just one of the several chiral centers, are called epimers. As shown in Fig. 6a and 6b pNP- $\beta$ Gal elutes before pNP- $\beta$ Glc, and pNP- $\beta$ GalNAc before pNP- $\beta$ GlcNAc, respectively. This indicates that the hydroxyl group at the C4 position in the Gal residue (or GalNAc



**Figure 7.** Structures of pNP and oNP oligosaccharides.

residue) engages in less interaction with the polar stationary phase than the hydroxyl group at the C4 position in the Glc residue (or GlcNAc residue).



**Figure 8.** Electrochromatograms of oNP derivatives of monosaccharides obtained on the CN-OH-monolithic column. Conditions: CN-OH-monolithic capillary column, 20/27 cm x 100  $\mu$ m I.D.; hydro-organic mobile phase, (a) 5mM and (b) 2.5mM  $\text{NH}_4\text{Ac}$  (pH 4.5) at (a) 95% and (b) 97.5% (v/v) ACN; voltage, 20kV; wavelength, 214nm; column temperature, 30  $^\circ\text{C}$ . Solutes: 1, toluene; 2, oNP- $\alpha$ GlcNAc; 2, oNP- $\beta$ GalNAc.

Figure 8 shows the separation of oNP- $\alpha$ GlcNAc and oNP- $\beta$ GalNAc. In this case, the nitrophenyl GlcNAc derivative is less retained than the nitrophenyl GalNAc derivative. This may be due to the fact that in the  $\beta$ -anomer (i.e., oNP- $\beta$ GalNAc) the

equatorial glycosidic oNP residue interacts less strongly with the axial hydrogen atom on C5 than in the  $\alpha$ -anomer (i.e., oNP- $\alpha$ GlcNac) where the glycosidic oNP residue occupies an axial position. In addition, the  $\alpha$ -anomer's (i.e., oNP- $\alpha$ GlcNac) glycosidic oNP residue is located on the same side as the polar acetylamine function, whereas in the  $\beta$ -anomer (i.e., oNP- $\beta$ GalNac) the glycosidic oNP residue is located on the opposite side. This allows oNP- $\beta$ GalNac to interact stronger with the stationary phase than oNP- $\alpha$ GlcNac since the acetylamine group is not sterically hindered by the label. An improved resolution between oNP- $\alpha$ GlcNac and oNP- $\beta$ GalNac (see Fig 7b) is readily obtained by increasing the ACN content of the mobile phase from 95% (v/v) ACN (Fig. 7a) to 97.5 % (v/v) ACN (Fig. 7b).

### Conclusions

Two synthetic routes have been introduced and evaluated for the preparation of hydrophilic silica-based monoliths possessing surface-bound cyano functions. Due to its stronger hydrophilic character, the CN-OH-monolith yielded higher retention and better selectivity than the CN-monolith. These monoliths with surface-bound stratified polar layers comprising a hydroxy sub-layer and a cyano top layer (i.e., CN-OH-monolith) proved very useful for NP-CEC of a wide range of polar compounds including; phenols, chlorophenols, nucleic acid bases, nucleosides, mono- and oligosaccharides. The extent of solute retention is readily adjusted by altering the acetonitrile content of the mobile phase, and the polar group (or residue) selectivity factor is strongly influenced by the group position within the solute and the organic content of the mobile phase. The CN-

OH-monolith exhibited a relatively strong EOF over a wide range of mobile phase composition, which resulted in rapid analysis times (i.e., less than 5 min) for most separations investigated.



## References

1. Knox, J.H., Grant, I.H., *Chromatographia* **1987**, 24, 135-143.
2. Yamamoto, H., Baumann, J., Erni, F., *J. Chromatogr.* **1992**, 593, 313-319.
3. Yan, C., Dadoo, R., Zhao, H., Zare, R.N., *Anal. Chem.* **1995**, 67, 2026-2029.
4. Dittmann, M., Wienand, K., Bek, F., Rozing, G.P., *LC-GC* **1995**, 13, 800-814.
5. Dittmann, M.M., Masuch, K., Rozing, G.P., *J. Chromatogr. A* **2000**, 887, 209-221.
6. Rathore, A.S., Wen, E., Horvath, C., *Anal. Chem.* **1999**, 71, 2633-2641.
7. Pretorius, V., Hopkins, B.J., Schieke, J.D., *J. Chromatogr.* **1974**, 99, 23-30.
8. Yang, C., El Rassi, Z., *Electrophoresis* **1998**, 19, 2061-2067.
9. Yang, C., El Rassi, Z., *Electrophoresis* **1999**, 20, 2337-2342.
10. Zhang, M., El Rassi, Z., *Electrophoresis* **1998**, 19, 2068-2072.
11. Zhang, M., Ostrander, G.K., El Rassi, Z., *J. Chromatogr. A* **2000**, 887, 287-297.
12. Churms, S.C., *High performance hydrophilic interaction chromatography of carbohydrates with polar sorbents*, in *Carbohydrate Analysis by Modern Chromatography and Electrophoresis*, Z. El Rassi, Editor. 2002, Elsevier: Amsterdam, pp. 121-163.
13. Alpert, A.J., *J. Chromatogr.* **1990**, 499, 177-196.
14. Wei, W., Luo, G.A., Hua, G.Y., Yan, C., *J. Chromatogr. A* **1998**, 817, 65-74.
15. Maruska, A., Pyell, U., *J. Chromatogr. A* **1997**, 782, 167-174.
16. Lai, E.P.C., Dabek-Zlotorzynska, E., *Electrophoresis* **1999**, 20, 2366-2372.

17. Que, A.H., Konse, T., Baker, A.D., Novotny, M.V., *Anal. Chem.* **2000**, *72*, 2703-2710.
18. Que, A.H., Novotny, M.V., *Anal. Chem.* **2002**, *74*, 5184-5191.
19. Ye, M., Zou, H., Kong, L., Lei, Z., Wu, R., Ni, J., *LC-GC* **2002**, August, 41-46.
20. Lammerhofer, M., Svec, F., Frechet, J.M.J., Lindner, W., *J. Chromatogr. A* **2001**, *925*, 265-277.
21. Allen, D., El Rassi, Z., *The Analyst* **2003**, in press.
22. Allen, D., El Rassi, Z., *Electrophoresis* **2003**, *24*, 408-420.
23. Ishizuka, N., Minakuchi, H., Nakanishi, K., Soga, N., Nagayama, H., Hosoya, K., Tanaka, C.K., *Anal. Chem.* **2000**, *72*, 1275-1280.
24. Hayes, J.D., Malik, A., *Anal. Chem.* **2000**, *72*, 4090-4099.

VITA

4

Darin James Allen

Candidate for the Degree of

Doctor of Philosophy

Thesis: MONOLITHIC SILICA – BONDED STATIONARY PHASES FOR  
CAPILLARY ELECTROCHROMATOGRAPHY

Major Field: Analytical Chemistry

Biographical:

Personal: Born in McCook, Nebraska, on January 8, 1975. The son of James Marshall Allen and Janis Rae Huff.

Education: Graduated from Canadian High School in Canadian, Oklahoma, in May of 1993; received Bachelor of Science degree in Chemistry from Southeastern Oklahoma State University in Durant, Oklahoma, in July of 1998. Completed the requirements for the Doctor of Philosophy Degree with a major in Chemistry at Oklahoma State University in Stillwater, Oklahoma, in December of 2003.

Experience: Undergraduate research assistant for Dr. Tim Smith from January of 1996 to August of 1998; graduate research assistant for Dr. Ziad El Rassi from August of 1998 to July of 2003; employed by Oklahoma State University, Department of Chemistry, as a teaching assistant from August of 1998 to December of 2003.

Professional Memberships: Phi Lambda Upsilon Honorary Chemical Society; American Chemical Society.